THE MITOCHONDRIAL ANTIOXIDANT DEFENSE SYSTEM AND OXIDATIVE METABOLISM DURING PERINATAL DEVELOPMENT: POTENTIAL ROLE IN MITOCHONDRIAL CALCIUM METABOLISM DURING REPERFUSION INJURY

by

Angelo Anthony Vlessis

A Dissertation

Presented to the Department of Biochemistry
School of Medicine
and the Graduate Division of the
Oregon Health Sciences University
in partial fulfillment of
the requirements for the degree of

Doctor of Philosophy

June 1989

APPROVED: [redacted]

(Professor in charge of thesis)

[redacted]

(Chairman, Graduate Council)

TABLE OF CONTENTS

LIST OF ILLUSTRATIONS

page

* These figures contain mean values connected by straight lines. The lines do not represent experimental data but are included merely to connect the mean values for each age group and to demonstrate gross trends in the dependent variable following birth.

LIST OF TABLES

ACKNOWLEDGEMENTS

I dedicate this thesis work to my parents, Christopher and Rosina Vlessis, and my siblings, Nick, Lisa and Damon, who have provided emotional support and encouragement throughout the many months spent researching and writing the contents of this book.

To my mentor, Dr. Leena Mela-Riker, I extend my deepest appreciation and thanks for nurturing my ideas, teaching me thoroughness, proper experimental technique and design, and most of all, for providing me with a sterling example of the type of scientist I hope to become.

I acknowledge the members of my Thesis Advisory Committee, Dr. Howard Mason, Dr. James Hare, Dr. John Bissonette, Dr. James Metcalfe and Dr. Buddy Ullman for their helpful advice, instruction and discussion.

I am grateful to the Medical Research Foundation of Oregon who has provided financial support while I pursue this degree.

ABSTRACT

Mammalian birth imposes a dramatic environmental change on the emerging organism. During adaptation to an altered oxygen and nutrient supply, the newborn animal exhibits an extreme resistance to various forms of oxidative stress, such as hyperoxia, selenite injection and ischemia-reperfusion. By understanding the mitochondrion's role in metabolic adaptation to extrauterine life, an understanding of possible biochemical mechanisms responsible for the newborn's tremendous resistance to oxidative challenge may evolve. Using isolated guinea pig heart, kidney and liver mitochondria, the perinatal development of the mitochondrial respiratory chain and antioxidant defense system were characterized both compositionally and functionally using a physiological chemistry approach. In order to assess perinatal changes in mitochondrial composition, ubiquinone, cytochromes b, c and oxidase, membrane fluidity, pyridine and adenine nucleotide pools, glutathione, glutathione reductase and peroxidase, and superoxide dismutase were determined. Cytochrome b and c concentrations, as well as the pyridine and adenine nucleotide pools, showed variable age and tissue specific changes during the perinatal period. Ubiquinone and cytochrome oxidase concentrations, as well as superoxide dismutase activity, increased in the mitochondria of all three tissues following birth. The liquid-gel phase transition temperature of the inner mitochondrial membrane increased transiently during the newborn period in all three tissues. Total glutathione concentration remained stable at all ages in heart and liver mitochondria, however, levels in kidney mitochondria declined steadily from the fetal to adult periods. The highest glutathione

reductase and peroxidase activities were seen in the mitochondria of fetal animals. Activities decreased immediately following birth and remained below fetal values thereafter except for glutathione peroxidase activity in heart and kidney which returned to fetal values. To assess perinatal changes in mitochondrial respiratory function, maximum state 3 respiratory rate with glucogenic (pyruvate), ketogenic (B-hydroxybutyrate), lipogenic (palmitylcarnitine) and amino acid (glutamate) substrates as well as succinate were determined. In general, respiration with all the substrates increased or remained unchanged during the newborn period except for pyruvate oxidation in the heart and kidney where rates declined abruptly following birth. To assess the function of the intact mitochondrial antioxidant defense system, NAD(P)H oxidation rates in the presence of two different oxidants, selenite and t-butylhydroperoxide, were determined. NAD(P)H oxidation rates with both oxidants were low during the fetal and early newborn period; rates increased significantly with increasing perinatal age. Additionally, oxidant-induced mitochondrial NAD(P)H oxidation was shown to induce mitochondrial calcium release and cycling, thereby substantiating the importance of the mitochondrial antioxidant defense system in oxidant-related injuries. Interestingly, mitochondria from newborn animals were less susceptible to oxidant-induced mitochondrial calcium release. The results are discussed in terms of the newborn's resilience to oxidative stress and the variable roles of the three tissues in whole body metabolism.

INTRODUCTION

Birth marks the beginning of an adaptive life for the emerging fetus in which the nurturing environment of the uterus is abandoned for an often hostile, unstable environment. The multitude of changes associated with birth make its study both a complex and intriguing enterprise. Three factors prompted this thesis work in perinatal metabolism. First, an academic interest in the normal metabolic adaptation to changing oxygen tensions and availability. Mammalian birth provides a model system to study this process. Second, the newborn animal exhibits an extreme tolerance to various oxidative challenges. An understanding of the biochemical differences between newborn and adult oxidative metabolism may elucidate possible therapeutic approaches to oxidant injuries in adults (e.g., adult respiratory distress syndrome, ischemia-reperfusion injury, oxygen toxicity). Third, an understanding of the metabolic complications which accompany prematurity and other perinatal diseases may evolve from an understanding of the normal biochemical changes associated with birth.

The first objective was to characterize the changes in mitochondrial respiratory chain function and composition in heart, kidney and liver during the perinatal period. Mitochondria orchestrate cellular metabolism, by regulating substrate entry into the various oxidative and reductive pathways as well as providing energy for cellular ion homeostasis. Although past research has focused on the development of the energy producing pathways, the mitochondrial antioxidant defense system has received very little attention.

Therefore, the second objective was to characterize the mitochondrial antioxidant defense system, for the first time, during perinatal development and emphasize its role in modulating substrate entry into oxidative pathways as well as regulating mitochondrial calcium balance.

The experiments described herein employed mitochondrial preparations made from whole tissues. Although each tissue contains many cell types, the mitochondria from the most prevalent cell types will predominate, i.e., myocyte, renal tubule cell and hepatocyte for the heart, kidney and liver respectively. The reader should be aware of this heterogeneity and its potential influence on the results herein.

The remainder of this introduction contains an extensive review of various topics in perinatal metabolism, biochemistry and physiology which are pertinent to this thesis. Information presented here does not reiterate nor replace the introductions of each manuscript, but instead provides the broad knowledge base necessary to interpret the results presented.

Alterations of mitochondrial function and composition in response to oxygen have been extensively studied in unicellular organisms. Anaerobically grown yeast do contain mitochondria (called promitochondria) but lack respiratory cytochromes [1]. The biosynthesis of several mitochondrial enzymes, such as cytochrome c [2], cytochrome c peroxidase [2] and cytochrome oxidase [3], are regulated by oxygen. These enzymes all contain heme as a prosthetic group. Since anaerobically grown yeast cells do not synthesize heme, the lack of heme-containing proteins during anaerobiosis was attributed to the absence of heme [3,4,5]. Heme has subsequently been shown to

regulate the expression of these oxygen-induced genes at the level of transcription [6]. Interestingly, the synthesis of mitochondrial manganese superoxide dismutase, a non-heme protein, is also regulated by oxygen [7]. Its expression may be controlled by the ROX1 gene product at the level of transcription [8]. Therefore, some of the effects of oxygen on mitochondrial function and composition may result from oxygen-sensitive changes in gene expression.

Circulatory changes at birth are accompanied by alterations in arterial oxygen tensions (P_aO_2). Prior to birth, the fetus derives oxygen from the placenta [9]. Oxygenated fetal blood (PO_2 ~ 25mmHg) flows from the placenta via the umbilical vein to the liver [10,11]. Blood courses through the liver capillary beds and is returned (PO_2 ~ 20 mmHg) to the heart [15,19,21,36]. After birth, systemic arterial pressure increases secondary to ductus arteriosus closure and loss of the low resistance placental circulation which received 40-50% of the fetal cardiac output [15]. Changes in the right and left atrial pressures induces foramen ovale closure and blood is forced through the pulmonary circulation for oxygenation. Arterial oxygen tension rises immediately after birth stabilizing at about 80 mmHg at 4 days post-birth [12,13,16,17], an increase of about 60 mmHg over fetal values. In sharp contrast, the blood supply to the liver post-birth consists primarily (95%) of poorly oxygenated portal venous blood [18,19]. Although the actual O_2 tensions in the liver vary widely depending on the lobe, the liver is not exposed to large increases in systemic arterial oxygen tension and, therefore, would be expected to show smaller oxygen-induced changes in mitochondrial structure and function

as compared to other systemic organs. For this reason, the liver provides an excellent comparison with other systemic organs when oxygen-induced changes in mitochondrial structure and function are studied.

Acute and chronic changes in P_aO_2 induce predictable changes in mitochondrial respiratory activities and cytochrome concentrations in both newborn and adult animals [12,20-22]. Local tissue oxygen tension is influenced by (1) tissue respiration, (2) diffusion conditions, (3) distance from the capillary, and (4) oxygen tension at the capillary wall [23]. An abrupt increase in P_aO_2 is associated with a rise in mean tissue PO_2 [24,25]. Mitochondria respond to the increased tissue PO_2 with an immediate decrease in maximal respiratory activity [13,26]. A new steady state level of respiratory activity is attained and cytochrome concentrations change after 6-10 days of exposure to a different level of oxygenation [13,16,26]. Birth provides an example of an organism's adaptation from a low oxygen tension to a high oxygen tension environment. In the term fetus, maximum mitochondrial respiratory activity per mole of cytochrome oxidase is several fold higher than the activity in adults [13,26,27]. Within the first 4 days post-birth, a dramatic decrease in respiratory activity occurs which correlates inversely with the rise in P_aO_2 [13,26]. As P_aO_2 stabilizes at adult levels, maximum respiratory activity per mole of cytochrome oxidase also stabilizes [13,26]. Support for oxygen as the stimulant of these changes in the newborn were obtained by simulating the hypoxic conditions of the uterus post-birth. Newborn animals kept in a low PO_2 (10-11%) environment following birth failed to show an increase in mitochondrial cytochrome content [16]. The process can be reversed by

changing an initially normoxic adult animal, P_aO_2 ~ 90 mmHg, to an acutely hypoxic state, P_aO_2 ~ 40 mmHg. In this case, respiratory activity abruptly increases [13]. Similarly, chronic hypoxia decreases cytochrome concentrations and increases maximum respiratory activity [26,28]. To summarize, acute and chronic changes in P_aO_2 appear to alter mitochondrial respiratory activity and cytochrome concentrations in a predictable fashion.

Although a rise in P_aO_2 is associated with a rise in mean tissue PO_2 [24,25], the actual PO_2 change at the level of the mitochondria remains speculative. Measurements in isolated cells have demonstrated significant intracellular oxygen concentration gradients [28]. Mitochondrial clustering, distribution and respiratory rate are major factors which determine the magnitude and location of intracellular oxygen concentration gradients [14,29,30]. A mathematical model of cellular oxygen diffusion has been established [31] in which the oxygen concentration at the mitochondrial outer membrane (C) is dependent on the extracellular oxygen concentration (C_i) minus the oxygen consumption rate (K) times the mitochondrial radius (b) squared over the intracellular diffusion coefficient (D) for oxygen:

$$C = C_i - (Kb^2)/(3D)$$

In the period immediately following birth, P_aO_2 rises abruptly [12,13,16,17] increasing the mean tissue PO_2 [24,25]. Since the mitochondrial radius and the oxygen diffusion coefficient initially remain constant, the oxygen concentration at the mitochondrial outer membrane becomes dependent on the extracellular oxygen concentration (approximately equal to mean tissue PO_2) minus the oxygen consumption

rate of the mitochondria. Therefore, the model predicts the oxygen concentration at the mitochondrial outer membrane will increase if mitochondrial oxygen consumption remains constant or decreases. Unfortunately, in vivo changes in mitochondrial oxygen consumption following birth are poorly defined. Studies on newborn infants have shown whole body oxygen consumption increases from 4.6 ml/kg/min to 7 ml/kg/min within 24 hours post-birth [32]. However, the source of the increased oxygen consumption remains unknown; heat production and brown fat metabolism are believed to be main contributors [33-35]. Univalent reduction pathways for O_2 may also be an important contributor to the rise in O_2 consumption post-birth since serum lipoperoxides and ethane/pentane expiration are elevated several-fold in the newborn [43,44]. In sheep, right ventricular myocardial oxygen consumption is decreased in the newborn as compared to the fetus [36], whereas, left ventricular myocardial oxygen consumption appears to increase [37,38]. In liver, oxygen consumption increases from 4 ml/min/100g to 7-9 ml/min/100g following birth [19]. Although the tissue oxygen consumption rate during the fetal to newborn transition may increase in some tissues, the actual in vivo PO_2 at the mitochondrial outer membrane remains speculative.

The structure and composition of mitochondria exhibit several interesting changes post-birth [39,40-42]. Isopycnic centrifugation of rat liver mitochondrial fractions show striking differences between the one-day prenatal and one-day postnatal animals [40]. Specifically, fetal mitochondria have a high osmotic space and a high hydrated matrix density, while neonatal mitochondria are devoid of an osmotic space and

the density of their hydrated matrix is lower [40]. The overall density of mitochondria changes from 1.236 g/ml at birth to 1.200 g/ml after two weeks [41]. Fortunately, these small, but significant, differences do not interfere with the composition of the isolated mitochondrial fraction obtained by standard differential centrifugation [40]. Interesting changes in the lipid composition of mitochondria occur following birth [39,42]. The phospholipid/ protein ratio declines from 0.255 +/- 0.015 (μmole/mg) in the 1 day-old to 0.207 +/- 0.005 in the 3 day-old [42]. The unsaturated/ saturated fatty acid ratio also decreases following birth rising again after 10 days to a new adult level [39,42]. These structural and compositional changes occur in the same time frame as the above mentioned alterations in respiratory activity.

The decrease in the phospholipid/ protein and unsaturated/ saturated fatty acid ratios may be explained by increased lipid peroxidation in the newborn [43,44]. Lipoperoxides are formed when reactive oxygen species remove hydrogen atoms from the methylene groups of unconjugated dienes [45-47]. Ethane and pentane, volatile hydrocarbon products of unsaturated fatty acid oxidation, are increased in the newborn (15 pmol pentane/ kg body wt) as compared to the adult (1.3 pmol pentane/ kg body wt) human [43]. In addition, lipoperoxides are low in the fetal rat serum but increase after birth reaching a peak at 10 days of life and then gradually decreasing to an intermediate adult level [44]. Lipid peroxidation is believed to increase phospholipase activity [48,49], thereby, liberating fatty acids from the membrane and contributing to the post-birth decline in the

phospholipid/ protein ratio.

The development of antioxidant defense enzyme systems in the newborn have been well documented for some tissue homogenates [50-54]. Unfortunately, the antioxidant defense system of mitochondria, the primary site of oxygen utilization and oxygen radical production [55], have received little attention [56]. Of the reactive oxygen species, mitochondria produce predominantly superoxide radical and H_2O_2 [55]. Superoxide will dismutate either enzymatically or spontaneously to H_2O_2. Univalent reduction of H_2O_2 by superoxide yields hydroxyl radical, the most reactive oxygen species (see Appendix D for additional details). Hydroxyl radical is responsible for initiating the lipid peroxidative chain reaction [45]. The mitochondrial antioxidant defense system functions to remove H_2O_2 through glutathione dependent pathways, thereby minimizing the formation of hydroxyl radical and preventing peroxidative membrane damage. Since superoxide generation by mitochondria increases linearly with PO_2 [46], increased tissue oxygen tensions in the newborn should increase oxygen radical formation. The inability to effectively remove reactive oxygen species may explain the observed increase in lipid peroxidation products during the newborn period [43,44]. The mitochondrial antioxidant defense system can influence mitochondrial function before signs of lipid peroxidation appear. For example, peroxide metabolism by mitochondria can modulate substrate entry into oxidative pathways. Pyruvate-driven ATP formation in isolated liver mitochondria is blocked by small quantities of peroxide. B-hydroxybutyrate and succinate oxidation, however, are not affected. The effect requires glutathione peroxidase

since glutathione peroxidase deficient mitochondria do not exhibit the peroxide-induced inhibition of pyruvate oxidation [57]. Characterization of the mitochondrial antioxidant defense system during the perinatal period should provide additional information not obtainable from the study of whole tissue homogenates.

Although rates of lipid peroxidation are enhanced in newborn animals, these animals exhibit an extreme tolerance to oxidative stress. Selenite is a potent oxidant which spontaneously oxidizes glutathione and other sulfhydryl compounds [58]. Newborn rats (3-4 days old) injected with 20 μmoles selenite/kg body weight have no toxic manifestation other than bilateral nuclear cataracts [59]. After 15 days of age, the frequency of cataract formation falls rapidly while mortality rate increases. Mortality approaches 100% at 50 days of age [60]. Newborn animals of various species are also resistant to the oxidative challenge imposed by hyperoxia [53]. Neonatal and adult guinea pigs have an LT 50 of 4.5 and 2.5 days respectively in >95% O_2 [61]. Although somewhat controversial, the neonatal myocardium appears to exhibit a tolerance to the oxidative stress imposed by ischemia/hypoxia-reoxygenation when compared to the adult myocardium [62-65]. Sixty minutes of hypoxia followed by reoxygenation reduced the maximum rate of tension development in neonatal and adult myocardium to 67% and 7% of control values respectively. In addition, resting tension, an indicator of post-reoxygenation tetany, increased 443% in the adult myocardium but remained unchanged in the neonatal myocardium. In conclusion, newborn animals exhibit a profound tolerance to various forms of oxidative stress. The etiology of this

tolerance remains unknown.

Manuscript #1 discusses the age-dependent, bimodal toxic manifestations of selenite. It reveals the importance of the mitochondrial antioxidant defense system on mitochondrial calcium metabolism during the perinatal period. Manuscripts #2 and #3 characterize the perinatal development of the mitochondrial respiratory chain and antioxidant defense system both functionally and compositionally. Appendix E, a minireview on mitochondrial calcium and peroxide metabolism, provides an indepth introduction to manuscript #4. Manuscript #4 demonstrates the important influence of the mitochondrial antioxidant defense system on mitochondrial calcium metabolism during periods of oxidative stress.

REFERENCES

1. Schatz,G. and Kovac, L. (1974). Isolation of promitochondria from anaerobically grown Saccharomyces cerevisiae. In: Methods in Enzymology. 31A: 627-632.

2. Djavadi-Ohaniance, L., Rudin, Y. and Schatz, G. (1978). Identification of enzymatically inactive apocytochrome c peroxidase in anaerobically grown Saccharomyces cerevisiae. J Biol Chem. 253: 4402-4407.

3. Woodrow, G. and Schatz, G. (1979). The role of oxygen in the biosynthesis of cytochrome c oxidase of yeast mitochondria. J Biol Chem. 254: 6088-6093.

4. Barlas, M., Ruis, H. and Sledziewski, A. (1979). Cell-free synthesis of Saccharomyces cerevisiae catalase T. FEBS Lett 99:242-246.

5. Mattoon, J.R., Lancashire, W.E., Sanders, H.K., Carvajal, E.,

Malamud, D.R., Braz, G.R.C. and Panek, A.D. (1979). Oxygen and catabolite regulation of hemoprotein biosynthesis in yeast. Biochem Clin Aspects Oxygen [Proc. Symp.]: 421-435.

6. Hortner, H., Ammerer, G., Hartter, E., Hamilton, B., Rytka, J., Bilinski, T. and Ruis, H. (1982). Regulation of the synthesis of catalases and iso-1-cytochrome c in Saccharomyces cerevisiae by glucose, oxygen and heme. Eur J Biochem. 128: 179-184.

7. Autor, A.P. (1982). Regulation of manganese superoxide dismutase by oxygen in Saccharomyces cerevisiae. Biochem Soc Trans. 10(2): 75-77.

8. Lowry, C.V. and Zitomer, R.S. (1984). Oxygen regulation of anaerobic and aerobic genes mediated by a common factor in yeast. Proc Natl Acad Sci USA. 81: 6129-6133.

9. Rudolph, A.M. (1984). Oxygenation in the fetus and neonate- a perspective. Seminars in Perinatology. 8(3): 158-167.

10. Dejours, P. (1981). Principles of Comparative Respiratory Physiology, 2nd Edition. Amsterdam: Elsevier/ North-Holland. p. 147-171.

11. Barron, D.H. and Meschia, G. (1954). A comparative study of the exchange of respiratory gases across the placenta. Cold Spring Harbor Symp Quant Biol. 19: 93-101.

12. Mela, L., Goodwin, C.W. and Miller, L.D. (1975). Correlations of mitochondrial cytochrome concentrations and activity to oxygen availability in newborn. Biochem Biophys Res Comm. 64(1):384-390.

13. Mela, L., Goodwin, C.W. and Miller, L.D. (1976). In vivo control of mitochondrial enzyme concentrations and activity by oxygen. Am J Physiol. 231: 1811-1816.

14. Anversa, P., Olivetti, G. and Loud, A.V. (1980). Morphometric study of early postnatal development in left and right ventricular myocardium of the rat. I. hypertrophy, hyperplasia and binucleation of myocytes. Circ Res. 46: 495-502.

15. Rudolph, A.M. and Heymann, M.A. (1970). Circulatory changes during growth in the fetal lamb. Circ Res. 26: 289-299.

16. Hallman, M. (1971). Changes in the mitochondrial respiratory chain proteins during prenatal development. Evidence of importance of environmental oxygen tension. Biochem Biophys Acta. 253: 360-372.

17. Harris, A.P., Sendak, M.J. and Donham, R.T. (1986). Changes in arterial oxygen immediately after birth in the human neonate. J Pediatrics. 109: 117-119.

18. Gleason, C.A., Roman, C. and Rudolph, A.M. (1985). Hepatic oxygen consumption, lactate uptake and glucose production in neonatal lambs. Circ Res. 19: 1235-1239.

19. Holzman, I.R. (1984). Fetal and neonatal hepatic perfusion and oxygenation. Seminars in Perinatology. 8: 234-244.

20. Park, C.D., Mela, L., Wharton, J., Reilly, J., Fishbein, P. and Aberdeen. (1973). Cardiac mitochondrial activity in acute and chronic cyanosis. J Surg Res. 14: 139-146.

21. Jones, C.T. (ed.). (1982). The development of metabolism in fetal liver. In: Biochemical Development of the Fetus and Neonate. Amsterdam: Elsevier. p. 249-286.

22. Aprille, J.R. and Asimakis, G.K. (1980). Postnatal development of rat liver mitochondria: State 3 respiration, adenine nucleotide translocase activity and net accumulation of adenine nucleotides.

Arch Biochem Biophys. 201: 564-575.

23. Lubbers, D.W. (1973). Local tissue PO_2: It's measurement and meaning. In: Oxygen Supply. (Kessler, et al, eds.). Univ. Park Press, Baltimore, Maryland. p. 151-155.

24. Schuchhardt, S. (1984). Myocardial oxygen pressure: Mirror of oxygen supply. Adv Exp Med Biol. 191: 21-35.

25. Skolasinska, K., Harbig, K., Lubbers, D.W. and Wodick, R. (1978). PO_2 and microflow histograms of the beating heart in response to changes in arterial PO_2. Basic Res Cardiol. 73: 307-319.

26. Mela, L., Goodwin, C.W. and Miller, L.D. (1977). In vivo adaptation of oxygen utilization to oxygen availability: Comparison of adult and newborn mitochondria. In: Oxygen and Physiological Function. Frans F. Jobsis, ed. Professional Information Library, p. 285-291.

27. Wells, R.J., Friedman, W.F. and Burton, E.S. (1972). Increased oxidative metabolism in the fetal lamb heart. Am J Physiol. 222: 1488-1493.

28. Jones, D.P. and Kennedy, F.G. (1986). Analysis of intracellular oxygenation of isolated adult cardiac myocytes. Am J Physiol. 250: C384-C390.

29. Jones, D.P. (1986). Intracellular diffusion gradients of O_2 and ATP. Am J Physiol. 250: C663-C675.

30. Jones, D.P. (1984). Effect of mitochondrial clustering on O_2 supply in hepatocytes. Am J Physiol. 247: C83-C89.

31. Boag, J.W. (1969). Oxygen diffusion and oxygen depletion problems in radiobiology. Curr Top Radiat Res. 5:141-195.

32. Scopes, J.W. (1966). Metabolic rate and temperature control in the human baby. Br Med Bull. 22: 88-91.

33. Hull, D. (1966). The structure and function of brown adipose tissue. Br Med Bull. 22: 92-96.

34. Heim, T. and Hull, D. (1966). The blood flow and oxygen consumption of brown adipose tissue in the newborn rabbit. J Physiol. 186: 42-55.

35. Dawes, G.S. (1968). In: Foetal and Neonatal Physiology. Chicago, Year Book. p. 195-200

36. Fisher, D.J., Heymann, M.A. and Rudolph, A.M. (1982). Regional myocardial blood flow and oxygen delivery in fetal, newborn and adult sheep. Am J Physiol. 243: H729-H731.

37. Fisher, D.J., Heymann, M.A. and Rudolph, A.M. (1980). Myocardial oxygen and carbohydrate consumption in fetal lambs in utero and in adult sheep. Am J Physiol. 238: H399-H405.

38. Fisher, D.J., Heymann, M.A. and Rudolph, A.M. (1981). Myocardial consumption of oxygen and carbohydrates in newborn sheep. Pediatr Res. 15: 843-846.

39. Nagatomo, T., Hattori, K., Ikeda, M. and Shimada, K. (1980). Lipid composition of sarcolemma, mitochondria and sarcoplasmic reticulum of newborn and adult rabbit cardiac muscle. Biochemical Medicine. 23: 108-118.

40. Mertens-Strijthagen, J., DeSchrijver, C., Wattiaux-DeConinck, S. and Wattiaux, R. (1979). A centrifugation study of rat liver mitochondria, lysosomes and peroxisomes during the perinatal period. Eur J Biochem. 98: 339-352.

41. Tolbert, N.E. (1979). Postnatal development of peroxisomal and mitochondrial enzymes in rat liver. J Cell Physiol. 101: 375-390.

42. Miyahara, M., Kitazoe, Y., Hiraoka, N., Takeda, K., Watanabe, S., Sasaki, J., Okimasu, E., Osaki, Y., Yamamoto, H. and Utsumi, K. (1984). Developmental changes in mitochondrial components in liver of newborn rats. Biol Neonate. 45: 129-141.

43. Wispe, J.R., Bell, E.F. and Roberts, R.J. (1985). Assessment of lipid peroxidation in newborn infants and rabbits by measurement of expired ethane and pentane. Influence of parental lipid infusion. Ped Res. 19: 374-379.

44. Yoshioka, T., Motoyama, H., Yamasaki, F. and Noma, J. (1982). Lipid peroxidation and it's protective mechanism during the developmental stage in rat. Acta Obst Gynaec JPN. 34(7): 966-970.

45. Kellogg, E.W. and Fridovich, I. (1975). Superoxide, hydrogen peroxide and singlet oxygen in lipid peroxidation by a xanthine oxidase system. J Biol Chem. 250: 8812-8817.

46. Kellogg, E.W. and Fridovich, I. (1977). Liposome oxidation and erythrocyte lysis by enzymatically generated superoxide and hydrogen peroxide. J Biol Chem. 252: 6721-6728.

47. Thomas, M.J., Mehl, K.S. and Pryor, W.A. (1978). The role of superoxide anion in the xanthine oxidase induced autoxidation of linoleic acid. Biochem Biophys Res Comm. 83: 927-932.

48. Beatrice, M.C., Stiers, D.L. and Pfeiffer, D.R. (1984). The role of glutathione in retention of Ca^{2+} by liver mitochondria. J Biol Chem. 259: 1279-1287.

49. Au, A.M., Chan, P.H. and Fishman, R.A. (1985). Stimulation of

phospholipase A_2 activity by oxygen derived free radicals in isolated brain capillaries. J Cell Biochem. 27: 449-453.

50. Yoshioka, T., Shimada, T. and Sekiba, K. (1980). Lipid peroxidation and antioxidants in the rat lung during development. Biol Neonate. 38: 161-168.

51. Gerdin, E., Tyden, O. and Eriksson, U,J. (1985). The development of antioxidant defense in the perinatal rat lung: Activities of superoxide dismutase, glutathione peroxidase and catalase. Ped Res. 19: 687-691.

52. Mavelli, I., Autuori, F., Dini, L., Spinedi, A. Ciriolo, M.R., Rotilio, G. (1981). Correlation between superoxide dismutase, glutathione peroxidase and catalase in isolated rat hepatocytes during fetal development. Biochem Biophys Res Comm. 102: 911-916.

53. Frank, L., Bucher, J.R. and Roberts, J.R. (1978). Oxygen toxicity in neonatal and adult animals of various species. J Appl Physiol. 45: 699-704.

54. Frank, L. and Groseclose, E.E. (1984). Preparation for birth in an O_2-rich environment: The antioxidant enzymes in the developing rabbit lung. Ped Res. 18: 240-244.

55. Boveris, A. (1977). Mitochondrial production of superoxide anion and hydrogen peroxide In: Oxygen and Physiological Function (F.F. Jobsis, ed.). Professional Information Library. p. 67-82.

56. Mavelli, I., Rigo, A., Federico, R., Ciriolo, M.R. and Rotolio, G. (1982). Superoxide dismutase, glutathione peroxidase and catalase in the developing rat brain. Biochem J. 204: 535-540.

57. Sies, H. and Moss, K.M. (1978). A role of mitochondrial

glutathione peroxidase in modulating mitochondrial oxidation in liver. Eur J Biochem. 84: 377-383.

58. Tsen, C.C. and Tappel, A.L. (1958). Catalytic oxidation of glutathione and other sulfhydryl compounds by selenite. J Biol Chem. 233: 1230-1232.

59. Bunce, G.E., Hess, J.L. and Batra, R. (1984). Lens calcium and selenite-induced cataract. Curr Eye Res. 3: 315-320.

60. Ostadalova, I., Babicky, A. and Obenberger, J. (1979). Cataractogenic and lethal effect of selenite in rats during postnatal ontogenesis. Physiol Bohemoslov. 283: 393-397.

61. Sosenko, I.R.S. and Frank, L. (1987). Guinea pig lung development: Antioxidant enzymes and premature survival in high O_2. Am J Physiol. 252: R693-R698.

62. Parish, M.D., Payne, A. and Fixler, D.E. (1987). Global myocardial ischemia in the newborn, juvenile and adult isolated isovolumic rabbit heart. Circ Res. 61:609-615.

63. Chu-Jeng Chiu, R. and Bindon, W. (1987). Why are newborn hearts vulnerable to global ischemia? Circulation. 76(Suppl V):V146-V149.

64. Young, H.H., Shimizu, T., Nishioka, K., Nakanishi, T. and Jarmakani, J.M. (1983). Effect of hypoxia and reoxygenation on mitochondrial function in the neonatal myocardium. Am J Physiol. 245: H998-H1006.

65. Grice, W.N., Konish, T. and Apstein, C.S. (1987). Resistance of the neonatal myocardium to injury during normothermic and hypothermic ischemic arrest and reperfusion. Circulation. 76(Suppl V):V150-V155.

Molecular Pharmacology 31: 643-646, 1987

SELENITE-INDUCED NAD(P)H OXIDATION AND CALCIUM RELEASE IN ISOLATED MITOCHONDRIA: RELATIONSHIP TO IN VIVO TOXICITY

by

Angelo A. Vlessis and Leena Mela-Riker, M.D.

Oregon Health Sciences University

Departments of Surgery and Biochemistry

Portland, Oregon 97201

ABSTRACT

The effects of selenite on the mitochondrial NAD(P)H/NAD(P)$^+$ ratio and calcium pool are described. Small quantities of selenite can (1) oxidize mitochondrial NAD(P)H and (2) induce calcium release from isolated mitochondria. Reduced NAD(P)H within intact mitochondria was monitored kinetically using the wavelength pair, 340-375 nm. NAD(P)H oxidation rates at various concentrations of selenite were calculated. Mitochondria from older animals can oxidize NAD(P)H faster than those of younger animals; maximum selenite-induced oxidation rates correlate well with age of the animal in both kidney (r=.920) and liver (r=.839) mitochondria, the oxidation rates in the adult (liver 15.4, kidney 34.8 nmoles/min/mg protein) being 3-5 times the rates in 1-2 day old newborn (liver 2.8, kidney 10.3 nmoles/min/mg protein). Calcium fluxes within mitochondrial suspensions were monitored kinetically using the calcium indicator, Arsenazo III, and the wavelength pair, 660-685 nm. Susceptibility to selenite-induced calcium release is age dependent; the mitochondria of older animals being more susceptible. Incubation time required to induce calcium release was 77±30 sec in the adult compared to 406±25 sec at the age of 0-4 days in the newborn. The bimodal toxic manifestations of selenite in vivo are discussed in view of the age dependent differences in selenite metabolism at the cellular level.

INTRODUCTION

The cellular metabolism of selenite has been extensively studied. As illustrated by the diagram in Figure 1 [1-7], selenite is reduced spontaneously by glutathione (GSH) and other sulfhydryl compounds in the cell [1, 2]. Oxidized sulfhydryl groups are reduced at the expense of NAD(P)H via GSSG reductase [2, 3, 4]. GSSG reductase can catalyze reactions II and III as well as the reduction of GSSG [4, 5]. Large quantities of cellular NAD(P)H may be consumed when metabolites of selenite enter redox cycles. Once formed, selenide, a very toxic metabolite [8], is methylated under physiological conditions to the non-toxic, volatile dimethyl selenide which is excreted through the lungs [5, 9, 10].

Curiously, the toxic manifestations of selenite in whole animals are dependent on age. Subcutaneous aqueous injection of 20 μmoles selenite/kg body weight in newborn rats causes bilateral nuclear cataracts within 3-4 days without any other toxic effects [11]. When rats are injected after 15 days of age, the frequency of cataract formation falls rapidly while mortality rate increases. Mortality approaches 100% at the adult age of 50 days [12]. The underlying mechanism for selenite toxicity and cataractogenesis are unknown.

Cellular calcium homeostasis can be profoundly affected by selenite-oxidized sulfhydryl compounds. In most mammalian cells, intracellular free calcium concentrations are controlled by several transport mechanisms which exist in the endoplasmic reticulum, mitochondrial and plasma membranes. Oxidation of GSH releases calcium from endoplasmic reticulum of isolated hepatocytes [13, 14]. Lehninger

and others [15, 16, 17] have demonstrated that decreases in the mitochondrial NAD(P)H/NAD(P)$^+$ ratio can elicit release of mitochondrial calcium. Since selenite can both (1) oxidize GSH and (2) deplete NAD(P)H via redox cycling, it probably has profound effects on cellular calcium homeostasis.

This paper describes experiments conducted to assess the effects of selenite on the mitochondrial calcium pool. Evidence is provided to show that: (1) mitochondrial NAD(P)H is oxidized in the presence of small quantities of selenite, (2) selenite causes calcium release from liver mitochondria and (3) the rates of selenite induced NAD(P)H oxidation and calcium release differ between the newborn and the adult.

MATERIALS AND METHODS

Topeka guinea pigs were used as experimental animals. Guinea pigs were chosen since the size of newborn animals is sufficient to allow isolation of mitochondrial preparations from one animal at a time. Adult animals were over 40 days of age. All animals were maintained on ad lib guinea pig chow and water. Newborns were kept with their mothers and allowed to nurse until the time of sacrifice.

Liver and kidney mitochondria were chosen as objects of the study because of the important role of these organs in glutathione metabolism [18, 19]. Mitochondria were isolated according to the methods of Widener and Mela-Riker [20]. Protein content of isolated mitochondria was determined according to Lowry, et al [21] .

NAD(P)H oxidation and calcium measurements were made kinetically using a Hitachi 557 dual wavelength spectrophotometer. NAD(P)H/NAD(P)$^+$

redox changes of the mitochondrial suspensions were monitored at 340-375 nm. Calcium uptake and release from mitochondria were monitored kinetically with the calcium indicator, Arzenazo III (50 μM) [22] using the wavelength pair 660-685 nm as described by Lehninger [15]. Calcium was added as calcium chloride. Mitochondria for both determinations were suspended in a medium containing 65 mM KCl, 125 mM sucrose, 8 mM Tris-Cl, 0.2 mM Tris-P04, 5 mM $MgCl_2$, 5 μM rotenone and 2 mM succinate at pH 7.2.

Respiratory activities of mitochondrial suspensions in State 3 and State 4 were determined using a Clark oxygen electrode (5 mM succinate, 1 mM ADP). Respiratory control ratios greater than 10 were obtained in all preparations.

RESULTS

The rate of NAD(P)H oxidation was determined at various concentrations of selenite in liver and kidney mitochondria isolated from animals of different ages. Isolated mitochondria were suspended in the medium described above at 1.7 - 2.3 mg protein/ml. Reduced NAD(P)H was monitored kinetically. Rotenone, a site I inhibitor present in the medium, prevents entry of electrons from NAD(P)H into the respiratory chain while allowing ATP synthesis via succinate and $FADH_2$. Examples of tracings obtained from 3.5 day old and adult liver mitochondria (both at 1.75 mg protein/ml) are shown superimposed in Figure 2. NAD(P)H oxidation was initiated by an addition of 10 μM selenite. The rate of mitochondrial NAD(P)H oxidation is more rapid in the adult than in the newborn. Similar results were obtained with kidney mitochondria (data not shown). The total amount of NAD(P)H oxidized by 10 nmoles of

selenite was calculated from the change in absorbance at 340 nm. Further calculation shows that 2.5-3.2 nmoles NAD(P)H are oxidized per nmole selenite which agrees well with the stoichiometry of selenite reduction shown in Figure 1.

The rates of NAD(P)H oxidation were plotted as a function of selenite concentrations for each animal after standardization as nmoles NAD(P)H per min per mg of mitochondrial protein. Figure 3 depicts titration curves constructed using liver mitochondria from animals of different ages. As the selenite concentration increases, the rate of NAD(P)H oxidation in all animals initially increases rapidly and then plateaus at about 300 μM selenite.

The maximal rates of NAD(P)H oxidation (at 500 μM selenite) in both liver and kidney mitochondria were plotted as a function of the age of the animal and are shown in Figure 4. The maximal rate of NAD(P)H oxidation in liver mitochondria at 500 μM selenite increases from 2.8 (nmoles/mg protein x minute) in the 1.5 day old to 15.4 in the adult; a 5.5 fold increase. The maximal rate of NAD(P)H oxidation in kidney mitochondria similarly increased from 10.3 in the 1.5 day old to 34.8 in the adult; a 3.4 fold increase.

Results from calcium uptake and release experiments using liver mitochondria from animals at different ages are displayed in Figures 5 and 6 and Table I. The medium contained reducing equivalents in the form of succinate (2 mM) in the presence of 5 μM rotenone. Calcium release was induced by selenite after preloading the mitochondria with 5-70 μM calcium. Mitochondria from the younger animals (Fig. 5 and Table I) were less susceptible to selenite-induced calcium release than

the mitochondria from the older animals (Fig. 6 and Table I). The preloading dose of calcium had no effect on this age dependent calcium release (data not shown).

Similar calcium uptake and release experiments were done using pyruvate (2 mM) and malate (0.7 mM) as substrates in the absence of rotenone. Calcium responses of liver mitochondria from 1.5, 2.75 and 6.5 day old animals showed similar age dependencies. Specifically, mitochondria from the 1.5 day old retained calcium in the presence of 500 μM selenite for longer than 8 minutes. In the presence of 50 μM selenite, mitochondria from 2.75 and 6.5 day old animals began releasing calcium after 2-2.5 minutes and 40-60 seconds respectively. Susceptibility to selenite-induced calcium release from liver mitochondria shows an age dependency, the older animals being more susceptible.

The effect of selenite on the integrity of the mitochondrial inner membrane was assessed by measuring State 3 respiratory rates (nmoles O_2 consumed/mg protein/min) in the presence and absence of selenite (500 μM) using succinate (5 mM) with rotenone (5 μM) as substrate. Maximum State 3 respiratory rates with selenite (49.4 $\pm$ 0.74) are reduced by only 10.7% when compared to control values (55.3 $\pm$ 1.06). The small reduction in respiratory rate may be explained by incomplete rotenone block (5 μM) allowing reversed electron flow to NAD(P)H.

DISCUSSION

Small quantities of selenite can oxidize liver and kidney mitochondrial NAD(P)H (Figure 2) resulting in the release of mitochondrial calcium. In adult liver mitochondria, the rate of NAD(P)H

oxidation in the presence of just 10 μM selenite is approximately 2.5-3.2 nmoles NAD(P)H per nmole selenite (per mg protein x minute). Similarly, small quantities of selenite can cause calcium release from the liver mitochondria of older animals (Figure 5 and Table I). Calcium release is known to occur in response to decreases in the NAD(P)H/NAD(P)$^+$ ratio induced by normal metabolites [15, 16, 17]. Selenite-induced oxidation of NAD(P)H is most likely responsible for the calcium release observed in the isolated liver mitochondria depicted in Figures 5 and 6 and Table I. Selenite concentrations which induce calcium release do not significantly impair respiration. Therefore, calcium release cannot be explained by generalized membrane damage.

Age dependent differences in the NAD(P)H oxidation rates of liver and kidney mitochondria may help explain the bimodal toxic manifestations of selenite. As described above, the cataractogenic effect of selenite is seen only in newborns less than 15 days of age. After 15 days, the same dose becomes non-cataractogenic and increasingly lethal [12]. Mortality in the adult may be explained by two mechanisms. First, the rapid reduction of selenite by adult mitochondria favors the complete 3-step reduction of selenite to selenide. Selenide, once formed, is very toxic [8] and methylation pathways become an important means of detoxification [5, 10]. Second, cellular calcium homeostasis can be altered by NAD(P)H consuming redox cycles [15, 16, 17] and GSSG [13, 14] leading to cell dysfunction and death [23]. Conversely, newborn liver and kidney mitochondria have a decreased capacity to reduce selenite, therefore, the formation of

toxic selenide is predictably much lower than that of the adult. Seemingly, a smaller percentage of the selenite dose becomes detoxified (i.e. methylated) by the newborn liver and kidney per unit time, and plasma selenite concentrations remain elevated for longer periods. Subsequently other sulfhydryl rich areas of the body which receive a small portion of the cardiac output, like the eye, gain the opportunity to sequester plasma selenite. In support of this hypothesis, Babicky et al [24] have recently shown that newborn rat lenses contain almost 500 times more radioselenium than adult lenses (per unit weight) at 2 hours after a subcutaneous injection of 30 μmoles selenite/kg body weight. Bunce et al [11] and Shearer and David [25] also emphasized the role of Ca^{2+} dyshomeostasis in selenium-induced cataracts. No previous evidence has been presented on the possible role of mitochondria in this response, although, selenite-induced alterations of glutathione metabolism in the lens have been confirmed [26, 27].

In summary, selenite-induced NAD(P)H oxidation rates of liver and kidney mitochondria at different ages are reported and correlated to the age-dependent susceptibility of selenite-induced mitochondrial calcium release. A possible mechanism for the observed increase in lens selenium of the newborn and the increased lethality in the adult is proposed.

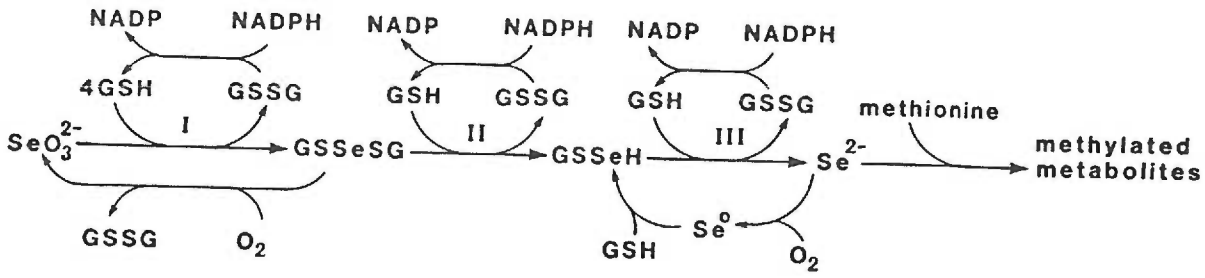

FIGURE 1. The metabolism of selenite (SeO_3^{2-}).

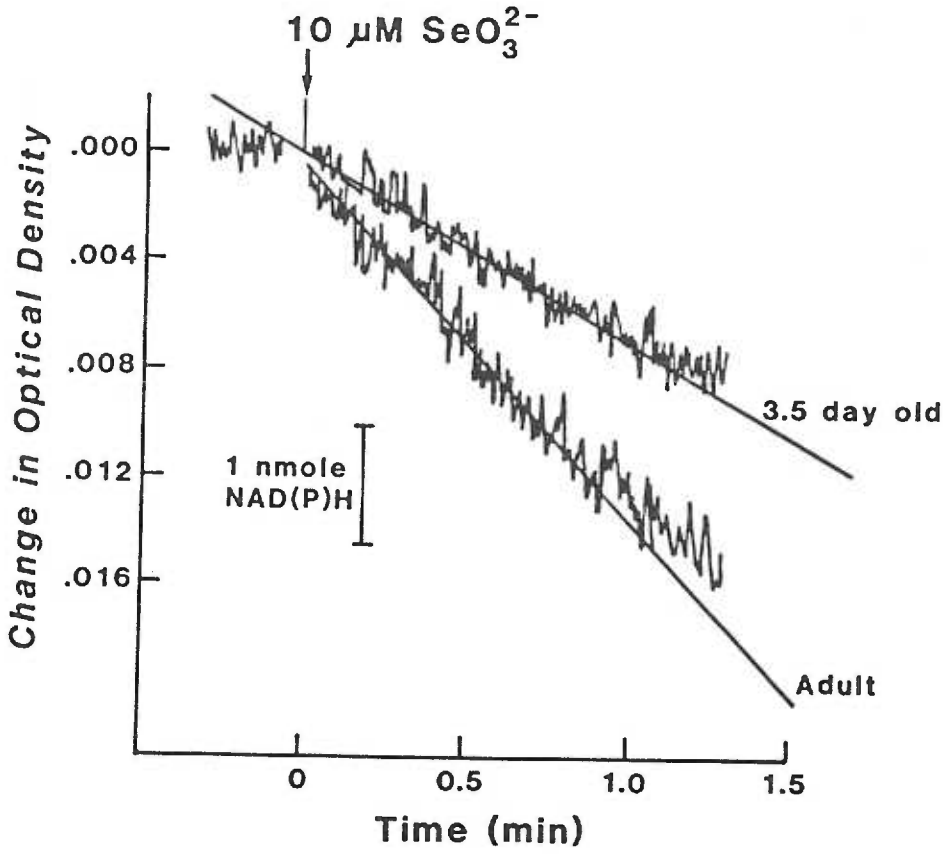

FIGURE 2. Selenite-induced oxidation of endogenous mitochondrial NAD(P)H. Tracings show the oxidation of NAD(P)H in isolated liver mitochondria following the addition of selenite. Tracings from 3.5 day old and adult are superimposed (both cuvettes contained 1.75 mg mitochondrial protein/ml).

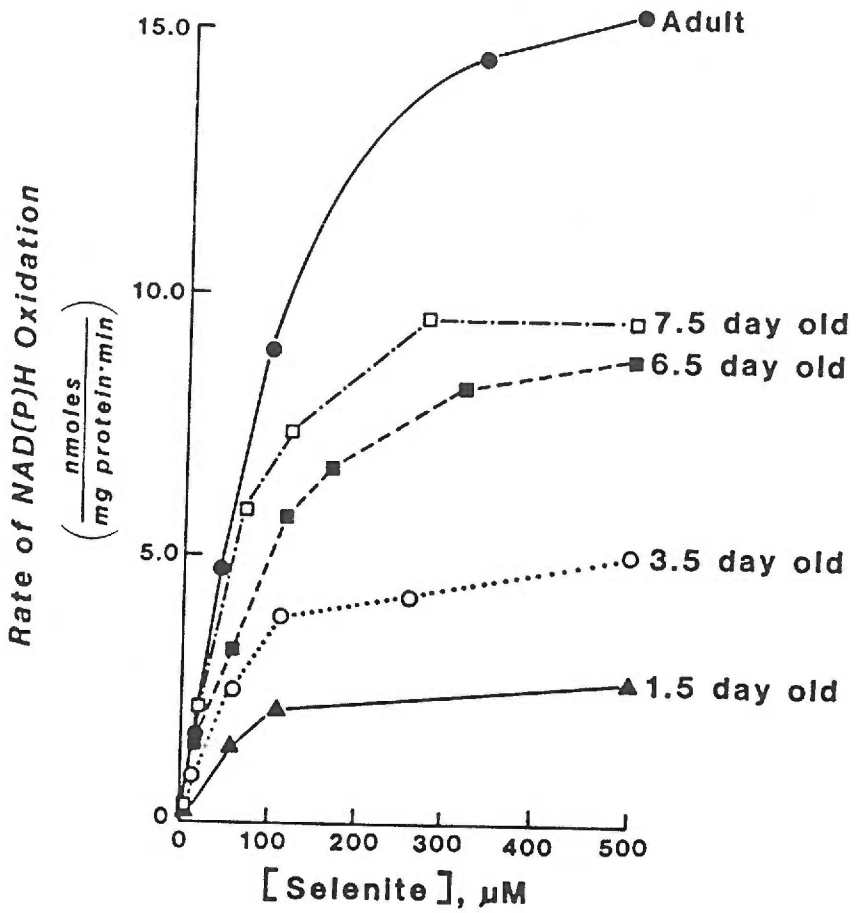

FIGURE 3. NAD(P)H oxidation rate in isolated liver mitochondria versus selenite concentration from animals of different ages. As the age of the animal increases, the maximum rate at which NAD(P)H is oxidized also increases. All rates are standardized per milligram of mitochondrial protein.

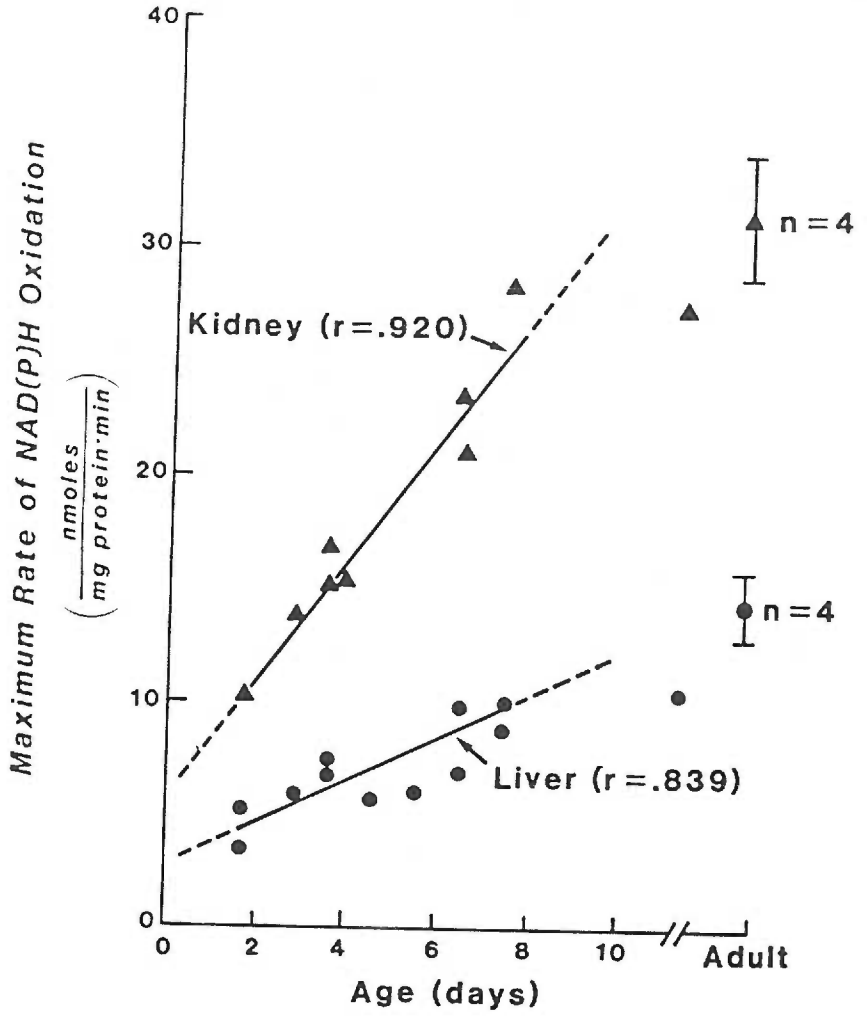

FIGURE 4. Maximum rate of selenite-induced NAD(P)H oxidation in isolated liver and kidney mitochondria versus postnatal age. Each symbol depicts the maximum rate obtained from a single animal. Adult rates are expressed as means ± one standard deviation.

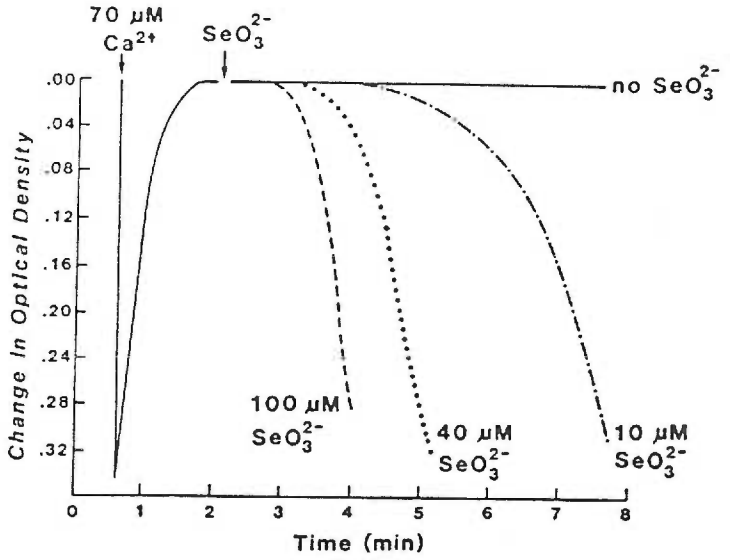

FIGURE 5. Selenite-induced release of calcium from the isolated liver mitochondria of a 7.5 day old animal. Ca^{2+} (70μM) is added to cuvettes containing 1.25 mg mitochondrial protein/ml. Once Ca^{2+} uptake by the mitochondria is complete, selenite is added. Four tracings are shown superimposed which demonstrate the Ca^{2+} -releasing effect of various concentrations of selenite.

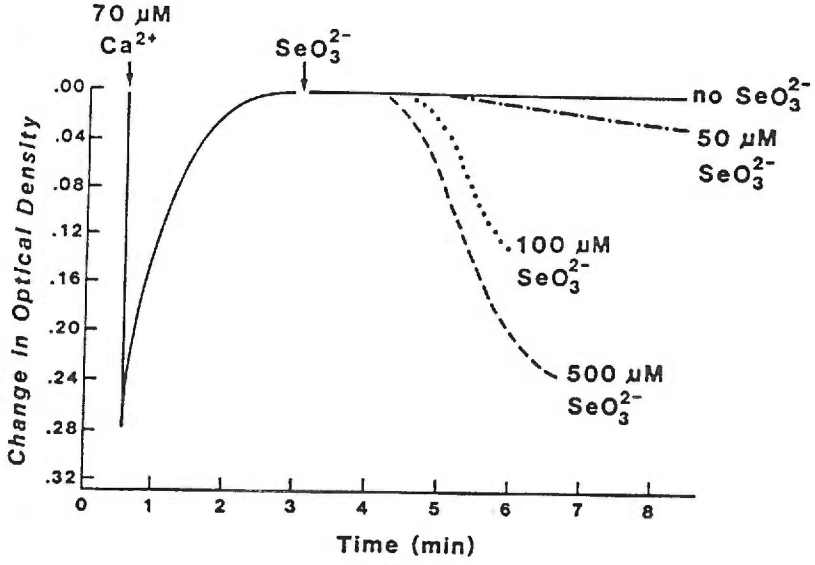

FIGURE 6. Selenite induced release of calcium from the isolated liver mitochondria of a 4.5 day old animal. Four tracings are shown superimposed. Ca^{2+} (70μM) is added to cuvettes containing 1.05 mg mitochondrial protein/ml. Compare with Figure 5 (7.5 day old). The 4.5 day old liver mitochondria are less susceptible to selenite induced Ca^{2+}-release.

Age (days)	Time (sec)
BIRTH - 4	406 ± 25
4 - 6	193 ± 36
6 - 12	75 ± 12
ADULT	77 ± 30

TABLE 1. Age-dependent changes in selenite-induced calcium release from isolated liver mitochondria. Mitochondria were incubated under conditions similar to those described for Figures 5. The time period between the addition of 500 μM selenite and the initiation of calcium release was recorded and standardized for micromoles selenite per milligram mitochondrial protein. Data are presented as mean ± standard deviation (n = a minimum of 3 in each group). Isolated mitochondria from the older animals are more susceptible to selenite-induced calcium release.

REFERENCES

1. Painter, E.P. The chemistry and toxicity of selenium compounds with special reference to the selenium problem. Chem Reviews 28:179-213 (1941).

2. Tsen, C.C. and Tappel, A.L. Catalytic oxidation of glutathione and other sulfhydryl compounds by selenite. J. Biol Chem 233:1230-1232 (1958).

3. Ganther, H.E. Selenotrisulfides. Formation by the reaction of thiols with selenious acid. Biochemistry. 7:2898-2905 (1968).

4. Ganther, H.E. Reduction of selenotrisulfide derivative of glutathione to a persulfide analog by glutathione reductase. Biochemistry. 10:4089-4098 (1971).

5. Hsieh, H.S. and Ganther, H.E. Acid-volatile selenium formation catalyzed by glutathione reductase. Biochemistry. 14:1632-1636 (1975).

6. Anundi, I., Stahl, A. and Hogberg, J. Effects of selenite on O_2 consumption, glutathione oxidation and NAD(P)H levels in isolated hepatocytes and the role of redox changes in selenite toxicity. Chem Biol Interaction 50:277-288 (1984).

7. Combs, G.F. and Combs, S.B. The nutritional biochemistry of selenium. Ann Rev Nutr 4:257-280 (1984).

8. Ganther, H.E. Metabolism of hydrogen selenide and methylated selenides. Adv Nutr Res 2:107-128 (1979).

9. Ganther, H.E. Enzyme synthesis of dimethyl selenide from sodium selenite in mouse liver extracts. Biochemistry.

5:1089-1098 (1966).

10. Stahl, A., Anundi, H. and Hogberg, J. Selenite biotransformation to volatile metabolites in an isolated hepatocyte model system. Biochem Pharmacol 32:1111-1117 (1984).

11. Bunce, G.E., Hess, J.L. and Batra, R. Lens calcium and selenite-induced cataract. Curr Eye Res 3:315-320 (1984).

12. Ostadalova, I., Babicky, A., and Obenberger, J. Cataractogenic and lethal effect of selenite in rats during postnatal ontogenesis. Physiologia Bohemoslovaca. 283:393-397 (1979).

13. Bellomo, G., Jewell, S.A., Thor, H. and Orrenius, S. Regulation of intracellular calcium compartmentation: Studies with isolated hepatocytes and t-butyl hydroperoxide. Proc Natl Acad Sci USA 79:6842-6846 (1982).

14. Jones, D.P., Thor, H., Smith, M.T., Jewell, S.A. and Orrenius, S. Inhibition of ATP-dependent microsomal Ca^{2+} sequestration during oxidative stress and its prevention by glutathione. J Biol Chem 258(10):6390-6393 (1983).

15. Lehninger, A.L., Vercesi, A. and Bababunmi, E.A. Regulation of Ca^{2+} release from mitochondria by oxidation-reduction state of pyridine nucleotides. Proc Natl Acad Sci USA 75(4):1690-1694 (1978).

16. Nicholls, D.G. and Brand, M.D. The nature of the calcium ion efflux induced in rat liver mitochondria by the oxidation of endogenous nicotinamide nucleotides. Biochem J 188:113-118 (1980).

17. Fiskum, G and Lehninger, A.L. Mitochondrial regulation of

intracellular calcium, in Calcium and Cell Function Vol II (Wai Yiu Cheung, ed.). Academic Press, Inc., New York, N.Y., 39-80 (1982).

18. Larrson, A., Orrenius, S., Holmgren, A. and Mannervik, B., eds. Functions of Glutathione: Biochemical, Physiological, Toxicological and Clinical Aspects. Raven Press, New York, N.Y. (1983).

19. Meister, A. and Anderson, M. E. Glutathione. Ann Rev Biochem 2:711-760 (1983).

20. Widener, L.L. and Mela-Riker, L.M. Verapamil pretreatment preserves mitochondrial function and tissue magnesium in the ischemic kidney. Circ Shock 13:27-37 (1984).

21. Lowry, O.H., Rosebrough, N.J., Farr, A.L. and Randall, R.J. Protein measurement with Folin phenol reagent. J Biol Chem 193:265-275 (1951).

22. Kendrick, N.C., Ratzlaff, R.W. and Blaustein, M.P. Arsenazo III as an indicator for ionized calcium in physiological salt solutions: Its use for determination of the CaATP dissociation constant. Anal Biochem 83:433-450 (1977).

23. Hu, M. and Spallholz, J.E. In vitro hemolysis of rat erythrocytes by selenium compounds. Biochem Pharmacol 32:957-961 (1983).

24. Babicky, A., Rychter, Z., Kopoldova, J. and Ostadalova, I. Age dependence of selenite uptake in rat lenses. Exp Eye Res 40:101-103 (1985).

25. Shearer, T.R. and David, L.L. Role of calcium in selenium

cataract. Curr Eye Res 2:777-784 (1982-1983).

26. Bunce, G.E. and Hess, J.L. Biochemical changes associated with selenite-induced cataract in the rat. Exp Eye Res 33:505-514 (1981).

27. David, L.L. and Shearer, T.R. State of sulfhydryl in selenite cataract. Toxicol Appl Pharmacol. 74:109-115 (1984).

To be submitted to Pediatric Research.

I. PERINATAL DEVELOPMENT OF THE MITOCHONDRIAL RESPIRATORY CHAIN AND OXIDATIVE PHOSPHORYLATION

by

Angelo A. Vlessis and Leena Mela-Riker

Departments of Surgery and Biochemistry

Oregon Health Sciences University

Portland, Oregon USA

ABSTRACT

The perinatal development of the mitochondrial respiratory chain and oxidative phosphorylation in guinea pig heart, kidney and liver are described. In all three tissues, mitochondrial cytochrome oxidase (127-160%) and ubiquinone concentration (160-290%) increased from the late fetal to adult period. Changes in cytochromes b and c showed variable tissue and age specific differences. State 3 respiration increased after birth in all tissues with most substrates tested, however, pyruvate-driven respiration in heart and kidney declined 60-65% from fetal values by 2-4 days of age. At all ages studied, succinate-driven state 3 respiration in liver and kidney far exceeded that of the other substrates while rates in heart remained low at all times. Liver mitochondrial adenine ribonucleotides increased transiently to 128% of fetal values immediately following birth. No change in heart or kidney adenine ribonucleotides were detected during the newborn period, however, levels in adult heart were 151-157% of fetal and newborn values. The mitochondrial pyridine nucleotide pool of kidney initially declined to 84% of fetal values then rose to 168% of fetal values by the adult period. In contrast, pyridine nucleotide levels in heart and liver mitochondria remained unchanged during the fetal and newborn period while adult values were 120% and 88% of newborn values in heart and liver respectively. In all 3 tissues, the inner mitochondrial membrane phase transition temperature (T_t) increased transiently during the newborn period. The rise in T_t is associated with a decrease in the energy of activation for succinate oxidation. The results are discussed in terms of the variable roles of

these 3 tissues in whole body metabolism as well as other known biochemical/hormonal changes associated with birth.

INTRODUCTION

Mammalian birth is accompanied by alterations in the circulation, O_2 availability and metabolism of the organism. The placental O_2 and nutrient supply is abandoned in exchange for pulmonary and splanchnic circulations. Systemic arterial O_2 tension (P_aO_2) rises as the switch to a more aerobic metabolism is initiated (1,2,51,52). The ability of the fetus to orchestrate its adaptation to extrauterine life has fascinated scientists for many years. Recently, interest in normal perinatal development has intensified as our ability to sustain the very premature infant has increased.

The multitude of changes which occur following birth make the study of metabolism during this period both a complex and intriguing enterprise. Following birth, the rise in systemic P_aO_2 stimulates mitochondrial biogenesis (3,4). Respiratory chain cytochrome concentrations also increase in whole tissue homogenates (5,6) as well as in mitochondrial fractions (7,8). Cytosolic (9,10) and mitochondrial (9,11) antioxidant defense systems develop. Rates of lipolysis, gluconeogenesis and glycogenolysis accelerate to compensate for the loss of the placental nutrient supply (12,13). The post-birth rise in serum catecholamines and glucagon alter the activity of the dehydrogenases as well as the glycogenic and gluconeogenic enzymes thereby regulating the flux of ketones, fatty acids, glucose, and amino acids to and from energy production (12,14-16). Transient neonatal

hyperiodothyroxinemia probably has a yet unrecognized effect on metabolism (17). Gastrointestinal enzyme and hormone secretion matures to accommodate the new source of fuel for growth, development and maintenance of life (18). All these factors coalesce to make the transition from intra- to extrauterine life possible. A knowledge of the normal developmental changes in cellular metabolism during perinatal adaptation may lead to a better understanding of the metabolic complications associated with prematurity and other perinatal diseases.

Since mitochondria play a central role in cellular energy metabolism, many studies have focused on elucidating sites of developmental change within this organelle during the perinatal period. The results are complicated by interspecies and tissue specific differences which reflect variations in ontology and fetal maturation at birth as well as the variable roles of different tissues in whole body metabolism. Although earlier studies employed whole tissue homogenates, more recent studies have employed isolated mitochondria. The intact, isolated mitochondrion can be used to study the enzymatic machinery as an integrated unit under various simulated cellular conditions. Also, many hormonally induced changes are retained when mitochondria are isolated from their native cellular mileau (19). Although our understanding of metabolism has advanced over the years, much remains to be learned from the study of isolated mitochondria during the perinatal period.

Previous studies by Mela, et al (8,20,21) reveal an interesting phenomenon. They document a precipitous decline in the state 3 respiratory rate of isolated puppy heart and guinea pig brain

mitochondria immediately following birth. These changes are believed to be secondary to the rise in systemic P_aO_2 since (a) the decrease in maximum state 3 respiration correlates well with the increase in P_aO_2 and (b) the effect can be reversed, i.e., maximum state 3 respiration increases when P_aO_2 is reduced in adult animals (8,20-23). Our objective was to determine if the decrease in respiratory activity is a phenomenon which exists in other tissues and is independent of substrate type (keto-, lipo- or glucogenic). In order to achieve this, the normal perinatal development of mitochondrial oxidative metabolism in guinea pig heart, kidney and liver was characterized. Specifically, changes in the mitochondrial respiratory chain components (i.e., ubiquinone and cytochrome b, c and oxidase), pyridine and adenine nucleotide pools and substrate oxidation rates are described during perinatal development. Also, alterations in inner mitochondrial membrane fluidity and the energy of activation for succinate oxidation are presented. The results are discussed in relation to the variable roles of these three tissues in whole body metabolism and changes in mitochondrial antioxidant metabolism which have been shown to modulate mitochondrial oxidative processes in vitro (24).

MATERIALS AND METHODS

Animals. Topeka guinea pigs, bred and housed at this institution, were used as experimental animals. Guinea pigs were chosen since the size of the newborn allows isolation of adequate quantities of heart, kidney and liver mitochondria from a single animal. Term fetuses were obtained by cesarean section 63 days (full gestation) following a one

week breeding period. Newborn animals in which the time of birth could not be accurately recorded (± 3 hours) were not used. All animals were maintained on ad libitum guinea pig chow and water. Newborns were kept with their mothers and allowed to nurse until the time of sacrifice.

Mitochondrial Preparations. Mitochondria were isolated according to the methods of Mela et al (8). Unanesthetized animals were sacrificed by decapitation and the tissue(s) of interest immediately removed and minced in ice cold MSE (150 mM mannitol, 130 mM sucrose, 1 mM EGTA). The minced sample was washed several times with cold MSE and then homogenized gently at 4°C with a Potter-Elvehjem homogenizing vessel. The homogenate was centrifuged at 480g to remove the large debris. Mitochondria were pelleted from the supernatant by centrifugation at 7700g. The pellet was washed twice with cold MS (150 mM mannitol, 130 mM sucrose) and resuspended in cold MS and kept on ice at all times. This suspension was analyzed for protein (25) and used to make the various determinations described below. All solutions were made with deionized/quartz distilled water.

Ubiquinone Assay. Mitochondrial suspensions were analyzed for ubiquinone using a modification of previously described methods (26,27). Samples were prepared in glass centrifuge tubes wrapped with aluminum foil to minimize light exposure. Isolated mitochondria were suspended in 1 ml of 120 mM KCl, 20 mM tris-Cl, 5% potassium hexacyanoferrate (III) and 0.1 M lauryl sulfate (pH 7.4) and vortexed for 30 seconds. Heptane and methanol (1 ml each) were added. The mixture was then vortexed vigorously for 2 minutes and centrifuged at 1000g for 2 minutes. 100-300 μl of the ubiquinone containing heptane layer was

drawn off the top of the solution for analysis.

Ubiquinone was quantitated by HPLC using a Resolve C_{18-5} column. The sample solution (15-30 μl) was loaded onto the column using 100% methanol and a flow rate of 1.2 ml/min. Over the first 5 minutes, the mobile phase was changed linearly to 25% heptane/75% methanol. Ubiquinone was detected at 275 nm as it eluted from the column. Standard curves were constructed using known quantities of Coenzyme Q_{10}. Quantitation was based on peak area.

The HPLC system consisted of a Waters 600 Multisolvent Delivery System and Waters 490 Programable Multiwavelength Detector. All injections were made using a Waters 712 Wisp equipped with a sample cooling unit held at minus 10°C. Data acquisition and analysis was performed using a Waters System Interface Module and an IBM-AT computer equipped with Waters 820 Chromatography software.

Mitochondrial Respiration. Maximum respiratory rates (nmoles O_2 consumed/min/mg protein) were determined by conventional methods using a Clark O_2 electrode. Mitochondria were suspended in a glass, water jacketed O_2 electrode chamber with 120 mM KCl, 10 mM tris-Cl and 10 mM tris-PO_4 at pH 7.4. The temperature was held at 25°C by circulating water from a bath through the water jacketed cell. O_2 consumption was monitored as a function of time and recorded onto chart paper. State 3 and state 4 respiratory rates were calculated following substrate and 1 mM ADP addition respectively. The following substrates were used: glutamate (5 mM)-malate (2 mM), pyruvate (5 mM)-malate (2 mM), β-hydroxybutyrate (6 mM)-malate (2 mM), palmitylcarnitine (20 μM)-malate (2 mM) and succinate (5 mM)-rotenone (5 μM). Respiratory control

ratios for all heart and kidney preparations were greater than 10; those of the liver were greater than 6.

Cytochrome Measurements. Cytochrome concentrations in isolated mitochondria were determined using a Hitachi 557 dual wavelength spectrophotometer (28). Using the oxidized (with 10 μM rotenone) minus the reduced (with succinate, $Na_2S_2O_4$) difference spectrum, the cytochrome concentrations were calculated from the following extinction coefficients: $E_{445-460}$ $a(a_3)$ = 164 mM^{-1} cm^{-1}, $E_{605-630}$ $a(a_3)$ = 26 mM^{-1} cm^{-1}, $E_{560-575}$ b = 24 mM^{-1} cm^{-1} and $E_{550-540}$ c = 20 mM^{-1} cm^{-1}. Cytochrome oxidase concentrations were obtained by averaging the values calculated from the spectrum at 445-460 nm and 605-630 nm.

Phase Transition Temperatures. The phase transition temperatures (T_t) of the inner mitochondrial membrane was determined via Arrhenius plots of succinate driven respiration (29,30). Heart, kidney and liver mitochondria from animals of various ages were isolated as described above. Maximum state 3 respiratory rates (5 mM succinate, 5 μM rotenone, 1 mM ADP) were determined between 8-40^{o}C. Arrhenius plots (log state 3 rate vs. 1/temperature (^{o}K)) were constructed by computer. Best fit lines were calculated according to the least squares prediction equation. T_t and the energy of activation above T_t were calculated from the intercept and the slope of the least squares lines, respectively (see Appendix A for additional details).

Statistical Analysis. Animals were grouped according to age and the results of the fetal and adult groups were compared individually with all other groups by one-way analysis of variance (ANOVA). Significant differences were confirmed using Dunnett's test. Additional

information is provided in the Results and figure legends.

RESULTS

Cytochrome Concentrations. Cytochrome concentrations were determined in heart, kidney and liver mitochondria isolated from animals of various ages. The levels of cytochrome b, c and oxidase vary with tissue type and perinatal age (Figure 1). Cytochrome b levels in heart and kidney mitochondria from adult animals were comparable to those of fetal animals (Figure 1A). Levels in newborn heart and kidney, however, were 116% and 80% of adult values respectively. Cytochrome b levels in liver mitochondria decreased to 47% of fetal values within 1-2 days of age; adult values remained 60% of fetal values. Cytochrome c levels showed a different trend with values in adult heart and kidney mitochondria 120-123% higher than fetal values (Figure 1B). Liver cytochrome c levels from fetal and adult animals were the same whereas values at 5 days of age were higher than either the fetal or adult values. Mitochondria from all tissues studied showed a significant increase in cytochrome oxidase content following birth (Figure 1C). Cytochrome oxidase levels in the adult heart, kidney and liver mitochondria were 127%, 148% and 160% of fetal values respectively. All cytochrome concentrations were consistently higher in the heart as compared to kidney or liver, possibly reflecting the high demand for aerobic metabolism in this tissue.

Ubiquinone Concentrations. Ubiquinone levels were also determined in isolated heart, kidney and liver from animals of various ages (Figure 2). Mitochondria from all tissues showed a significant increase in

ubiquinone content with increasing age. Adult levels in heart, kidney and liver mitochondria were 160%, 198% and 290% of fetal values. The magnitude of change far exceeded that of the cytochromes. In fact, the ratio of ubiquinone to cytochrome b increased from the fetal to the adult period (Figure 3). A higher ratio of ubiquinone to cytochrome b should increase the efficiency of electron transfer from complexes I and II to cytochrome b of complex III, since diffusion of ubiquinone between complex I (or II) and III is believed to be the rate limiting factor in electron transfer through the respiratory chain (31).

Mitochondrial Respiration. The respiratory activities of isolated heart, kidney and liver mitochondria from animals of various ages were determined as described above. All values were standardized per nmole of cytochrome oxidase to correct for any variation in microsomal contamination among preparations. Figure 4 summarizes the results obtained with the various substrates. Pyruvate-driven respiration (Figure 4A) in isolated heart and kidney mitochondria declined 60-65% from fetal values by 2-4 days of age. Liver mitochondria displayed a much different pattern with fetal rates which started low, increased to 161% by day 1 and then declined steadily back to fetal values by day 5. Pyruvate-driven respiratory rates in adult heart, kidney and liver mitochondria were similar to those in the fetal group. Rates in the adult liver, however, were significantly lower than those at 0.5-2.0 days of age. β-hydroxybutyrate driven respiration (Figure 4B) in heart and kidney mitochondria increased to 280% and 180% of fetal values respectively by 2 days of age while adult rates remained 150-180% higher than those of the fetal group. In contrast, β-hydroxybutyrate

driven respiratory rates in fetal liver mitochondria were not significantly different from values obtained during the newborn or adult period. Rates at 0.5-2.0 days of age, however, were higher than those of the adult group. Palmitylcarnitine driven respiration in isolated heart, kidney and liver mitochondria increased to 140-180% of fetal values by 2 days of age (Figure 4C). Rates declined to pre-birth values by 4-5 days of age and remained so up to the adult period. Succinate driven respiratory rates in isolated heart mitochondria were low (120-150 nmoles O_2/min·nmole cytochrome oxidase) at all ages studied and lacked significant differences in rates between age groups (data not shown). In sharp contrast, succinate driven respiratory rates in kidney and liver mitochondria were consistently higher than those obtained with any other substrate (Figure 4D). Rates increased to 144% and 200% of fetal values in kidney and liver mitochondria respectively by 0.5-2.0 days of age. Succinate driven respiratory rates remained at 150% of adult liver mitochondria values while rates with adult kidney mitochondria were comparable to the fetal group. Glutamate driven respiratory rates in isolated heart and kidney mitochondria displayed no age related changes while rates in liver mitochondria increased (178%) transiently from fetal and adult values between 0.5-2.0 days of age (data not shown). As a general rule, heart, kidney and liver mitochondrial respiratory activity, with most of the substrates studied, increased following birth. Pyruvate driven respiration in heart and kidney was the exception, where rates declined following birth.

Adenine Nucleotide Concentrations. Perinatal changes in the mitochon-

drial adenine nucleotides (ATP + ADP + AMP) are shown in Figure 5. No significant differences were seen during the fetal and newborn periods in heart and kidney, however, the liver showed a transient increase immediately following birth. In addition, the heart mitochondria from adult animals displayed levels which were 151 - 157% of fetal or newborn values. Therefore, tissue and age-dependent changes in mitochondrial adenine nucleotide content do exist.

Pyridine Nucleotide Concentrations. Large tissue and age-dependent changes in mitochondrial pyridine nucleotide content also exist during the perinatal period (Figure 6). Kidney mitochondria showed the most variation with an initial drop to 84% of fetal values by 1 day of age. The trend then reversed with 130% and 168% higher values in the 3 - 4 day old and adult groups, respectively. Less variation was seen in the heart and liver mitochondria. Specifically, values in the adult liver group were significantly lower than those of the fetal group while heart mitochondria showed the opposite pattern with higher values in the adult as compared to the fetal and newborn groups. In addition to the changes in total pyridine nucleotide content, the mitochondrial NADP(H)/NAD(H) ratio exhibited large tissue-specific differences (data not shown). The NADP(H)/NAD(H) ratio was similar in heart and kidney mitochondria with a range of 0.18 - 0.23 while that of liver mitochondria ranged from 1.6 - 2.0.

Phase Transition Temperatures. The fluid properties of the inner mitochondrial membrane were assessed during perinatal development using Arrhenius plots of succinate driven respiration. Liquid-gel phase transition temperatures (T_t) and energies of activation (E_a) were

calculated as described in Materials and Methods. Mitochondria from all three tissues showed a transient increase in T_t (Figure 7A) and a transient decrease in E_a (Figure 7B) following birth. Therefore, inner mitochondrial membrane fluidity decreased post-birth. This decrease in fluidity was accompanied by changes in the E_a for succinate oxidation, possibly through membrane lipid-protein interactions. Note that the largest changes in T_t were seen in the heart mitochondria, the tissue with the highest mitochondrial ubiquinone content of the three tissues studied.

DISCUSSION

The preparation of mitochondria from whole organs resulted in a heterogeneous pool of mitochondria with regard to cell type. Therefore, the results presented reflect the characteristics of these whole organ preparations.

The concentrations and stoichiometry of the mitochondrial respiratory chain components change during perinatal development (Figures 1 & 2). Cytochrome b and c concentrations fluctuate up or down depending on tissue type and perinatal age. In contrast, cytochrome oxidase and ubiquinone concentrations increase steadily following birth in heart, kidney and liver mitochondria. The increase in ubiquinone concentration exceeds that of cytochrome b in all three tissues leading to an increase in the ubiquinone/cytochrome b ratio (Figure 3) from the fetal to adult period. Since ubiquinone diffusion from complex I or II to complex III may be the rate limiting factor in electron transfer (31), an increase in this ratio may facilitate

respiration. The postnatal rise in mitochondrial cytochrome, and possibly ubiqinone, concentrations may be triggered by the rising systemic p_aO_2 since postnatal hypoxia inhibits the increase in mitochondrial cytochrome concentration (32).

Mitochondrial adenine nucleotide content varies in a tissue and age dependent manner during perinatal development (Figure 5). The transient increase in liver mitochondrial adenine nucleotides following birth has been previously reported (33,34) and implicated in the initiation of gluconeogenesis in the liver by activating pyruvate carboxylase (35). The elevated serum glucagon/insulin ratio and catecholamine surge associated with birth increases lipolysis and accelerates gluconeogenesis in the newborn (12,36). The rise in liver mitochondrial ATP, a substrate for pyruvate carboxylase, in conjunction with an increase in acetyl CoA (a positive allosteric effector) accelerate flux through pyruvate carboxylase (16). The importance of glucose synthesis and release by the newborn liver for maintenance of blood glucose levels and survival is well known (37). Factors which interfere with the rise in liver mitochondrial ATP, such as hypoxia and maternal diabetes, will inhibit the normal gluconeogenic response in the newborn (38). In this manner, hypoglycemia may contribute to the brain insult imposed by neonatal hypoxia. Although the kidney has the ability to synthesize glucose, no change in kidney or heart mitochondrial adenine nucleotide levels were detected from the fetal to newborn period. In adult heart, the elevated mitochondrial adenine nucleotide levels may be important in stimulating gluconeogenesis for replenishment of myocardial glycogen stores rather than glucose release

since this tissue lacks glucose-6-phosphatase. Therefore, age related changes in mitochondrial adenine nucleotide concentrations may play a role in stimulating gluconeogenic pathways in liver and heart during the newborn and adult periods, respectively.

Tissue specific differences in the total pyridine nucleotide content, as well as the NADP(H)/NAD(H) ratio exist in heart, kidney and liver mitochondria during perinatal development (Figure 6). The large increase in pyridine nucleotide levels in kidney mitochondria from the fetal to adult period may be related to changes in mitochondrial glutathione. The glutathione content of kidney mitochondria decreases steadily from the fetal to adult period while values in heart and liver do not change significantly (11). NADPH (and NADH via the transhydrogenase reaction) functions to maintain mitochondrial glutathione in the reduced state via glutathione reductase (39). Therefore, a larger NAD(P)H pool in kidney mitochondria of adult animals may provide a reserve of electrons to maintain reduction of the smaller glutathione pool during periods of oxidative stress. The function of a high NADP(H)/NAD(H) ratio in liver mitochondria, as compared to heart or kidney mitochondria, remains unknown. Traditionally, NADPH plays a biosynthetic role in cell metabolism by providing reducing equivalents for fatty acid, deoxyribonucleic acid and cholesterol synthesis. In liver mitochondria, however, NADPH may have an oxidative function by providing electrons to the respiratory chain via the transhydrogenase reaction.

Figures 4 illustrate changes in respiratory activity which, in part, support the earlier observations of Mela et al (20-23). The

maximum pyruvate driven state 3 respiratory rate of isolated heart and kidney mitochondria does indeed decrease following birth. Respiratory rates with the other substrates tested, however, increase (β-hydroxy-butyrate, palmityl-carnitine and succinate) or remain unchanged (glutamate). An explanation for these differential findings can be provided by appreciating the concomitant alterations in the mitochondrial antioxidant defense system and their effect on modulating oxidative processes in mitochondria.

According to Boag's model of diffusion (40), the post-birth rise in P_aO_2 should increase the PO_2 at the inner mitochondrial membrane, assuming that the mitochondrial O_2 consumption rate, O_2 diffusion coefficient and mitochondrial radius do not, at least initially, change. Under normal conditions, Boveris predicts that 1 - 4% of the O_2 reduced by an animal is via univalent pathways forming superoxide anion radical (41). Since the rate of superoxide generation increases as PO_2 increases, a post-birth rise in P_aO_2 should lead to an elevated mitochondrial superoxide and, consequently, H_2O_2 production rate. Mitochondria metabolize H_2O_2 via glutathione peroxidase forming oxidized glutathione. Glutathione reductase then re-reduces glutathione consuming NAD(P)H (39). Interestingly, peroxide-induced NAD(P)H oxidation rates in the intact, isolated mitochondria from newborn heart, kidney and liver are lower than adult values (11). Therefore, a heightened steady state rate of superoxide generation in newborn's may exceed the endogenous mitochondrial antioxidant capacity. In support of this hypothesis, lipid peroxidation increases transiently during the newborn period (42-45).

Sies and Moss have elegantly demonstrated that small quantities of peroxide can modulate substrate entry into oxidative pathways (24). In isolated mitochondria, peroxide restricts ATP production from pyruvate but not β-hydroxybutyrate or succinate. The effect requires peroxide metabolism since selenium-deficient animals, which lack significant glutathione peroxidase activity, were resistant to the peroxide-induced inhibition of pyruvate utilization (24). Therefore, elevated mitochondrial superoxide production, as evidenced by increased serum lipoperoxides (45) and increased ethane and pentane expiration (43,44), may contribute to the post-birth decrease in pyruvate oxidation and the apparent increase in β-hydroxybutyrate oxidation seen in heart and kidney mitochondria. The effect of systemic hormones (elevated glucagon/ insulin ratio, increased serum catecholamines, hyperiodothyronemia), however, cannot be discounted (12-17). Also other factors appear to be operative in liver mitochondria since the pyruvate driven respiratory rate increases post-birth (Figure 4A). For example, the rise in matrix adenine nucleotides will increase pyruvate carboxylase activity forming oxaloacetate which can then enter oxidative cycles and increase the apparent pyruvate driven respiratory rate.

Birth is also associated with a transient increase in the phase transition temperature (T_t) of the heart, kidney and liver inner mitochondrial membrane (Figure 7A). T_t is an intrinsic property of the membrane lipids attributable to a liquid-gel phase change (29). An increase in T_t corresponds to a decrease in membrane fluidity. The large increase in T_t seen in heart mitochondria may be related indirectly to its high ubiquinone content. The steady-state production

of superoxide radical by mitochondria occurs predominantly at the ubiquinone site through the reaction of O_2 with the semiquinone (41). Superoxide formed within the matrix can spontaneously or enzymatically dismutate to H_2O_2. Elevated levels of superoxide and H_2O_2 within the matrix increase the likelihood of forming hydroxyl radical, a highly reactive intermediate which can initiate the lipid peroxidative chain reaction. Lipid peroxidation can decrease membrane fluidity by converting polyunsaturated acyl chains from the unconjugated diene structure to the more solidifying conjugated diene configuration (47).

The changes in membrane fluidity are associated with a decrease in the E_a of succinate oxidation (Figure 7B). Other investigators have demonstrated alterations in the E_a of membrane associated enzymes and transport in response to diet-induced membrane fluidity changes (48). The effect has been attributed to alterations in lipid-protein interactions which may shift the configuration of the functional protein leading to changes in substrate/effector affinity at the active/allosteric sites, thereby altering enzyme activity (49). Changes in the binding affinities of the enzyme would be reflected by alterations in the K_m for substrate. Although changes in the K_m for succinate oxidation were not investigated here, others have shown large perinatal changes in the K_m of succinate for succinate oxidase (50) and ADP for the ADP/ATP translocase, enzymes embedded within the inner mitochondrial lipid bilayer.

To summarize, perinatal changes in heart, kidney and liver mitochondrial respiratory chain components (ubiquinone, cytochromes b, c and oxidase), pyridine and adenine nucleotide pools and substrate

oxidation rates were described. Alterations in inner mitochondrial membrane fluidity and E_a for succinate oxidation were also described. Collectively, these individual measurements characterize the development of the mitochondrial respiratory system and oxidative phosphorylation in three important body tissues during the perinatal period. By comparison with experimental models of prematurity, neonatal hypoxia, etc., possible therapeutic options may become self-evident. These results also elucidate other pathways which have a potential influence on perinatal metabolism. Of particular interest is the possible involvement of mitochondrial peroxide metabolism and lipid peroxidation in the respiratory changes seen in heart and kidney mitochondria as well as the transient decrease in inner mitochondrial membrane fluidity post-birth. Perinatal development of the mitochondrial antioxidant defense system, a previously unstudied area, may help define this relationship.

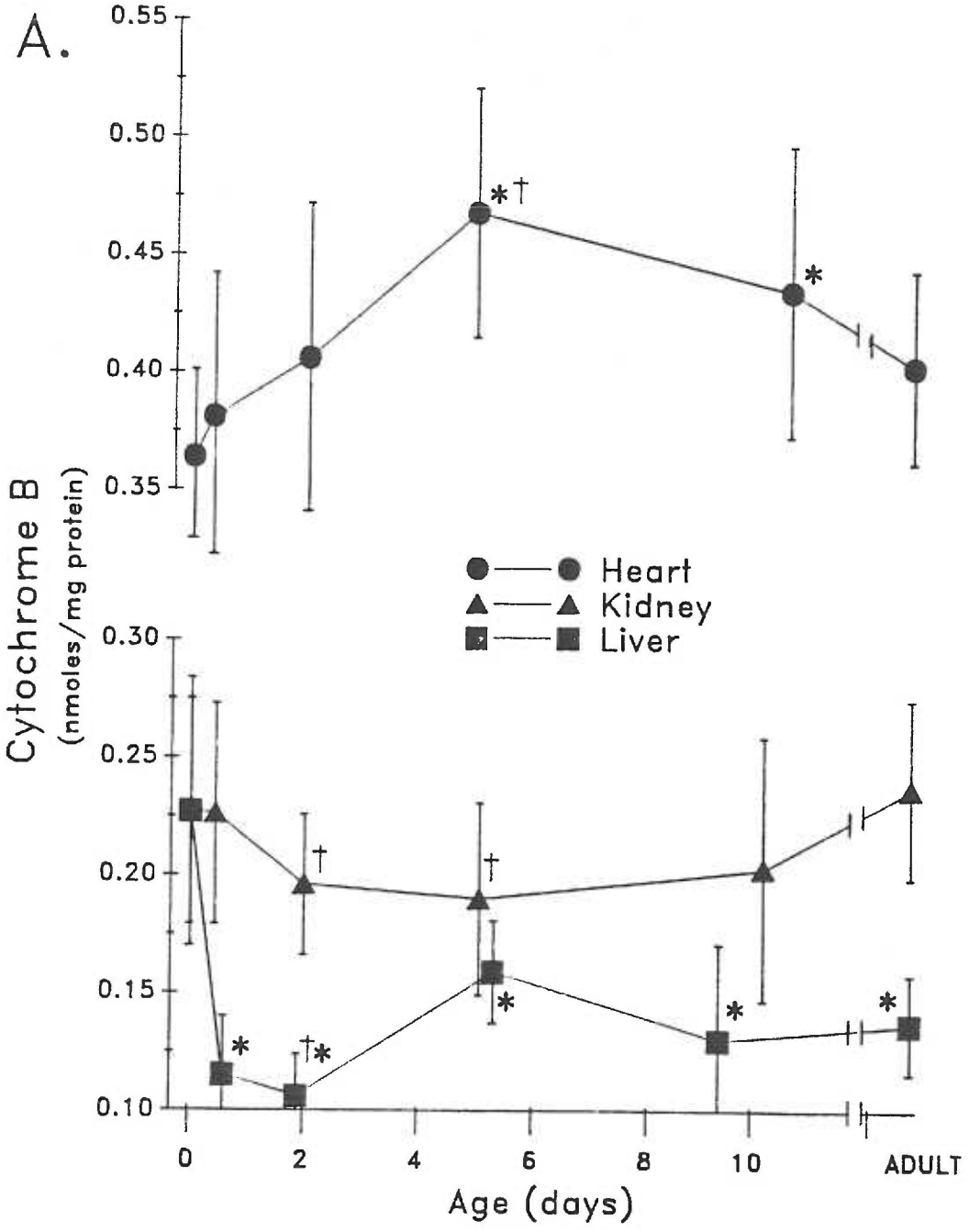
A.
0.55
0.50
0.45
0.40
0.35
0.30
0.25
0.20
0.15
0.10
Cytochrome B
(nmoles/mg protein)
Heart
Kidney
Liver
0
2
4
6
8
10
ADULT
Age (days)

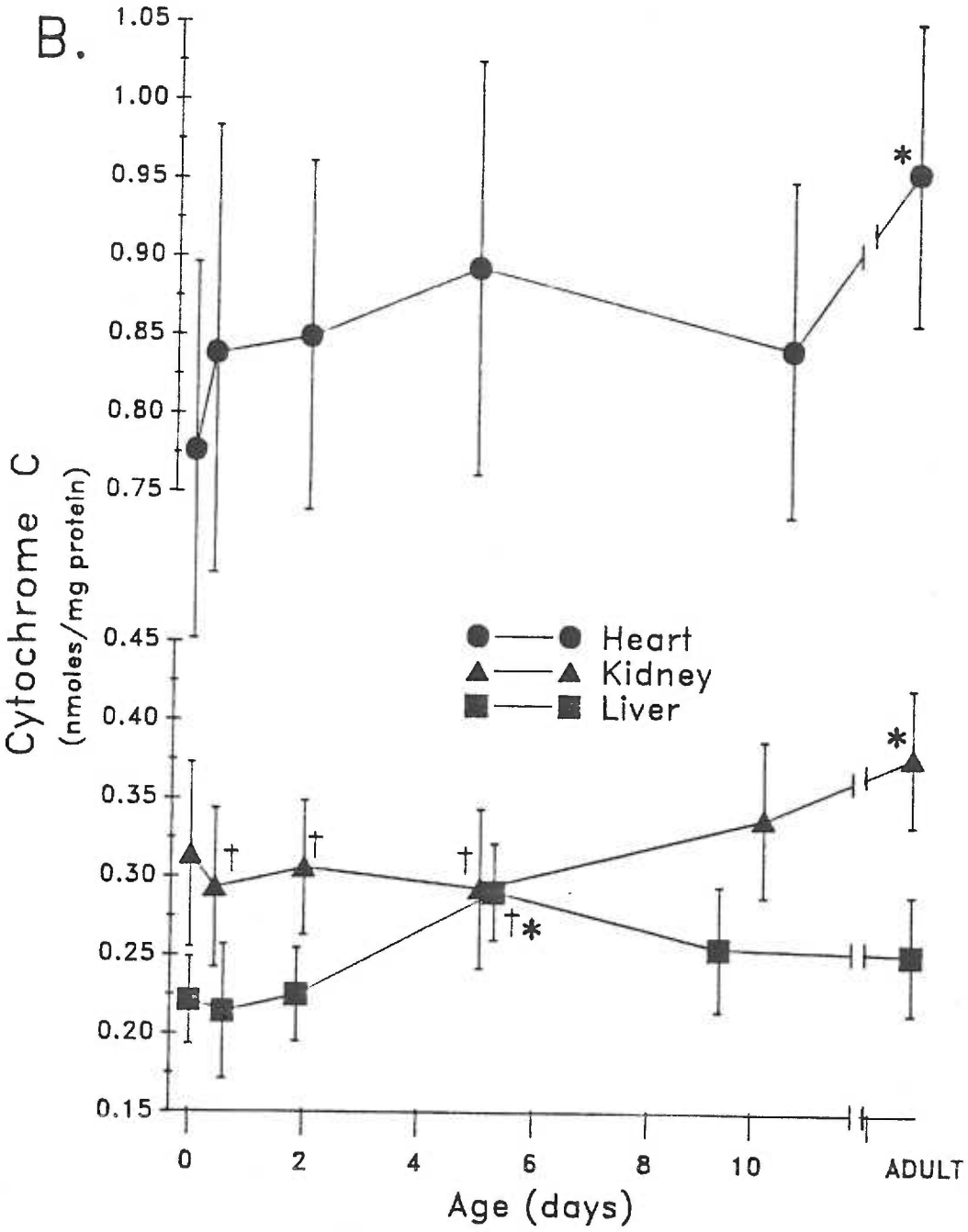
B.
Cytochrome C
(nmoles/mg protein)
1.05
1.00
0.95
0.90
0.85
0.80
0.75
0.45
0.40
0.35
0.30
0.25
0.20
0.15
Heart
Kidney
Liver
*
†
0
2
4
6
8
10
ADULT
Age (days)

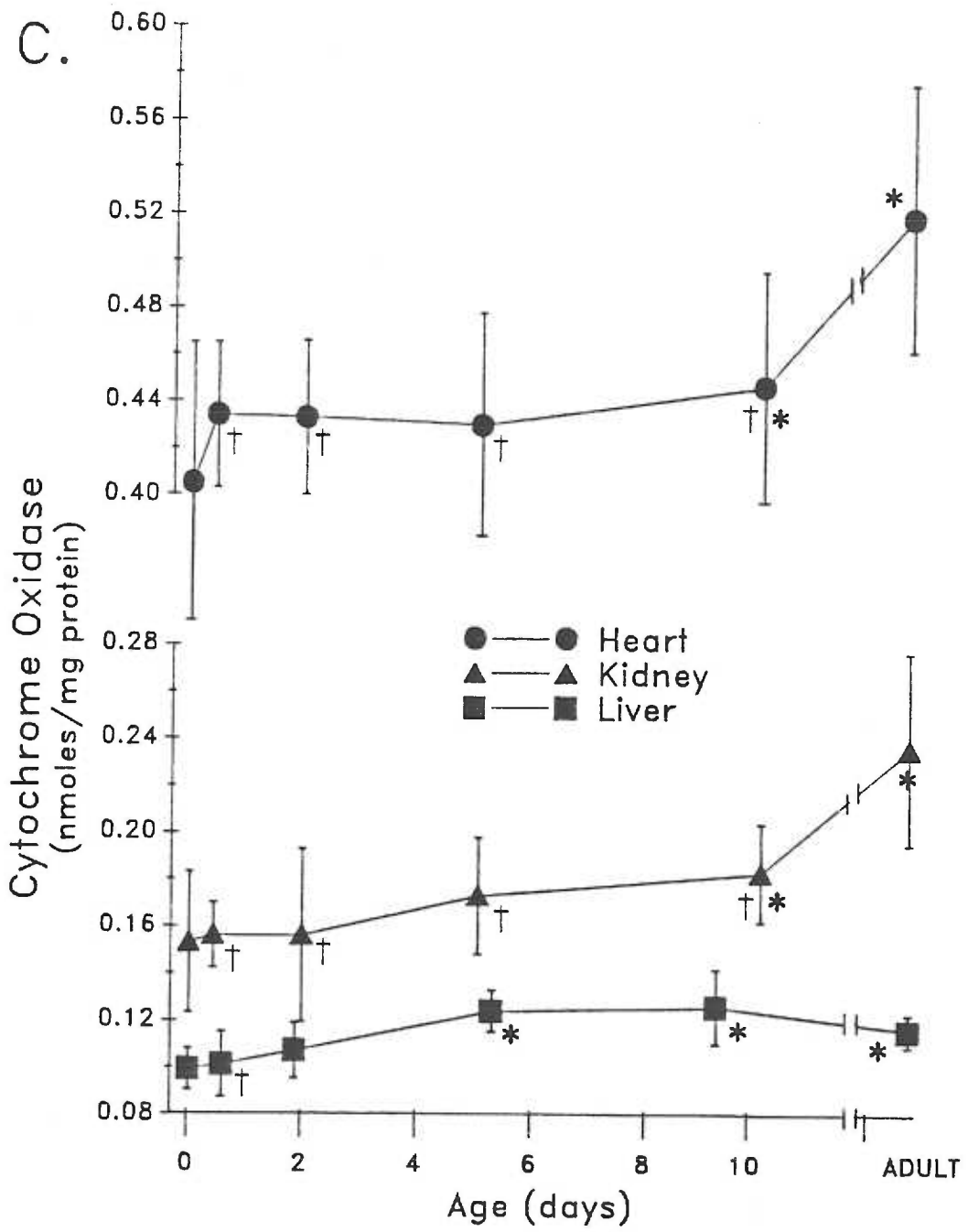
C.
Cytochrome Oxidase
(nmoles/mg protein)
0.60
0.56
0.52
0.48
0.44
0.40
0.28
0.24
0.20
0.16
0.12
0.08
Heart
Kidney
Liver
0
2
4
6
8
10
ADULT
Age (days)

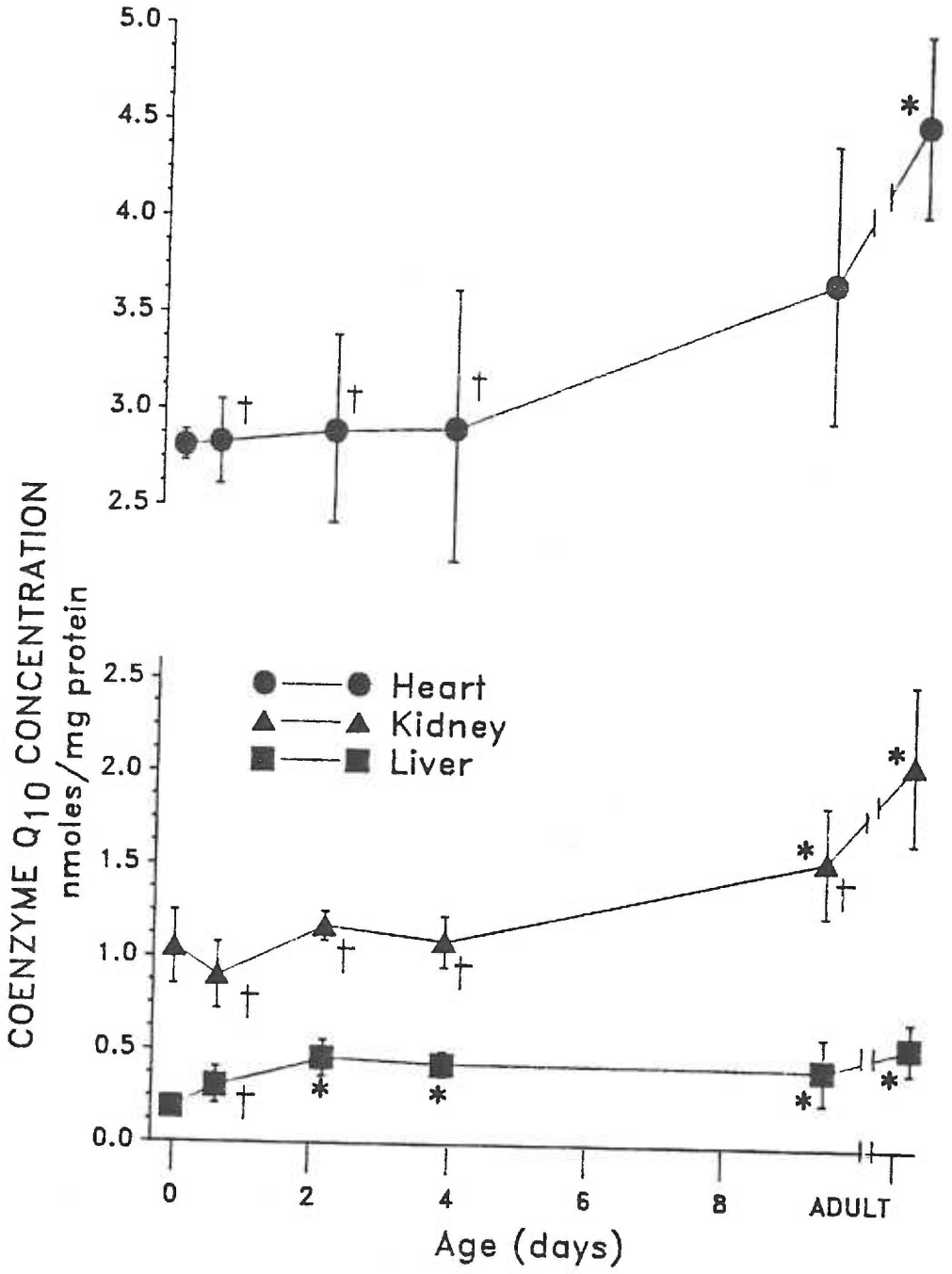

Figure 2. Mitochondrial ubiquinone concentration in isolated heart, kidney and liver mitochondria from fetal (day 0), newborn and adult animals. Each symbol depicts the mean concentration and age of each group. The bracket includes +/- one standard deviation from the mean. The n values averaged 5 with a range of 3-6 animals in each group. * and † denotes a significant difference of at least $\alpha < 0.05$ from the fetal and adult group respectively.

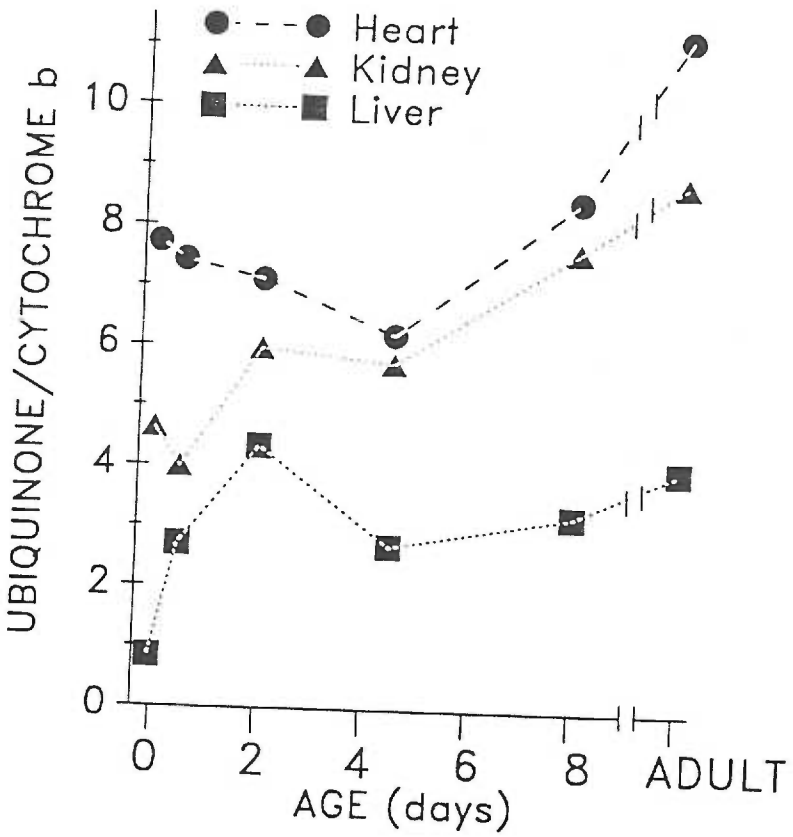

Figure 3. The ubiquinone to cytochrome b ratio in isolated heart, kidney and liver mitochondria from fetal (day 0), newborn and adult animals. Each symbol depicts the values obtained by dividing the mean ubiquinone concentration by the mean cytochrome b concentration for each age group.

Figure 4. Rate of A) pyruvate, B) β-hydroxybutyrate, C) palmitylcarnitine and D) succinate driven state 3 respiration in isolated heart, kidney and liver mitochondria from fetal (day 0), newborn and adult animals. Each symbol depicts the mean respiratory rate and age for each group. The bracket includes +/- standard error of the mean. The n values averaged 7 with a range of 4-10 animals in each group.

* and † denotes a significant difference of at least $\alpha < 0.05$ from the fetal and adult groups respectively.

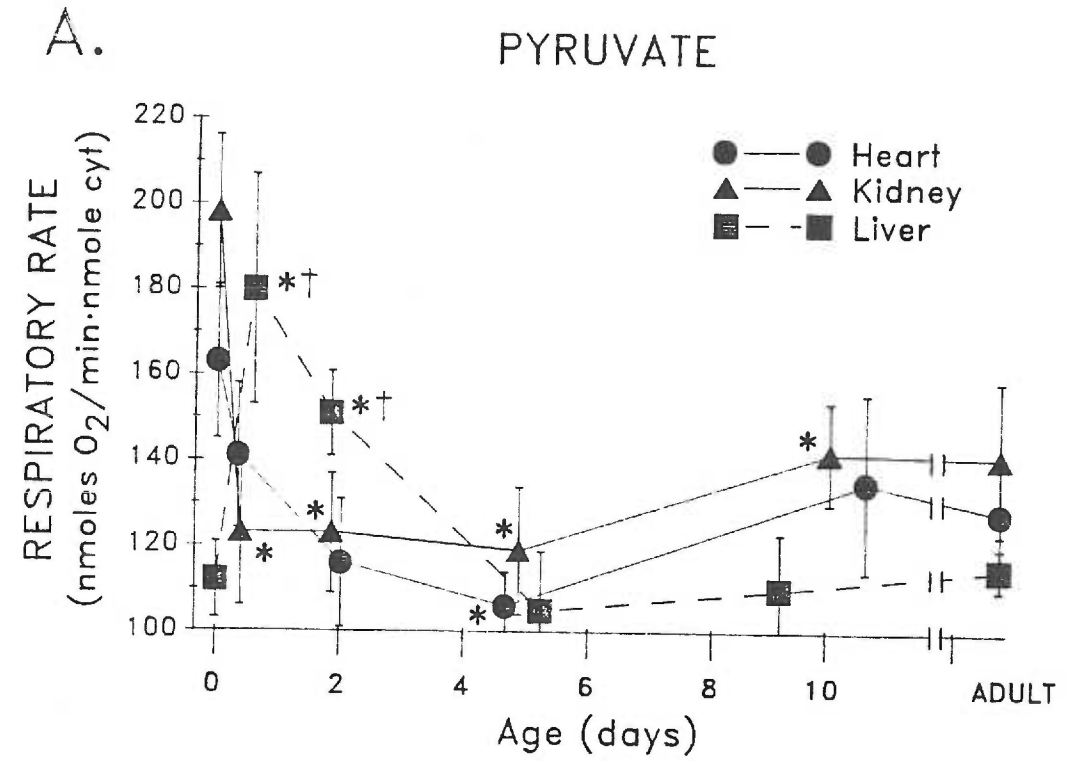
A.
PYRUVATE
RESPIRATORY RATE
(nmoles O_2/min·nmole cyt)
220
200
180
160
140
120
100
Heart
Kidney
Liver
0
2
4
6
8
10
ADULT
Age (days)

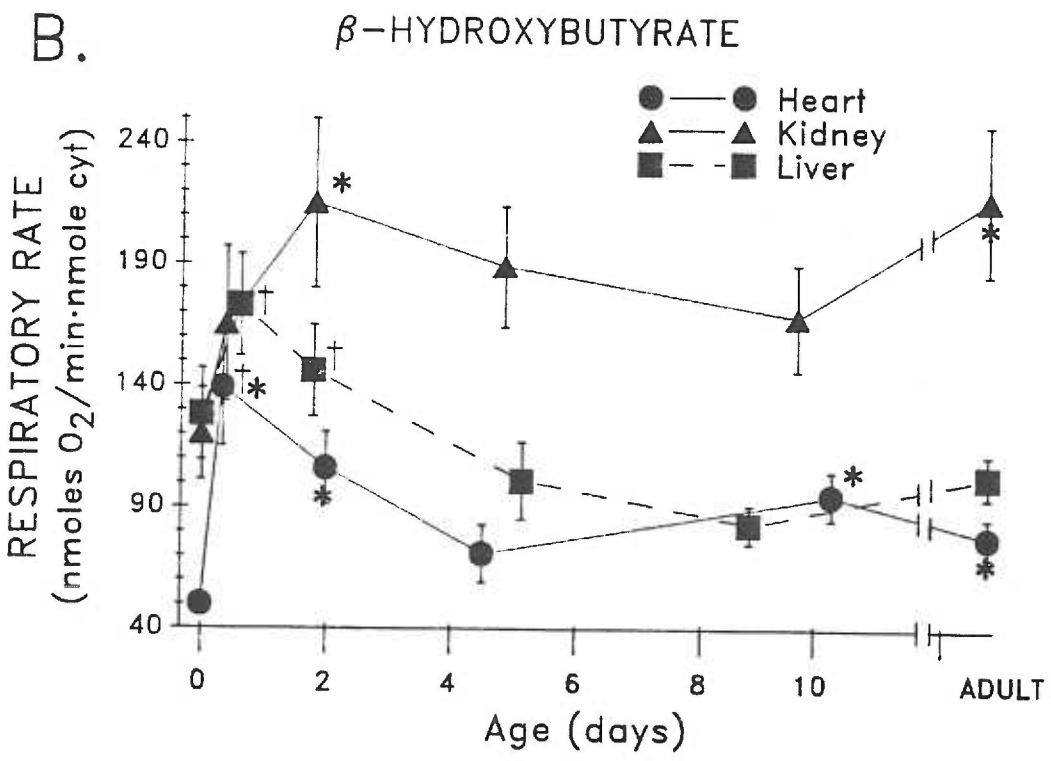
B.
β–HYDROXYBUTYRATE
RESPIRATORY RATE
(nmoles O_2/min·nmole cyt)
240
190
140
90
40
Heart
Kidney
Liver
0
2
4
6
8
10
ADULT
Age (days)

C.

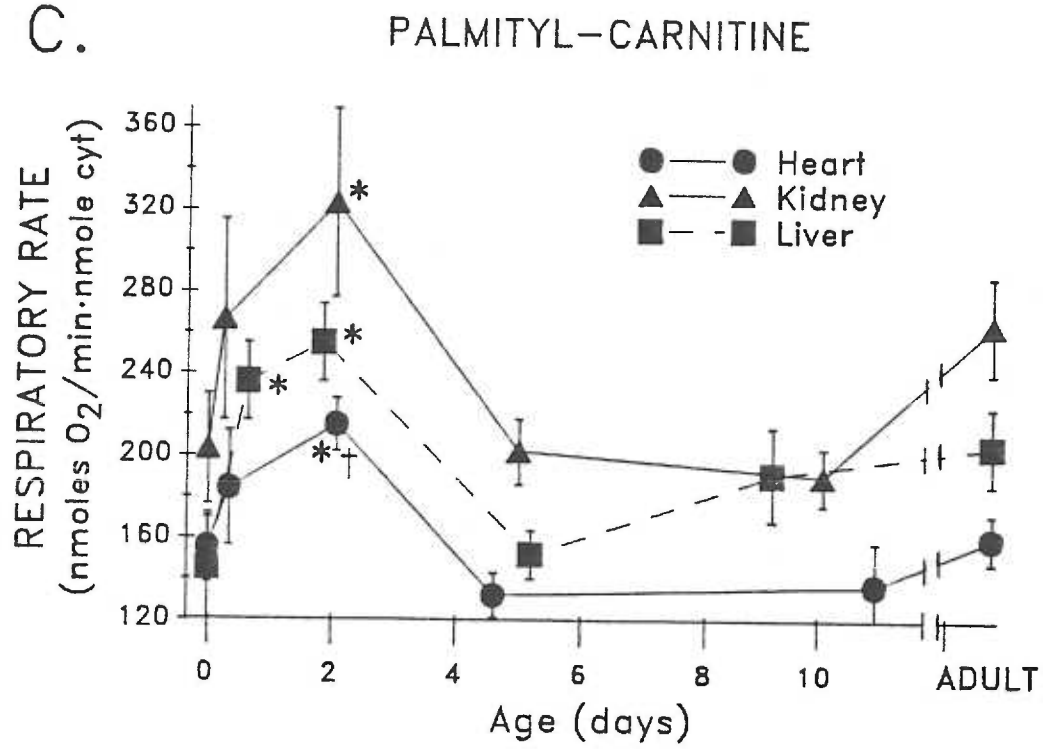
PALMITYL–CARNITINE
RESPIRATORY RATE
(nmoles O_2/min·nmole cyt)
360
320
280
240
200
160
120
Heart
Kidney
Liver
0
2
4
6
8
10
ADULT
Age (days)

D.

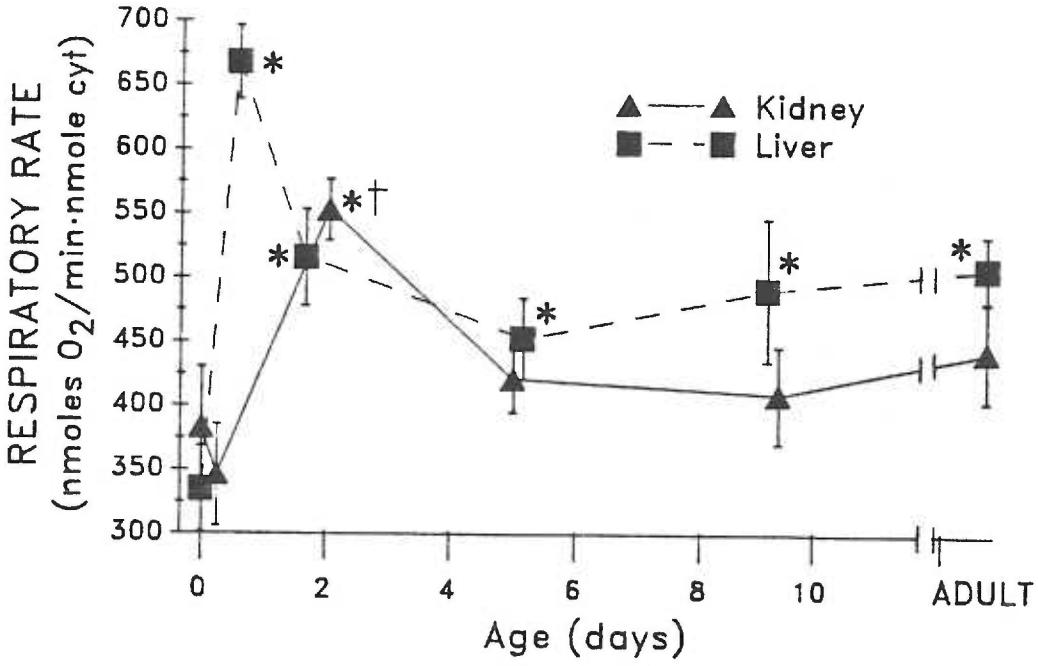
SUCCINATE
RESPIRATORY RATE
(nmoles O_2/min·nmole cyt)
700
650
600
550
500
450
400
350
300
Kidney
Liver
0
2
4
6
8
10
ADULT
Age (days)

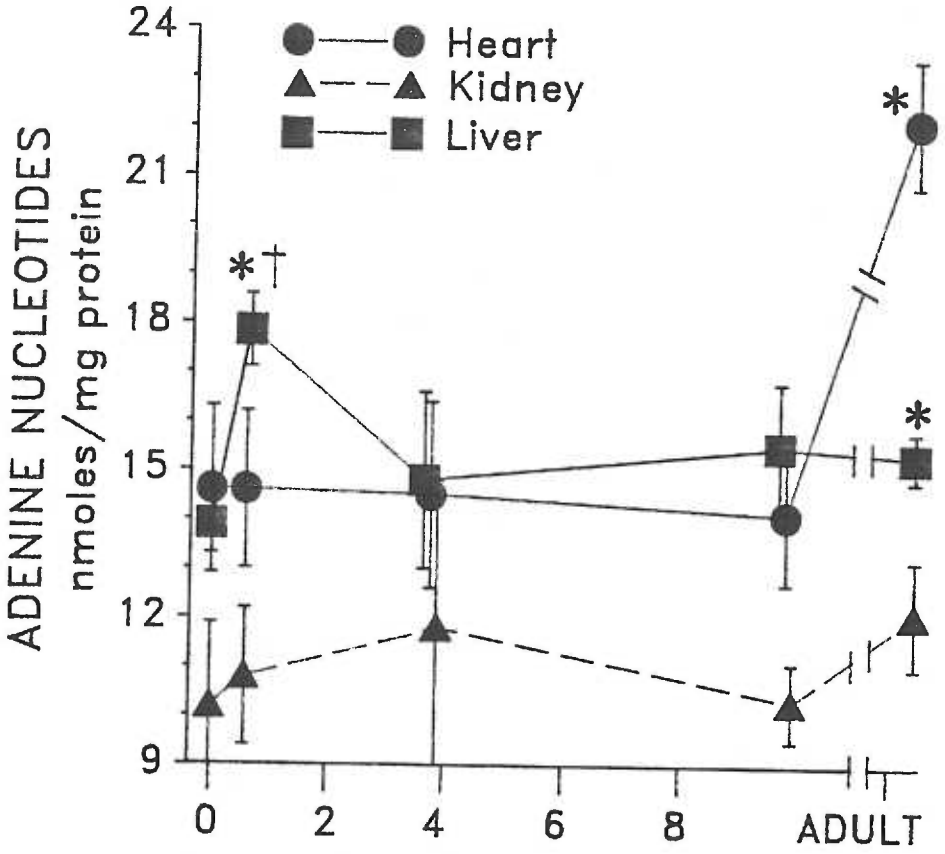

Figure 5. Mitochondrial adenine ribonucleotide levels in isolated heart, kidney and liver mitochondria from fetal (day 0), newborn and adult animals. Each symbol depicts the mean concentration and age of each group. The bracket includes +/- one standard deviation from the mean. The n values averaged 4 with a range of 4-5 animals in each group.

* and † denotes a significant difference of at least $\alpha < 0.05$ from the fetal and adult groups respectively.

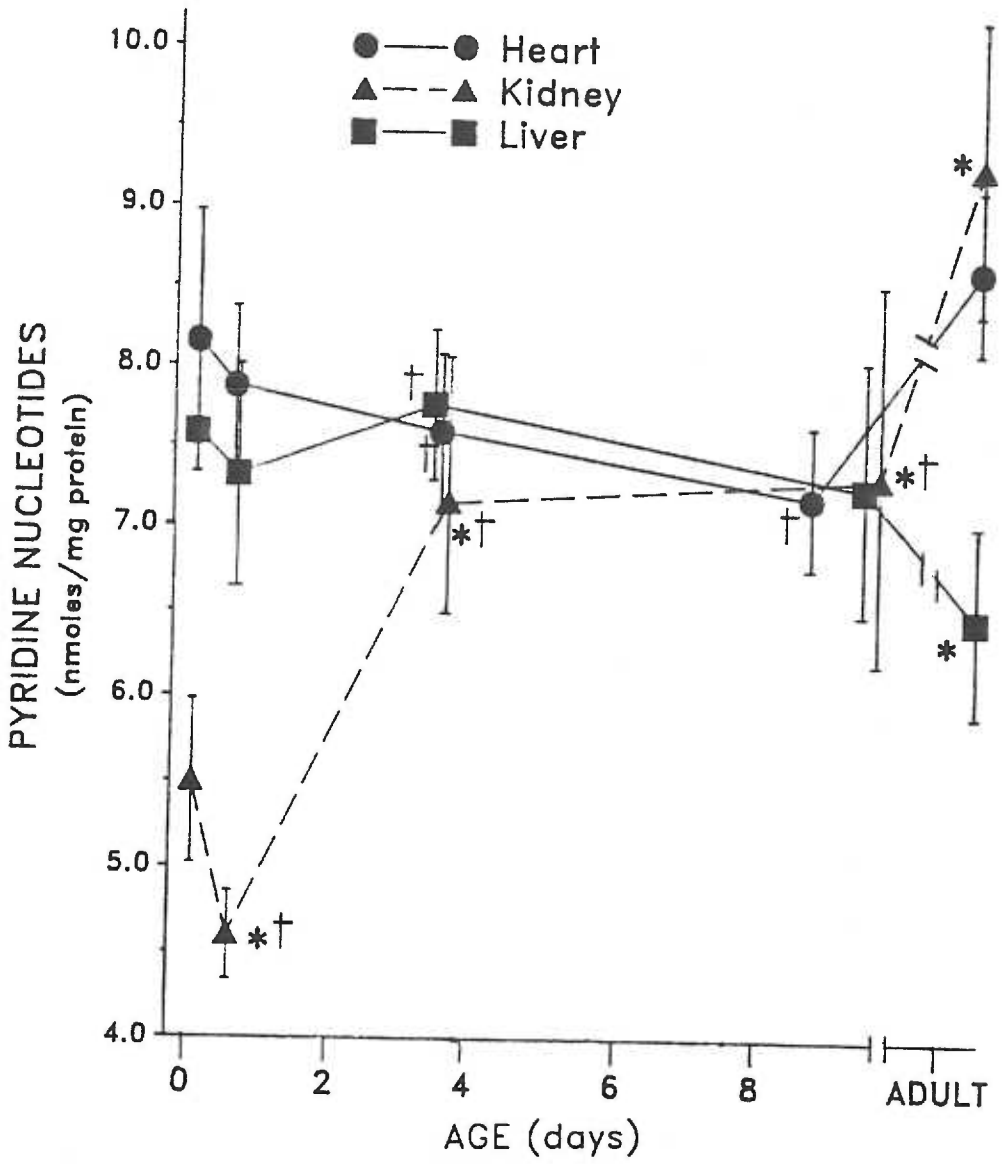

Figure 6. Total pyridine nucleotide content, NAD(H) plus NADP(H), in isolated heart, kidney and liver mitochonria from fetal (day 0), newborn and adult animals. Each symbol depicts the mean concentration and age of each group. The bracket includes +/- one standard deviation from the mean. The n values averaged 4 with a range or 4-5 animals in each group.

* and † denotes a significant difference of at least $\alpha < 0.05$ from the fetal and adult groups respectively.

REFERENCES

1. Harris AP, Sendak MJ, Donham RT 1986 Changes in arterial oxygen immediately after birth in the human neonate. J Pediatrics 109:117-119.

2. Itskovitz J, Goetzman BW, Roman C, Rudolph AM 1984 Effects of fetal-maternal exchange transfusion on fetal oxygenation and blood flow distribution. Am J Physiol 247:H655-H660.

3. Kanamura S, Kanai K, Oka M, Shugyo Y, Watanabe J 1985 Quantitative analysis of development of mitochondrial ultrastructure in differentiating mouse hepatocytes during postnatal period. J Ultrastruct Res 93:195-204.

4. Smith HE, Page E 1977 Ultrastructural changes in rabbit heart mitochondria during the perinatal period. Develop Biol 57:109-117.

5. Jakovcic S, Haddock J, Getz GS, Rabinowitz M, Swift H 1971 Mitochondrial development in liver of foetal and newborn rats. Biochem J 121:341-347.

6. Hallman M, Maenpaa P, Hassinen I 1972 Levels of cytochromes in heart, liver, kidneys and brain in the developing rat. Separatum Experimentia 28:1408-1410.

7. Hallman M 1971 Changes in mitochondrial respiratory chain proteins during perinatal development: Evidence of the importance of enviromental oxygen tension. Biochim Biophys Acta 253:360-372

8. Mela L, Goodwin CW, Miller LD 1975. Correlation of mitochondrial cytochrome concentration and activity to oxygen availability in the newborn. Biochem Biophys Res Commun 64:384-390.

9. Mavelli I, Rigo A, Federico R, Ciriolo MR, Rotilio G 1982 Superoxide dismutase, glutathione peroxidase and catalase in developing rat brain. Biochem J 204:535-540.

10. Gerdin E, Tyden O, Eriksson UJ 1985 The development of antioxidant enzymatic defense in the perinatal rat lung: activities of superoxide dismutase, glutathione peroxidase and catalase. Pediatr Res 19:687-691.

11. Vlessis AA, Mela-Riker L 1988 II. Perinatal development of the mitochondrial antioxidant defense system. Submitted for publication to Pediatr Res.

12. Sutton R, Pollak JK 1980 Hormone-initiated maturation of rat liver mitochondria after birth. Biochem J 186:361-367.

13. Sinclair JC, Warshaw JB 1975 Perinatal energy metabolism. In: Hafez ESE (ed) The Mammalian Fetus: Comparative Biology and Methodology. Charles C. Thomas, Springfield, Illinois, pp 104-119.

14. Martin A, Caldes T, Benito M, Medina JM 1981 Regulation of glycogenolysis in the liver of the newborn rat in vivo: inhibitory effect of glucose. Biochim Biophys Acta 672:262-267.

15. Lenartowicz E, Olson MS 1978 The inhibition of α-ketoglutarate oxidation by fatty acids in rat liver mitochondria. J Biol Chem 253:5990-5996.

16. Thienen WD, Davis EJ 1981 The effects of energetic steady state, pyruvate concentration and octanoyl-(-)-carnitine on the relative rates of carboxylation and decarboxylation of pyruvate by rat liver mitochondria. J Biol Chem 256:8371-8378.

17. Fisher DA 1975 Thyroid function in the fetus and newborn. Medical Clinics of North America 59:1099-1107.

18. Aynsley-Green A 1986 The role of regulatory peptides in postnatal metabolic adaptation. Acta Endocrinol 113 (Suppl) 279:422-427.

19. Halestrap AP 1978 Stimulation of pyruvate transport in metabolizing mitochondria through changes in the transmembrane pH gradient induced by glucagon treatment of rats. Biochem J 172:389-398.

20. Mela L 1979 Development of the newborn to meet its own energy requirements. Proc Amer Phil Soc 123:293-297.

21. Mela L, Goodwin CW, Miller LD 1976 In vivo control of mitochondrial enzyme concentrations and activity by oxygen. Am J Physiol 231:1811-1816.

22. Goodwin CW, Mela L, Deutsch C, Forster RE, Miller LD, Delivoria-Papadopoulos M 1976 Development and adaptation of heart mitochondrial respiratory chain function in fetus and in newborn. Adv Exp Med Biol 75:713-719.

23. Mela L, Goodwin CW, Miller LD 1977 In vivo adaptation of O_2 utilization to O_2 availability: comparison of adult and newborn mitochondria. In: Jobsis FF (ed) Oxygen and Physiological Function. Professional Information Library, pp 285-291.

24. Sies H, Moss KM 1978 A role of mitochondrial glutathione peroxidase in modulating mitochondrial oxidations in liver. Eur J Biochem 84:377-383.

25. Lowry OH, Rosebrough NJ, Farr AL, Randall RJ 1951 Protein measurement with folin phenol reagent. J Biol Chem 193:265-275.

26. Lang JK, Gohl K, Packer L 1986 Simultaneous determination of tocopherols, ubiquinols, and ubiquinones in blood, plasma, tissue homogenates, and subcellular fractions. Anal Biochem 157:106-116.

27. Okamoto T, Fukui K, Nakamoto M, Kishi T 1985 High-performance liquid chromatography of coenzyme Q-related compounds and its application to biological materials. J Chromatogr 342:35-46.

28. Chance B, Hagihara B 1963 Direct spectroscopic measurements of interaction of components of the respiratory chain with ATP, ADP, phosphate and uncoupling agents. In: Proceedings of the Fifth International Congress of Biochemistry, Oxford. Pergamon Press, Elmsford, New York, p 3.

29. Kumamota J, Raison JK, Lyons JM 1971 Temperature "breaks" in Arrhenius plots: a thermodynamic consequence of a phase change. J Theor Biol 31:47-51.

30. Sandermann, Jr. H 1978 Regulation of membrane enzymes by lipids. Biochim Biophys Acta 515:209-237.

31. Ragan CI, Reed JS 1986 Regulation of electron transfer by the quinone pool. J Bioenerg Biomembr 18:403-418.

32. Kinnula VL, Hassinen I 1977 Effect of hypoxia on mitochondrial mass and cytochrome concentrations in rat heart and liver during postnatal development. Acta Physiol Scand 99:462-466.

33. Aprille JR 1986 Perinatal development of mitochondria in rat liver. In: Fiskum G (ed) Mitochondrial Physiology and Pathology. Van-Nostrand Reinhold, New York, pp 66-99.

34. Tullson PC, Aprille JR 1987 Regulation of mitochondrial adenine nucleotide content in newborn rabbit liver. Am J Physiol 253:

44. Wispe JR, Knight M, Roberts RJ 1986 Lipid peroxidation in newborn rabbits: effects of oxygen, lipid emulsion, and vitamin E. Pediatr Res 20:505-510.

45. Yoshioka T, Motoyama H, Yamasaki F, Noma J 1982 Lipid peroxidation and its protective mechanism during developmental stage in rat. Acta Obst Gynaec JPN 34:966-970.

46. Pryor WA 1986 Oxy-radicals and related species: their formation, lifetimes, and reactions. Ann Rev Physiol 48:657-667.

47. Vladimirov YA, Olenev VI, Suslova TB, Cheremisina ZP 1980 Lipid peroxidation in mitochondrial membrane. Adv Lipid Res 17:173-249.

48. McMurchie EJ, Raison JK 1979 Membrane lipid fluidity and its effect on the activation energy of membrane-associated enzymes. Biochim Biophys Acta 554:364-374.

49. Stubbs CD, Smith AD 1984 The modification of mammalian membrane polyunsaturated fatty acid composition in relation to membrane fluity and function. Biochim Biophys Acta 779:89-137.

50. Aw TY, Jones DP 1987 Respiratory characteristics of neonatal rat hepatocytes. Pediatr Res 21:492-496.

51. Van Rossum GDV 1963 Respiration and glycolysis in liver slices prepared from rats of different foetal and post-natal ages. Biochem Biophys Acta 74:15-23.

52. Faulkner A, Jones CT 1975 Changes in the activities of some glycolytic enzymes during the development of the guinea pig. Int J Biochem 6:789-792.

To be submitted to Pediatric Research.

II. PERINATAL DEVELOPMENT OF THE MITOCHONDRIAL ANTIOXIDANT DEFENSE SYSTEM

by

Angelo A. Vlessis and Leena Mela-Riker

Departments of Surgery & Biochemistry

Oregon Health Sciences University

Portland, Oregon, U.S.A.

ABSTRACT

The mitochondrial antioxidant defense system was studied to assess its potential role in the newborn mammal's tolerance to oxidative challenge and to gain insight into the fetal adaptation to a relatively hyperoxic adult environment. Isolated heart, kidney, and liver mitochondria from fetal, newborn, and adult guinea pigs were used. In situ function of the antioxidant enzymes was estimated in mitochondrial suspensions following selenite or t-butylhydroperoxide (tBOOH) addition by determining NAD(P)H oxidation rates spectrophotometrically at 340-375 nm. Mitochondria from newborn animals were less susceptible to selenite and tBOOH-induced NAD(P)H oxidation. The pattern of change varied widely with tissue type. Kidney mitochondria displayed the largest change with a 3-4 fold increase in rate from the fetal to adult period. NAD(P)H oxidation rates in intact mitochondria did not correlate consistently with glutathione reductase and peroxidase activities in sonicated mitochondria suggesting in situ regulation by other endogenous factors. Immediately following birth, mitochondrial glutathione reductase and peroxidase activities dropped 38-50% and 50-70%, respectively, in all tissues studied. Total glutathione content of heart and liver mitochondria did not change with age. Adult kidney mitochondrial glutathione, however, declined to 24% of fetal values. Mitochondrial superoxide dismutase activity increased 150-300% from the fetal to the adult period in all tissues studied. Perinatal changes in the mitochondrial antioxidant system and their relationship to mitochondrial calcium metabolism are discussed in terms of the newborn's resistance to oxidative stress.

INTRODUCTION

Mammalian birth introduces a dramatic environmental change on the emerging organism. Altered circulation and oxygen availability necessitate adaptive changes in metabolism. Prior to birth, fetal oxygen tensions (P_aO_2) are low (25 mmHg). After birth, average P_aO_2 rises (80-90 mmHg) initiating the switch to a more aerobic metabolism [5,15,18,32]. In the newborn period, rising tissue PO_2 accompanies increased formation of reactive oxygen species which stimulate lipid peroxidation, as measured by ethane and pentane expiration [48,49], as well as serum malondialdehyde [29] and lipoperoxide levels [51]. As antioxidant defense systems develop, lipid peroxidation decreases to adult levels between 10-20 days of age [29,51].

Despite increased lipid peroxidation at birth, newborn mammals are more resistant to a variety of oxidative challenges when compared to adult animals of the same species [10,50]. Although the biochemical mechanism of this tolerance remains unknown, the mitochondrial antioxidant system is likely to play a key role. When mitochondria metabolize oxidants, large quantities of NAD(P)H are consumed through glutathione dependent redox cycles [2,25,30]. An increase in the matrix NAD(P)/NAD(P)H ratio will induce calcium efflux [21,25,34]. Interestingly, isolated mitochondria from newborn animals are less susceptible to oxidant-induced NAD(P)H oxidation and calcium release [46]. Therefore, tolerance to oxidative stress in newborn animals may stem from differences in the mitochondrial antioxidant defense system.

Mitochondria generate reactive oxygen species at rates dependent on the surrounding oxygen tension [44,45]. Under normal physiological

conditions, the mitochondrial respiratory chain produces superoxide radical and hydrogen peroxide (H_2O_2), accounting for 1-4 % of the total oxygen consumed [4]. The rate of production increases linearly with PO_2 [44,45]. Therefore, a rise in average tissue PO_2 at birth should enhance in vivo superoxide and H_2O_2 production by the mitochondrial respiratory chain. In support of this, mitochondria exhibit a decrease in membrane fluidity following birth [33], consistent with heightened lipid peroxidation in these membranes.

Superoxide radicals and H_2O_2 liberated by the mitochondrial respiratory chain are reduced to water by antioxidant enzyme systems within the matrix. Superoxide can dismutate to H_2O_2 spontaneously or enzymatically [12]. Glutathione peroxidase reduces H_2O_2 to water forming oxidized glutathione (GSSG) from reduced glutathione (GSH). Glutathione reductase then regenerates GSH from GSSG consuming NAD(P)H [36]. Failure to remove H_2O_2 and superoxide increases the likelihood of forming hydroxyl radicals, highly reactive intermediates which can initiate the lipid peroxidative chain reaction [12]. Conversely, effective removal of H_2O_2 will oxidize NAD(P)H and induce calcium efflux [2,21,25,34]. This type of efflux can uncouple oxidative phosphorylation via calcium cycling involving the Ca^{2+}/H^+ antiport and Ca^{2+}-uniport systems [7,11]. In addition, oxidation of mitochondrial GSH and NAD(P)H may modulate substrate oxidations in mitochondria [38].

The development of antioxidant defense systems have been studied extensively in newborn animals, using tissue homogenates [9,10,28,41,50]. Little is known, however, about the development of the mitochondrial antioxidant defense system [28]. This system is of

paramount importance since: (1) mitochondria are a known source of reactive O_2 species under normal physiological conditions [4,44,45], (2) the rate of mitochondrial superoxide radical and H_2O_2 generation increases linearly with PO_2 [44,45], (3) mitochondrial metabolism of peroxides can increase free intracellular calcium [7] and deplete cellular ATP by inducing calcium efflux and futile calcium cycling, respectively, and (4) it may play a role in modulating substrate entry into oxidative pathways in mitochondria [38].

The purpose of this study was to characterize the mitochondrial antioxidant defense system during the perinatal period and to assess its potential role in the newborn mammal's tolerance to oxidative stress. To do this, mitochondria from fetal, newborn and adult guinea pigs were studied using two approaches. First, the ability of intact, isolated mitochondria to reduce the oxidants selenite and t-butyl hydroperoxide (tBOOH) were determined. Second, NAD(P)H oxidation rates were compared to the mitochondrial glutathione reductase and peroxidase activities, as well as the endogenous substrate levels. Mitochondrial manganese-containing superoxide dismutase (SOD) were also assayed as an indirect indicator of in vivo superoxide production.

MATERIALS AND METHODS

Animals. Topeka guinea pigs, bred and housed at this institution, were used as experimental animals. Guinea pigs were chosen since the size of the newborns allows isolation of adequate quantities of heart, kidney and liver mitochondria from a single animal. Term fetuses were obtained by cesarean section 63 days (full gestation) following a one

week breeding period. Newborn animals in which the time of birth could not be accurately recorded (± 3 hours) were not used. All adult animals were maintained on ad libitum guinea pig chow and water. Newborn animals were kept with their mothers and allowed to nurse until the time of sacrifice.

Mitochondrial Preparations. Mitochondria were isolated according to conventional methods as described previously by Mela et al [32] and Widener and Mela-Riker [47]. Unanesthetized animals were sacrificed by decapitation and the tissue(s) of interest immediately removed and minced in ice cold MSE (150 mM mannitol, 130 mM sucrose, 1 mM EGTA). The minced sample was washed several times with cold MSE and then homogenized gently at 4°C in a Potter-Elvehjem homogenizing vessel. The homogenate was centrifuged (4° C) at 480g to remove the large debris. Mitochondria were pelleted from the supernatant by centrifugation at 7700g. The pellet was washed twice with cold MS (150 mM mannitol, 130 mM sucrose) and resuspended in cold MS and kept on ice at all times. This suspension was analyzed for protein [26] and used to make the various determinations described below. All solutions were made with deionized/quartz distilled water. This procedure yields heart and kidney mitochondria with respiratory control ratios greater than 10; those of the liver are greater than 6.

Oxidation of Mitochondrial NAD(P)H. NAD(P)H oxidation was monitored kinetically in intact mitochondria using a Hitachi 557 dual wavelength spectrophotometer using a modification of the method described by Lehninger et al [21]. Isolated mitochondria were suspended in 65 mM KCl, 125 mM sucrose, 20 mM tris-chloride, 0.2 mM tris-phosphate, 10 μM

rotenone and 2 mM succinate at pH 7.4. Rotenone, a site I inhibitor, functions to prevent entry of electrons from NAD(P)H into the respiratory chain while allowing ATP synthesis via succinate and $FADH_2$. Rotenone also inhibits the reverse flow of electrons from $FADH_2$ to NAD(P)H. NAD(P)H oxidation was monitored kinetically following the addition of 500 μM sodium selenite or 500 μM t-butyl hydroperoxide (tBOOH). These quantities of selenite and tBOOH elicit maximal NAD(P)H oxidation rates [25,46]. The change in optical density versus time was recorded onto chart paper. The extinction coefficient for NADPH at 340-375 nm was calculated by additions of known quantities of NADPH to a blank cuvette. NAD(P)H oxidation rates were calculated as nmoles NAD(P)H oxidized per minute per mg of mitochondrial protein.

Nucleotide Assay. ATP, ADP, AMP, $NADP^+$ and NADPH were assayed using a modification of the methods employed by Stocchi [40]. Isolated mitochondria were suspended at room temperature in 200 μl of 120 mM KCl, 10 mM tris-Cl, 10 mM tris-PO_4, 5 mM succinate, 10 μM rotenone at pH 7.4. The suspension was alkalinized by adding 400 μl of 0.5 M KOH, vortexed for 15 seconds and then allowed to cool for 1 minute in an ice bath. The pH was adjusted to 6.5-7.0 with 180 μl 1 M KH_2PO_4 and the resulting solution was centrifuged at 10,000g for 3 minutes. The supernatant was filtered (at 4^oC) using a Rainin 0.45 μm filter. The filtrate was assayed for nucleotides by HPLC.

Nucleotides were separated on a RESOLVE C_{18-5} column (3.9 mm X 15 cm). All samples and standards were analyzed using the following solvent gradient: 0-9 minutes, flow 0.8 ml/min with 100% 0.1 M KH_2PO_4; 9-15 minutes, flow was increased linearly to 1.3 ml/min and the mobile

phase was changed linearly to 2% methanol and 98% 0.1 M KH_2PO_4; 15-20 minutes, flow was maintained at 1.3 ml/min and the mobile phase was changed linearly to 10% methanol and 90% 0.1 M KH_2PO_4; 20-30 minutes, flow was maintained at 1.3 ml/min, mobile phase 10% methanol and 90% 0.1 M KH_2PO_4. Two wavelengths were employed for detection: 254 nm and 340 nm. Standard curves were constructed using external standards containing known quantities of nucleotides. Quantitation was based on peak area.

The HPLC system consisted of a Waters 600 Multisolvent Delivery System and Waters 490 Programable Multiwavelength Detector. All injections were made using a Waters 712 Wisp equipped with a sample cooling unit which was held at 4°C. Data acquisition and analysis was performed using a Waters System Interface Module and an IBM-AT computer equipped with Waters 820 Chromatography software.

Glutathione Reductase and Peroxidase Assays. Isolated mitochondria were sonicated under buffered hypotonic (60 mM KCl, 10 mM tris-chloride and 10 mM tris-phosphate at pH 7.4) conditions in a saline ice bath and assayed immediately for glutathione reductase and peroxidase activity.

For the reductase assay [35], 50-200 μl aliquots of the sonicate were mixed with 800-950 μl of 120 mM KCl, 10 mM tris-chloride, 10 mM tris-phosphate and 5 mM GSSG at pH 7.4. The reaction was started by adding 0.3 mM NADPH and its disappearance was monitored kinetically at 340-375 nm.

Glutathione peroxidase was assayed by the method of Tappel [42]. Aliquots (100-250 μl) of sonicate were mixed with 750-900 μl of 120 mM

KCl, 50 mM tris-Cl, 0.1 mM EDTA, 0.25 mM glutathione, 0.3 mM NADPH and glutathione reductase (2 units/ml) at pH 7.4. The reaction was started by addition of 1.2 mM t-butyl hydroperoxide. The disappearance of NADPH was monitored kinetically and recorded onto chart paper. The spontaneous NADPH oxidation rate under these conditions was determined in the absence of added sonicate and subtracted from the observed rates with sonicate.

All measurements were done at room temperature in a Hitachi 557 dual wavelength spectrophotometer. Glutathione reductase and peroxidase activities were calculated from chart paper recordings as nmoles NADPH oxidized per minute per mg of mitochondrial protein.

Glutathione Assay. Total glutathione content of isolated mitochondria was assayed enzymatically using glutathione reductase and 5-5'-dithiobis-2-nitrobenzoate (DTNB) [14]. This method guarantees specificity for glutathione via a cycling reaction involving glutathione reductase and DTNB.

Mitochondria were sonicated as described above and kept frozen at -70°C until assayed. Aliquots (100-200 μl) of the thawed sonicate were mixed with 800-900 μl of 120 mM KCl, 30 mM tris-chloride, 6.3 mM EDTA, 1 mM NADPH and 0.6 mM DTNB at pH 7.4. The cycling reaction was initiated by addition of 4 units of glutathione reductase/ml. The rate of 5-thio-2-nitrobenzoate formation at 412-540 nm was directly proportional to glutathione concentration. A standard curve was constructed with known concentrations of glutathione. Sample concentrations were calculated as μmoles glutathione per mg of mitochondrial protein.

Manganese Superoxide Dismutase Assay. Mitochondrial superoxide dismutase (SOD) was assayed by its ability to inhibit the reaction of nitroblue tetrazolium (NBT) with superoxide anion radical [8]. Mitochondria were sonicated as described above. For each sample, 10 cuvettes were prepared with 0-400 μl of sonicate in each. The final volume was adjusted to 1 ml with 120 mM KCl, 40 mM tris-chloride, 2 mM NaCN, 6 mM EDTA and 0.05 mM NBT at pH 7.8. Following the addition of 2 μM riboflavin, the cuvettes were illuminated uniformly in a dark-light box with a 25 watt cylindrical fluorescent light. Superoxide radical, generated by the reaction of photoreduced riboflavin with oxygen, reduces the colorless NBT to a blue formazan (absorbance maximum 560 nm). SOD present in the sonicate inhibits color formation by converting superoxide radical to H_2O_2 and O_2. Cyanide inhibits any contaminating Cu-Zn superoxide dismutase, the cytoplasmic isoenzyme. Optical density at 560-700 nm is inversely proportional to the logarithm of SOD activity. Best fit exponential curves of sonicate added versus optical density change were constructed by computer and the quantity of sonicate needed for 50% inhibition of color formation (defined as 1 unit of SOD) was calculated. SOD activities were calculated as units per mg of mitochondrial protein.

Ubiquinone Assay. Heart, kidney and liver mitochondrial suspensions were analyzed for ubiquinone by high pressure liquid chromatography using a $C_{18\text{-}5}$ column as previously described [33].

Statistical Analysis. Animals were grouped according to age and the results of the fetal and adult groups were compared individually with all other groups by one-way analysis of variance (ANOVA). Significant

differences were confirmed using Dunnett's test. Additional information is provided in the Results and figure legends.

RESULTS

NAD(P)H Oxidation. Heart, kidney and liver mitochondria from fetal and newborn animals were assayed for their ability to reduce selenite and tBOOH. Figure 1 illustrates selenite and tBOOH induced oxidation of endogenous NAD(P)H in isolated mitochondria. Selenite catalyzes the non-enzymatic oxidation of glutathione (GSH) forming glutathione disulfide (GSSG) [43]. The metabolism of tBOOH involves glutathione peroxidase which utilizes GSH to reduce tBOOH to an alcohol, also forming GSSG. Once formed, GSSG is reduced by glutathione reductase consuming mitochondrial NADPH. NADH is also oxidized via the transhydrogenase reaction [36].

Age related differences in mitochondrial NAD(P)H oxidation rates with selenite and tBOOH are shown in Figure 2. Mitochondria were suspended in buffered medium and the rate of endogenous NAD(P)H oxidation was determined following the addition of selenite or tBOOH as described above. Rates are dependent on the age of the animal and the tissue used. Fetal kidney mitochondria (day 0) exhibit low rates of selenite and tBOOH metabolism. Rates decline further during the first day and then rise steadily with age resulting in adult values which are 3-4 fold higher than fetal values. Heart mitochondria display low NAD(P)H oxidation rates with both selenite and tBOOH at all ages. Rates with selenite and tBOOH at 4-5 days, however, were significantly decreased from adult values. Liver mitochondria display a much

different pattern. Fetal NAD(P)H oxidation rates with selenite and tBOOH are high and decline rapidly during the first day. Rates with tBOOH remain low up to 8 days with adult rates persisting approximately 32% below fetal values. Rates with selenite are lowest at day 2 then increase slightly up to day 8-9; adult rates are comparable to those of the fetal group. Note that selenite-induced NAD(P)H oxidation rates are consistently higher than those obtained with tBOOH (Figures 1 & 2), suggesting that glutathione peroxidase, and not GSSG reduction, is rate limiting in tBOOH metabolism. To summarize, isolated mitochondria exhibit large age and tissue dependent differences in selenite and tBOOH-induced NAD(P)H oxidation rates with similar patterns of change for both oxidants.

Glutathione Reductase and Peroxidase Activities. In order to better understand the age dependent differences in NAD(P)H oxidation, mitochondrial glutathione reductase and peroxidase activities were assayed as described above. Several important differences require emphasis. First, fetal mitochondria possess the highest glutathione reductase activities in all tissues tested (Figure 3A). Activity drops in all tissues during the first day with adult values remaining 15-33% below fetal values. Kidney mitochondria exhibit higher glutathione reductase activities than liver or heart at all ages studied. Glutathione peroxidase activity of all mitochondria follow a similar age dependent pattern, although significant tissue specific differences exist (Figure 3B). Most notably, mitochondrial glutathione peroxidase activities in fetal and newborn liver are higher than those of kidney or heart. Adult values in liver and kidney are similar, while the

activities in heart mitochondria remain much lower.

An interesting paradox emerges when the mitochondrial glutathione reductase activities are compared with the selenite-induced NAD(P)H oxidation rates in intact mitochondria. Since selenite rapidly oxidizes GSH forming GSSG, the rate of endogenous NAD(P)H oxidation with selenite should reflect mitochondrial glutathione reductase activity (Figure 1). As expected, mitochondrial glutathione reductase activity (Figure 3A) shows some correlation with the selenite-induced NAD(P)H oxidation rate (Figure 2A) in liver ($r = 0.73$) and heart ($r = 0.81$). In sharp contrast, glutathione reductase activities in kidney mitochondria do not correlate ($r = 0.21$) with the selenite-induced NAD(P)H oxidation rates. In fetal kidney mitochondria (Figure 2A), when NAD(P)H oxidation rates are low, glutathione reductase activities are at their highest (Figure 3A). Conversely, in adult kidney mitochondria, glutathione reductase activities are 80% of fetal values and selenite-induced NAD(P)H oxidation rates are paradoxically 300% higher. Changes in glutathione reductase activities may explain age-related differences in selenite-induced NAD(P)H oxidation rates in heart and liver but other factors are clearly involved in kidney mitochondria.

Another paradox exists between tBOOH-induced NAD(P)H oxidation rates in intact mitochondria and mitochondrial glutathione peroxidase activities. NAD(P)H oxidation rates with tBOOH should reflect endogenous glutathione peroxidase activity. The peroxidase utilizes GSH to reduce tBOOH to an alcohol forming GSSG. GSSG is then reduced (via glutathione reductase) consuming NAD(P)H (Figure 1). For heart

mitochondria, this assumption appears to hold true; tBOOH-induced NAD(P)H oxidation rates (Figure 2B) parallel endogenous glutathione peroxidase activity (Figure 3B). Additionally, mitochondrial glutathione peroxidase activities in fetal kidney are 41% lower than fetal liver and, as expected, tBOOH-induced NAD(P)H oxidation rates in fetal kidney mitochondria are equally low (42%) when compared to fetal liver mitochondria. This assumption fails when liver mitochondria from older animals are compared to those of kidney. Kidneys from animals over 2 days of age have mitochondrial glutathione peroxidase activities which are consistently lower than those of the liver (Figure 3B), yet kidney mitochondria display paradoxically high tBOOH-induced NAD(P)H oxidation rates; up to 280% higher than liver mitochondria. The rates of tBOOH metabolism in intact mitochondria reflect glutathione peroxidase activities for heart, as well as, fetal kidney and liver mitochondria. Other factors appear to regulate tBOOH metabolism in older (>2 day) kidney and liver mitochondria.

Mitochondrial Glutathione Content. Since the selenite and tBOOH-induced NAD(P)H oxidation rates could be limited by substrate availability, the endogenous glutathione content of the isolated mitochondria were determined (Table I). Heart and liver mitochondria show no consistent age related change in total glutathione content. In contrast, kidney mitochondria exhibited a steady decline in total glutathione as the age of the animal increased; adult values for kidney mitochondria were 24% of fetal values. Values in kidney mitochondria from adult animals were also significantly lower than those of adult heart (39%) or liver (13%) mitochondria ($\alpha < 0.025$). Glutathione

concentrations do not limit tBOOH or selenite-induced NAD(P)H oxidation rates since adult kidney mitochondria have the lowest GSH content and yet exhibit the highest NAD(P)H oxidation rates.

Adenine and Pyridine Nucleotides. Several nucleotides are known inhibitors of glutathione peroxidase [22,23,52]. NADPH and NADP+ inhibit activity 30 to 55% at concentrations of 0.26 and 0.7 mM respectively. Figure 4 displays the total NADP(H) concentrations in isolated heart, kidney and liver mitochondria as a function of age. Note that liver mitochondria possess 2.5 - 5.6 fold higher NADP(H) levels than heart or kidney. ATP is also known to affect glutathione peroxidase activity, causing 30% inhibition at 0.7 mM concentrations [22]. Table II shows adenine nucleotide concentrations in isolated heart, kidney and liver mitochondria as a function of age. Heart and liver show significant increases in mitochondrial adenine nucleotides with age, however, no change in kidney mitochondria was detected.

Superoxide Dismutase Activity. Heart, kidney and liver mitochondrial superoxide dismutase (SOD) activities were significantly ($\alpha < 0.01$) higher in adults than in fetal animals (Figure 5). Note the liver mitochondria initially showed a significant drop ($\alpha < 0.05$) in SOD at day 4, whereas heart SOD activity rose significantly by day 5-6. Higher SOD activities suggest augmented superoxide radical formation by the mitochondrial respiratory chain. Since the rate of mitochondrial superoxide generation is known to increase linearly with ubiquinone concentration [44], the ubiquinone content of isolated heart, kidney and liver mitochondria from animals of various ages were determined. Animals were placed into groups according to age. As previously

described [33], mitochondrial ubiquinone increased post-birth in all 3 tissues (data not shown). Figure 6 shows the ubiquinone content versus SOD activity for each age group. The changes in ubiquinone correlated well with the changes in SOD activity in heart ($R = 0.97$) and kidney ($R = 0.94$) mitochondria. The correlation in liver mitochondria was insignificant ($R = 0.52$, $\alpha = 0.14$).

DISCUSSION

Isolated mitochondria show large age and tissue specific differences in selenite and tBOOH-induced NAD(P)H oxidation rates (Figure 2). Both oxidants exhibit similar patterns of change which correspond to known differences in tissue PO_2. For example, fetal rates are highest in liver mitochondria, the organ experiencing the highest PO_2 in utero [17]. Rates in kidney are lower, reflecting a lower P_aO_2 supply. After birth, circulatory changes elevate the systemic P_aO_2 [15,32] thereby increasing average tissue PO_2 [27,37] in the kidney; liver tissue PO_2 remains the same or declines [17]. As expected, newborn (>2 day) and adult oxidant-induced NAD(P)H oxidation rates are higher in kidney and lower in liver. Heart shows little variation in rates, possibly reflecting increased oxygen consumption [6] and clustering [16] of mitochondria following birth, thereby effectively maintaining a low PO_2 at the mitochondrial inner membrane despite increased average tissue PO_2.

Interestingly, oxidant-induced NAD(P)H oxidation rates in kidney mitochondria are 3-4 fold higher in the adult than in the fetus. This large difference in rates cannot be explained by elevated glutathione

reductase or peroxidase activities. In fact, adult kidney mitochondrial glutathione reductase activities are 70% of fetal values, yet selenite-induced NAD(P)H oxidation rates are 300% higher. Likewise, kidney glutathione peroxidase activities are similar in the fetal and adult period despite 460% higher tBOOH-induced NAD(P)H oxidation rates in the adult. A similar discrepancy exists between tBOOH-induced NAD(P)H oxidation rates and glutathione peroxidase activity in liver and kidney. Newborn (>2 day) and adult liver mitochondria have elevated or similar glutathione peroxidase activities when compared to kidney mitochondria of the same age. Intact kidney mitochondria, however, consistently display higher NAD(P)H oxidation rates than age-matched liver mitochondria. Therefore, mitochondrial glutathione reductase and peroxidase activities in sonicated mitochondria are not necessarily indicative of the antioxidant function of the intact organelle. Estimation of antioxidant function merely on the basis of enzyme activities in disrupted mitochondria may be misleading since other factors appear to be regulating the activities of these antioxidant defense enzymes in situ.

Several factors present in the mitochondrial matrix are known regulators of glutathione peroxidase and reductase activity. NADPH and $NADP^+$ inhibit glutathione peroxidase activity 30 - 50% at 0.26 mM and 0.7 mM concentrations, respectively [22,23]. Figure 4 reveals 2.5-5.6 fold higher NADP(H) levels in liver mitochondria than those of kidney or heart. This corresponds to matrix NADP(H) concentrations of 4.2 -5.0 mM in liver mitochondria, assuming a matrix volume of 1 μl per mg mitochondrial protein. Therefore, NADP(H) inhibition of glutathione

peroxidase in situ may be responsible for lower tBOOH-induced NAD(P)H oxidation rates despite higher glutathione peroxidase activity in older (>2 day) liver versus kidney mitochondria. Incubation of glutathione reductase with NADPH or NADH causes reversible inactivation of the enzyme. This type of inhibition may have an important regulatory role [24]. Adenine ribonucleotides are competitive inhibitors of glutathione peroxidase with increased hydroperoxide levels enhancing the inhibitory effect [22]. No correlation, however, was found between the age-related changes in mitochondrial ATP content (Table II) and tBOOH-induced NAD(P)H oxidation rates. Coenzyme A is also a potent inhibitor of glutathione peroxidase with a K_i of < 5 μM. Binding the sulfhydryl group of Coenzyme A reduces the inhibitory effectiveness 6-fold [23]. All these potential regulators are present within the mitochondria at concentrations known to affect the enzymatic rate. Therefore, mitochondrial antioxidant function, estimated solely by enzyme activities in disrupted mitochondria, should be interpreted with caution.

Superoxide dismutase activities are higher in adult heart, kidney and liver mitochondria when compared to the fetus (Figure 5) suggesting heightened superoxide radical production in adult mitochondria. Similar increases in rat brain mitochondrial SOD following birth have been described [28]. Two known factors which influence the rate of superoxide formation by mitochondria require emphasis. First, the rate of superoxide formation increases linearly with the pO_2 at the mitochondrial inner membrane [44,45]. This depends, in part, on changes in organ blood flow and incoming P_aO_2, factors which vary with

perinatal age and the tissue in question. For example, in utero, the liver receives oxygenated blood directly from the placenta via the umbilical vein. After birth, the liver receives approximately 90% of its blood supply from the splanchnic bed, a low PO_2 source [13,17]. In contrast, heart and kidney have a systemic arterial supply which dramatically increases in oxygen tension post-birth. Tissue and age related changes in mitochondrial clustering [20], oxygen consumption rates and diffusion distances from the capillary wall [19] will also contribute to the pO_2 adjacent to the inner mitochondrial membrane. Secondly, the concentration of mitochondrial ubiquinone, the predominant site of superoxide radical formation [44], is known to increase in heart, kidney and liver post-birth [33]. Assuming the pO_2 at the inner membrane does not change, mitochondrial superoxide formation should increase with ubiquinone content. In fact, mitochondrial SOD activity correlates well with ubiquinone content in heart and kidney (Figure 6). In conclusion, the rise in mitochondrial SOD from the fetal to adult period is a complex phenomenon. Although the exact etiology remains speculative, the rise in SOD activity suggests heightened mitochondrial superoxide radical generation. The postnatal increase in heart and kidney mitochondrial ubiquinone could indirectly lead to elevated SOD activity by increasing the rate of superoxide radical formation [44]. In liver mitochondria, the lack of correlation between ubiquinone content and SOD activity suggests that other factors (e.g., pO_2, other sources of superoxide, translobular heterogeneity) may be operative in liver.

Selenite or tBOOH-induced oxidation of endogenous NAD(P)H in

intact mitochondria may be a more reliable indicator of mitochondrial antioxidant function than determination of enzyme activities in disrupted mitochondria. Nevertheless, other yet unstudied pathways may interfere with interpretation of data obtained by this method. In certain cell types, GSSG formed during oxidant metabolism can be actively extruded from the cell [39]. A similar GSSG transport system may exist in mitochondria which could compete with glutathione reductase for GSSG, thereby decreasing the NAD(P)H oxidation rate. In addition, succinate with rotenone, used as substrate in these experiments, may give falsely low NAD(P)H oxidation rates in the presence of $NADP^+$-malate dehydrogenase. Heart mitochondria are known to contain substantial levels of this enzyme [1], possibly accounting for the low levels of oxidant-induced NAD(P)H oxidation (Figures 2). $NADP^+$-malic enzyme may also be an important source of reducing equivalents necessary for mitochondrial oxidant detoxification. The significance of mitochondrial GSSG transport and $NADP^+$-malate dehydrogenase activity in the mitochondrial antioxidant defense system are currently under investigation.

Mitochondrial antioxidant function may provide resistance to oxidative stress in the newborn period by stabilizing the mitochondrial calcium pool. Mitochondria continually cycle Ca^{2+} through separate uptake and efflux systems. Under normal conditions, low steady-state extramitochondrial Ca^{2+} concentration is maintained against a continual slow efflux by an active Ca^{2+} uniport [7]. Oxidation of mitochondrial NAD(P)H, by a variety of substances, accelerates Ca^{2+} efflux, possibly through activation of a Ca^{2+}/H^+ antiport [11,34]. Efflux initiates a

futile Ca^{2+} cycle as the uniport system actively takes up released Ca^{2+}. ATP levels drop since Ca^{2+} uptake continues at the expense of ATP production [31] and extramitochondrial ATP becomes hydrolyzed to maintain active uptake. During the newborn period, the mitochondrial antioxidant system displays significantly lower oxidant-induced NAD(P)H oxidation rates than those of adult animals (Figure 2). Lower NAD(P)H oxidation should prevent mitochondrial Ca^{2+} efflux. To support this, liver mitochondria from newborn animals are indeed less susceptible to oxidant-induced Ca^{2+} efflux than those of adult animals [46]. The ability of the mitochondrial antioxidant system to resist NAD(P)H oxidation in the newborn period may provide tolerance to oxidative challenge by stabilizing the mitochondrial Ca^{2+} pool.

To summarize, the following conclusions and inferences can be made: (1) Intact mitochondria from newborn animals were less susceptible than those of adults to oxidant-induced NAD(P)H oxidation. Since mitochondrial calcium efflux has been linked to oxidant-induced NAD(P)H oxidation, the newborn's resistance to oxidant-induced NAD(P)H oxidation, and thus calcium efflux, may underly their tolerance to hyperoxia [10,50] and other exogenous oxidants [46]. (2) Age and tissue specific differences in mitochondrial glutathione reductase do exist. In the term fetus, mitochondrial glutathione reductase activities were higher than those of the newborn or adult groups. Activity dropped during the first day in all tissues studied with adult values which remained below those of the fetus. Mitochondrial glutathione peroxidase showed a similar age-dependent pattern; activities declined post-birth in all three tissues. (3) Mitochondrial

SOD activities were increased in adult mitochondria as compared to fetal or newborn animals. This suggests an increase in the rate of superoxide radical generation by the mitochondria. (4) NAD(P)H oxidation rates in intact mitochondria were not consistently correlated with glutathione reductase and peroxidase activities in disrupted mitochondria. This finding suggests involvement of additional endogenous regulatory factors in antioxidant-related responses in situ.

ACKNOWLEDGEMENTS

The authors wish to thank Stephanie Thompson for her help in the preparation of the manuscript.

These studies were supported in part by a grant from the National Institutes of Health (GM-33267). Angelo A. Vlessis is an M.D./Ph.D. scholar supported by the Medical Research Foundation of Oregon.

TABLE I

Total glutathione content of isolated kidney, heart, and liver mitochondria from animals of various ages.

AGE (days)	KIDNEY	HEART	LIVER
Fetus (term)	5.1 ± 0.3 (3)	3.6 ± 0.3 (3)	9.8 ± 3.4 (4)
0.5 ± 0.4	4.0 ± 1.6 (7)	4.2 ± 0.9 (6)	10.6 ± 2.4 (7)
1.1 ± 0.1	4.0 ± 1.9 (4)	3.7 ± 2.0 (4)	7.5 ± 2.3 (3)
3.0 ± 0.5	3.6 ± 0.5 (3)*	4.5 ± 1.2 (4)	6.9 ± 2.4 (5)
5.2 ± 0.3	3.2 ± 1.7 (7)	4.5 ± 1.4 (6)	8.9 ± 2.9 (7)
8.1 ± 1.8	1.7 ± 0.8 (5)**	2.4 ± 1.0 (5)	8.2 ± 0.4 (5)
Adult	1.2 ± 0.8 (7)**	3.2 ± 1.6(6)	9.7 ± 1.6 (6)

Values are expressed as means +/- one standard deviation. Numbers in parentheses are the numbers of animals in each group.

* and ** denote a significant difference of $\alpha < 0.01$ and $\alpha < 0.001$ from the fetal group respectively.

TABLE II

Adenine ribonucleotide content (ATP + ADP + AMP) of isolated kidney, heart and liver mitochondria from animals of various ages (values expressed as nmoles/mg protein).

AGE (days)	KIDNEY	HEART	LIVER
Fetus (term)	10.2 ± 1.7 (4)	14.6 ± 1.7 (4)	13.9 ± 0.6 (4)
0.5 ± 0.3	10.8 ± 1.4 (4)	14.6 ± 1.6 (4)	17.8 ± 0.7 (4)*
3.2 ± 0.3	11.8 ± 3.0 (4)	14.5 ± 1.9 (4)	14.8 ± 1.8 (4)
9.0 ± 1.0	10.3 ± 0.8 (5)	14.1 ± 1.4 (5)	15.5 ± 1.3 (5)
Adult	12.1 ± 1.1 (4)	22.1 ± 1.3 (4)**	15.3 ± 0.5 (4)

Values are expressed as means +/- one standard deviation. Numbers in parentheses are the numbers of animals in each group.

* and ** denote a significant difference of $\alpha < 0.025$ and $\alpha < 0.001$ from the fetal group, respectively.

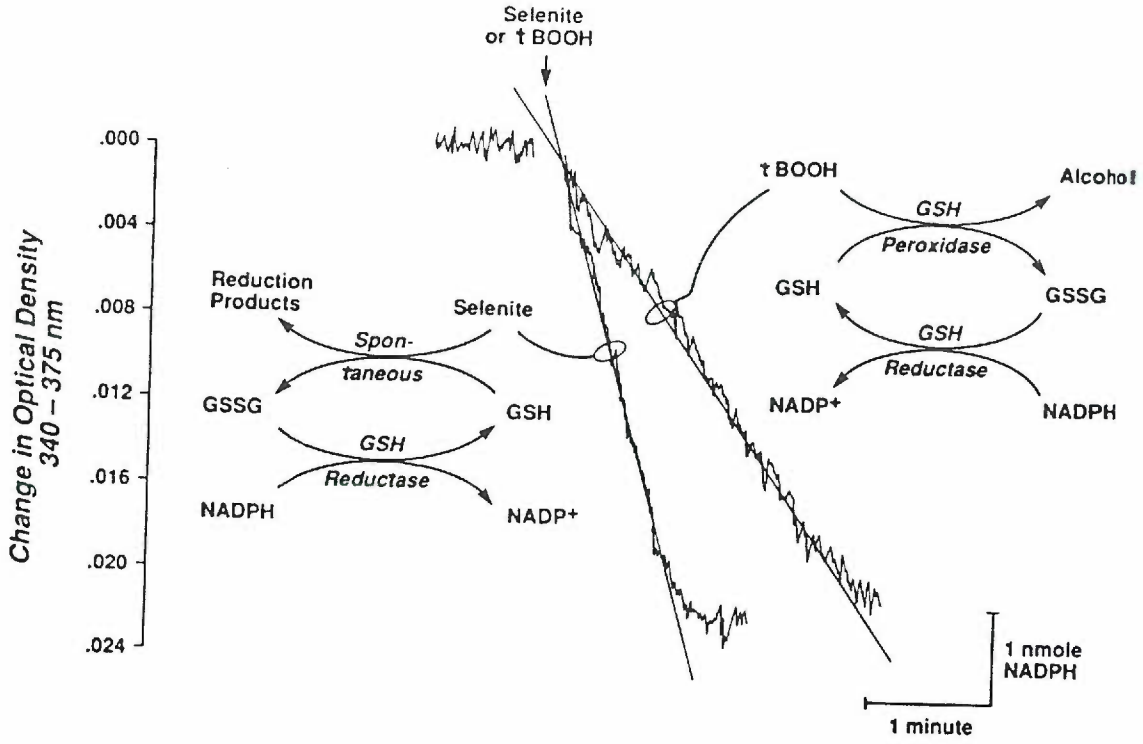

Figure 1. Oxidation of endogenous NAD(P)H by selenite and tBOOH in isolated liver mitochondria from a 7.2 day old animal. Mitochondria were suspended in buffered medium at 1.55 mg protein/ml and endogenous NAD(P)H was monitored kinetically at 340-375nm as described in Materials and Methods. Two tracings are shown superimposed in which either selenite (500 μM) or tBOOH (500 μM) were added to initiate NAD(P)H oxidation. Rates were calculated from the slope of a line drawn through each tracing. A simplified schematic of the metabolic pathways leading to NAD(P)H oxidation is shown for each oxidant.

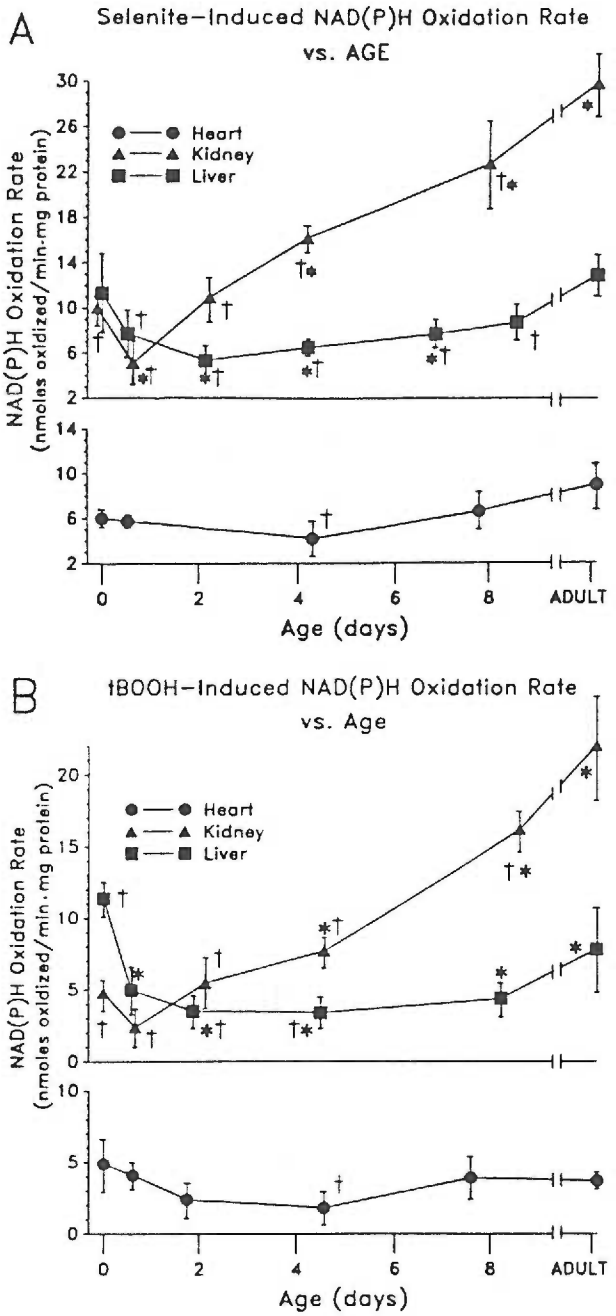

Figure 2. Rate of A) selenite and B) tBOOH-induced NAD(P)H oxidation by isolated heart, kidney and liver mitochondria from fetal (day 0), newborn and adult animals. Rates were calculated as described in the legend to Figure 1. Each symbol depicts the mean NAD(P)H oxidation rate and age of each group. The bracket includes +/- one standard deviation from the mean. The n values averaged 5 with a range of 3-8 animals in each group.

* and † denotes a significant difference of at least $\alpha < 0.05$ from the fetal and adult group respectively.

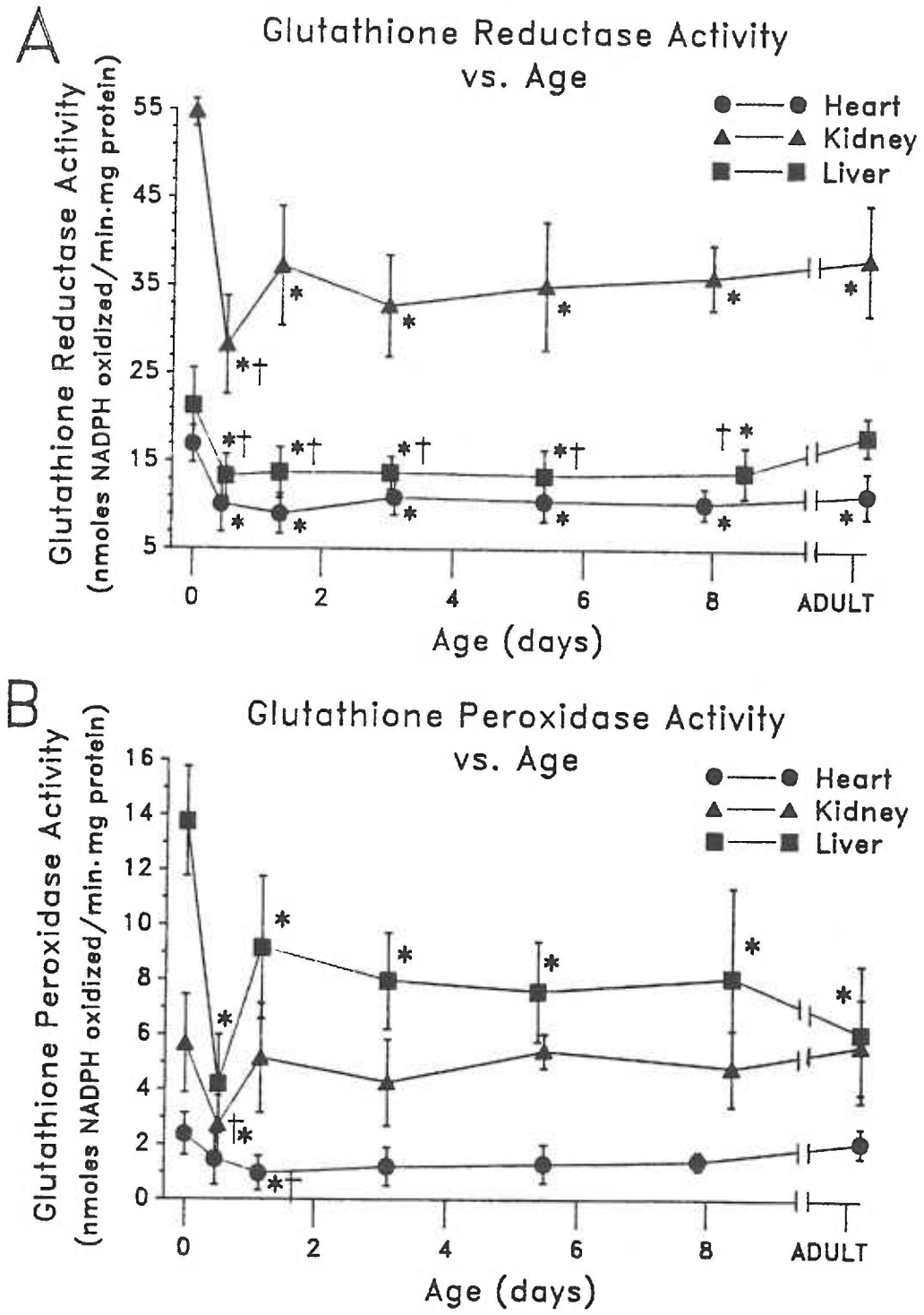

Figure 3. Glutathione reductase A) and peroxidase B) activity in sonicated heart, kidney and liver mitochondria from fetal (day 0), newborn and adult animals. Each symbol depicts the mean enzyme activity and age for each group. The bracket includes +/- one standard deviation from the mean. The n values averaged 6 with a range of 3-9 animals in each group.

* and † denotes a significant difference of at least $\alpha < 0.05$ from the fetal and adult group respectively.

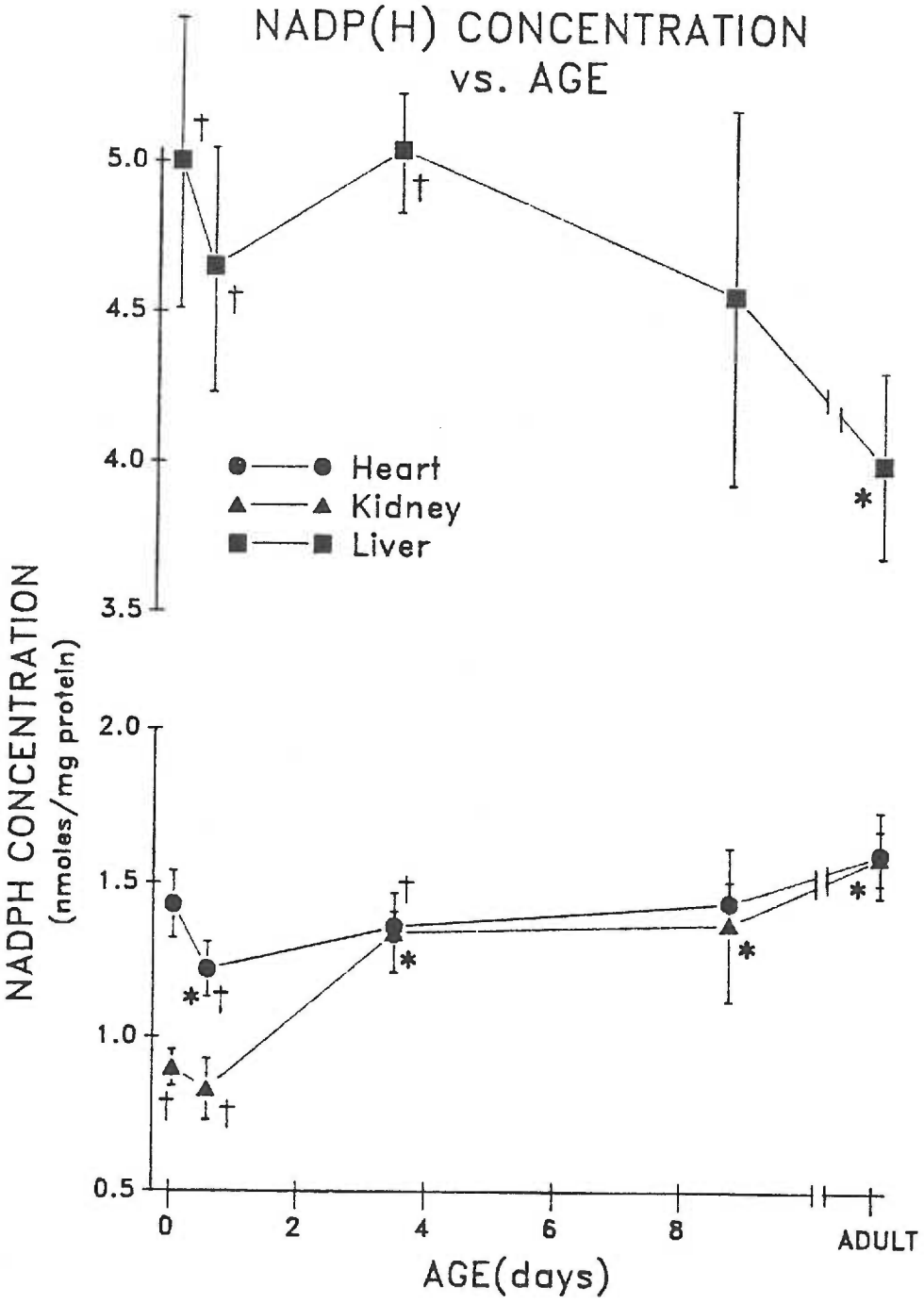

Figure 4. NADP(H) concentration in isolated heart, kidney and liver mitochondria from fetal (day 0), newborn and adult animals. Each symbol depicts the mean NAD(P)H concentration and age for each group. The bracket includes +/- one standard deviation from the mean (n = 4 or 5 animals in each group).
* and † denotes a significant difference of at least $\alpha < 0.05$ from the fetal and adult group respectively.

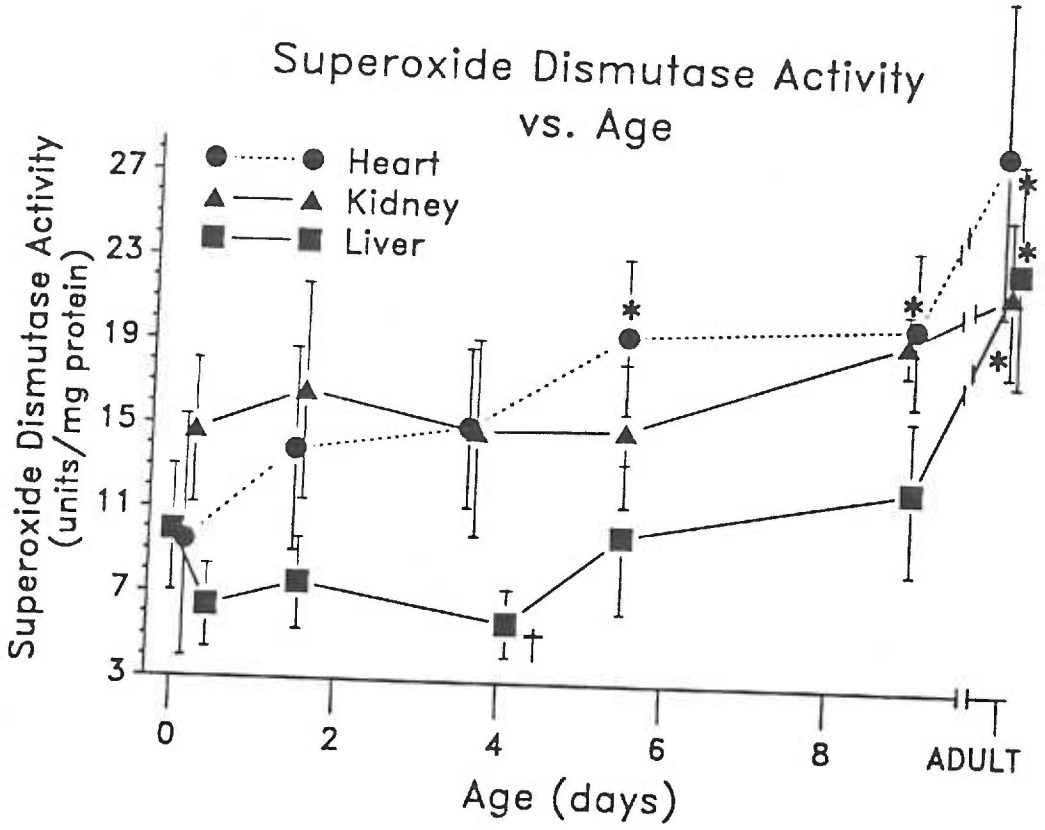

Figure 5. Mitochondrial SOD activity in sonicated mitochondria from fetal (day 0), newborn and adult animals. Each symbol depicts the mean SOD activity and age for each group. The bracket includes +/- one standard deviation. The n values averaged 5 and ranged from 3-7 animals in each group.

* and † denotes a significant difference of $\alpha < 0.01$ and $\alpha < 0.05$ respectively from the fetal group.

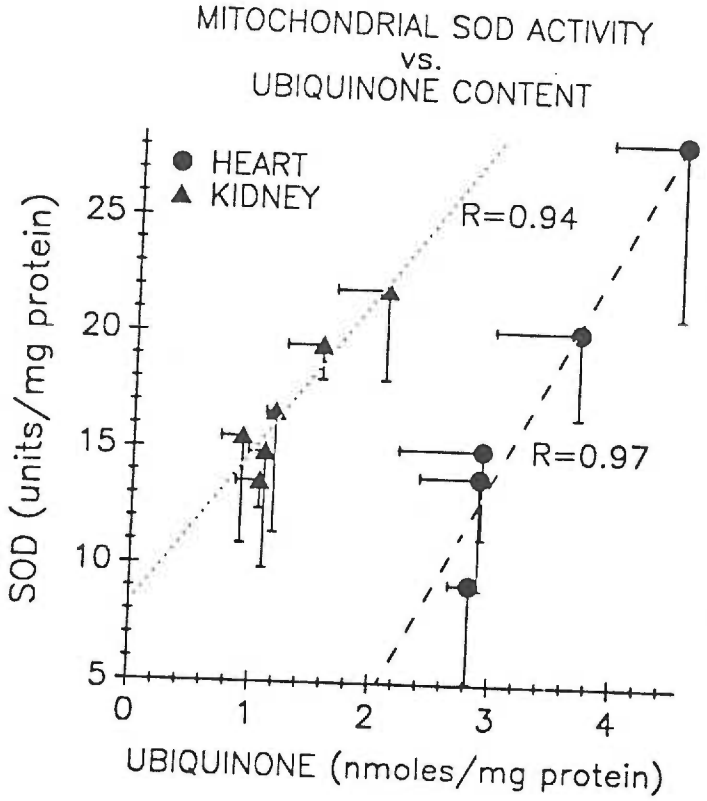

Figure 6. Mitochondrial ubiquinone content versus SOD activity in heart and kidney mitochondria from animals of various ages. Animals were placed into groups according to animal age. Each symbol depicts the mean value obtained from each age group. The brackets below and left of each symbol include one standard deviation from the mean SOD activity and ubiquinone content respectively. The n values for each group averaged 5 and ranged from 3-7 animals in each group. Both correlations are significant at $\alpha < 0.002$.

REFERENCES

1. Andres, A., J. Satrustegui, and A. Machado. 1980. Development of NAD(P)H-producing pathways in rat heart. *Biochem. J.* 186:799-803, 1980.

2. Beatrice, M.C., D.L. Stiers, and D.R. Pfeiffer. The role of glutathione in retention of Ca^{2+} by liver mitochondria. *J. Biol. Chem.* 259:1279-1287, 1984.

3. Brook, W.H., S. Connell, J. Cannata, J.E. Maloney, and A.M. Walker. Ultrastructure of the myocardium during development from early fetal life to adult life in sheep. *J. Anat.* 137:729-741, 1983.

4. Chance, B., H. Sies, and A. Boveris. Hydroperoxide metabolism in mammalian organs. *Physiol. Rev.* 59:527-605, 1979.

5. Fischer, D.J., M.A. Heymann, and A.M. Rudolph. Regional myocardial blood flow and oxygen delivery in fetal, newborn and adult sheep. *Am. J. Physiol.* 243:H729-H731, 1982.

6. Fischer, D.J., M.A. Heymann, and A.M. Rudolph. Myocardial consumption of oxygen and carbohydrates in newborn sheep. *Pediatr. Res.* 15:843-846, 1981.

7. Fiskum, G. and A.L. Lehninger. Mitochondrial regulation of intracellular calcium. IN: Calcium and Cell Function, Vol. II, edited by W.Y. Cheung. New York: Academic Press, Inc., 1982, p. 39-80.

8. Flohe, L. and F. Otting. Superoxide dismutase assays. *Methods in Enzymology*. 105:93-104, 1984.

9. Frank, L. and E.E. Groseclose. Preparation for birth into an O_2-

rich environment: the antioxidant enzymes in the developing rat lung. *Ped. Res.* 18:240-244.

10. Sosenko IRS, Frank L 1987. Guinea pig lung development: Antioxidant enzymes and premature survival in high O_2. *Am J Physiol* 252:R693-R698.

11. Frei, B., K.H. Winterhalter, C. Richter. Quantitative and mechanistic aspects of hydroperoxide-induced release of Ca^{2+} from rat liver mitochondria. *Eur. J. Biochem.* 149:633-639, 1985.

12. Fridovich, I. Superoxide dismutase in biology and medicine. IN: Pathology of Oxygen, edited by A.P. Autor. New York: Academic Press, Inc., 1982, p. 1-17.

13. Gleason, C.A., C. Roman, and A.M. Rudolph. Hepatic oxygen consumption, lactase uptake and glucose production in neonatal lambs. *Circ. Res.* 19:1235-1239, 1985.

14. Griffith, O.W. Determination of glutathione and glutathione disulfide using glutathione reductase and 2-vinyl pyridine. *Anal. Biochem.* 106:207-212, 1980.

15. Harris, A.P., M.J. Sendak, and R.T. Donham. Changes in arterial oxygen immediately after birth in the human neonate. *J. Pediatrics.* 109:117-119, 1986.

16. Heinz, D., R. Meyer, I. Marx, H. Guski, and K. Wenzelides. Morphometric characterization of left ventricular myocardial cells of male rats during postnatal development. *J. Mol. Cell Cardiol.* 11:631-638, 1979.

17. Holzman, I.R. Fetal and neonatal hepatic perfusion and oxygenation. *Sem. Perinatol.* 8:234-244, 1984.

18. Itskovitz, J., B.W. Goetzman, C. Roman, and A.M. Rudolph. Effects of fetal-maternal exchange transfusion on fetal oxygenation and blood flow distribution. *Am. J. Physiol.* 247:H655-H660, 1984.

19. Jones, D.P. Intracellular diffusion gradients of O_2 and ATP. *Am. J. Physiol.* 250:C663-C675, 1986.

20. Jones, D.P. Effect of mitochondrial clustering on O_2 supply in hepatocytes. *Am. J. Physiol.* 247:C83-C89, 1984.

21. Lehninger, A.L., A. Vercesi, and E.A. Bababunmi. Regulation of Ca^{2+} release from mitochondria by the oxidation-reduction state of pyridine nucleotides. *Proc. Natl. Acad. Sci. USA.* 75:1690-1694, 1978.

22. Little, C., R.M. Olinescu, K.G. Reid, and P.J. O'Brien. Properties and regulation of glutathione peroxidase. *J. Biol. Chem.* 245:3632-3636, 1970.

23. Little, C., R.M. Olinescu, and P.J. O'Brien. Inhibition of glutathione peroxidase by coenzyme A. *Biochem. Biophys. Res. Comm.* 41:287-293, 1970.

24. Lopez-Barea, J., and C.Y. Lee. Mouse-liver glutathione reductase. Purifications, kinetics, and regulation. *Eur. J. Biochem.* 98:487-499, 1979.

25. Lotscher, H.R., K.H. Winterhalter, E. Carafoli, and C. Richter. Hydroperoxide-induced loss of pyridine nucleotides and release of calcium from rat liver mitochondria. *J. Biol. Chem.* 255:9925-9930, 1980.

26. Lowry, O.H., N.J. Rosebrough, A.L. Farr, and R.J. Randall.

Protein measurement with the folin phenol reagent. *J. Biol. Chem.* 193:265-275, 1951.

27. Lubbers, D.W. Local tissue PO_2: Its measurement and meaning. IN: Oxygen Supply, edited by M. Kessler. Baltimore, Maryland: University Park Press, 1973, p. 151-155.

28. Mavelli, I., A. Rigo, R. Federico, M.R. Ciriolo, G. Rotilio. Superoxide dismutase, glutathione peroxidase, and catalase in developing rat brain. *Biochem. J.* 204:535-540, 1982.

29. McCarthy, K., M. Bhogal, M. Naudi, and D. Hart. Pathogenic factors in bronchopulmonary dysplasia. *Pediatr. Res.* 18:483-488, 1984.

30. McIntyre, T.M. and N.P. Curthoys. The interorgan metabolism of glutathione. *Int. J. Biochem.* 12:545-551, 1980.

31. Mela, L. Mechanism and physiological significance of calcium transport across mammalian mitochondrial membranes. IN: Current Topics in Membranes and Transports, Vol. 9., edited by F. Bronner and A. Kleinzeller. New York: Academic Press, Inc., 1977, p. 321-362.

32. Mela, L., C.W. Goodwin, and L.D. Miller. Correlations of mitochondrial cytochrome concentrations and activity to oxygen availability in the newborn. *Biochem. Biophys. Res. Comm.* 64:384-390, 1975.

33. Vlessis AA, Mela-Riker L 1988 I. Perinatal development of the mitochondrial respiratory chain and oxidative phosphorylation. Submitted to Pediatr. Res.

34. Nicholls, D.G., and M.D. Brand. The nature of calcium ion efflux

induced in rat liver mitochondria by the oxidation of endogenous nicotinamide nucleotides. *Biochem. J.* 188:113-118, 1980.

35. Podrazky, V., and F.S. Steven. Reversible inhibition by its coenzyme as a source of error in glutathione reduction assays. *Clinica. Chimica. Acta.* 137:349-354, 1984.

36. Reed, D.J. Regulation of reductive processes by glutathione. *Biochem. Pharmacol.* 35:7-13, 1986.

37. Schuchhardt, S. Myocardial oxygen pressure: mirror of oxygen supply. *Adv. Exp. Med. Biol.* 191:21-35, 1984.

38. Sies, H., and K.M. Moss. A role of mitochondrial glutathione peroxidase in modulating mitochondrial oxidations in liver. *Eur. J. Biochem.* 84:377-383, 1978.

39. Sies, H., and T.P.M. Akerboom. Glutathione disulfide (GSSG) efflux from cells and tissues. *Methods in Enzymology.* 105:445-451, 1984.

40. Stocci V., L. Cucchiarini, M. Magnani, L. Chiarantini, P. Palma, and G. Crescentini. Simultaneous extraction and reverse-phase high performance liquid chromato-graphic determination of adenine and pyridine nucleotides in human red blood cells. *Anal. Biochem.* 146:118-124, 1985.

41. Tanswell, K.A., and B.A. Freeman. Pulmonary antioxidant enzyme maturation in fetal and neonatal rat. I. Developmental profiles. *Ped. Res.* 18:584-587, 1984.

42. Tappel, A.L. Glutathione peroxidase and hydroperoxides. *Methods in Enzymology.* 105:506-513, 1984.

43. Tsen, C.C., and A.L. Tappel. Catalytic oxidation of glutathione

and other sulfhydryl compounds by selenite. *J. Biol. Chem.* 233:1230-1232, 1958.

44. Boveris A 1977 Mitochondrial production of superoxide radical and hydrogen peroxide. In: Reivich M, Coburn R, Lahiri S, Chance B (eds) Tissue Hypoxia and Ischemia. Plenum Press, New York, London, pp 67-81.

45. Turrens, J.F., B.A. Freeman, J.G. Levitt, and J.D. Crapo. The effect of hyperoxia on superoxide production by lung submitochondrial particles. *Arch. Biochem. Biophys.* 217:401-410, 1982a.

46. Vlessis, A.A., and L. Mela-Riker. Selenite-induced NAD(P)H oxidation and calcium release in isolated mitochondria: relationship to *in vivo* toxicity. *Mol. Pharmacol.* 31:643-646, 1987.

47. Widener, L.L., and L.M. Mela-Riker. Verapamil pretreatment preserves mitochondrial function and tissue magnesium in the ischemic kidney. *Circ. Shock.* 13:27-37, 1984.

48. Wispe, J.R., E.F. Bell, and R.J. Roberts. Assessment of lipid peroxidation in newborn infants and rabbits by measurements of expired ethane and pentane: influence of parenteral lipid infusion. *Pediatr. Res.* 19:374-379, 1985.

49. Wispe, J.R., M. Knight, and R.J. Roberts. Lipid peroxidation in newborn rabbits: effects of oxygen, lipid emulsion, and Vitamin E. *Pediatr. Res.* 20:505-510, 1986.

50. Yam, J., L. Frank, and R.J. Roberts. Oxygen toxicity: comparison of lung biochemical responses in neonatal and adult

rats. *Pediatr. Res.* 12:115-119, 1978.

51. Yoshioka, T., H. Motoyama, F. Yamasaki, and J. Noma. Lipid peroxidation and its protective mechanism during developmental stage in rat. *Acta. Obst. Gynaec. Jpn.* 34:966-970, 1982.

52. Zakowski, J.J., and A.L. Tappel. Purification and properties of rat liver mitochondrial glutathione peroxidase. *Biochem. Biophys. Acta.* 526:65-76, 1978.

American Journal Physiology, submitted in revised form, in review.

THE POTENTIAL ROLE OF MITOCHONDRIAL CALCIUM METABOLISM DURING REPERFUSION INJURY

by

Angelo A. Vlessis and Leena Mela-Riker

Departments of Surgery and Biochemistry

Oregon Health Sciences University

Portland, Oregon USA

ABSTRACT

Ischemia-reperfusion injury has been associated with intracellular H_2O_2 and superoxide radical production from accumulated hypoxanthine (HX) and xanthine oxidase (XO). The effect of H_2O_2 and superoxide radical on mitochondrial Ca^{2+} efflux was characterized in isolated renal mitochondria using a HX/XO system. Mitochondria were suspended in buffered medium containing 200 μM HX. Extramitochondrial Ca^{2+} was monitored kinetically at 660-685 nm using the Ca^{2+} indicator arsenazo III. After preloading mitochondria with 18-25 nmoles Ca^{2+}/mg protein, addition of XO to the medium caused a rapid oxidation of mitochondrial NAD(P)H followed by Ca^{2+} release. Ca^{2+} efflux was attributed to mitochondrial metabolism of H_2O_2 since efflux could be prevented with catalase but not superoxide dismutase. The Ca^{2+} efflux rate ($r = 0.995$) and lag time to Ca^{2+} efflux ($r = 0.987$) both correlate well with the NAD(P)H oxidation rate. Exogenous ATP prevents Ca^{2+} efflux in a dose-dependent fashion (K_m = 35 μM ATP) without affecting NAD(P)H oxidation; ATP plus oligomycin however did not prevent efflux. XO-induced Ca^{2+} efflux increased state 4 respiration 148% via a futile Ca^{2+} cycle involving the Ca^{2+}-uniport. The increase in state 4 respiration could be reversed with ruthenium red ($\alpha < 0.001$) or ATP ($\alpha < 0.01$); ATP plus oligomycin however had no effect. The results are discussed in relation to the oxygen free radical theory of reperfusion injury.

INTRODUCTION

In recent years, the role of oxygen radicals and hydrogen peroxide (H_2O_2) in ischemia-reperfusion injury has been realized [21,22,35] and the following scheme for the observed changes has been outlined.

During ischemia, anoxia results in the rapid hydrolysis of cellular ATP to AMP. Tissue hypoxanthine concentration increases as AMP is catabolized via adenosine and inosine [4,16]. The loss of ATP leads to the failure of ion pumps resulting in an increase in cytosolic Na^+ and Ca^{2+} [7,33]. Anaerobiosis also releases mitochondrial Ca^{2+} by reversal of the Ca^{2+}-uniport [5]. Elevated cytosolic Ca^{2+} is believed to activate a protease, via a calmodulin-dependent process [32], which converts xanthine dehydrogenase to xanthine oxidase (XO). In rat heart and kidney, the XO content has been shown to double after 8 and 30 minutes of non-perfusion, respectively [32].

During reperfusion, tissue oxygen tension rises and XO catalyzes the reaction of accumulated hypoxanthine to xanthine and xanthine to uric acid. The oxidation of fully reduced XO involves four steps. The first two steps are bivalent reductions forming hydrogen peroxide (H_2O_2), while the following two steps are univalent reductions forming superoxide anion radical [13,29].

$$\mathrm{XO(6)} \xrightarrow{H_2O_2} \mathrm{XO(4)} \xrightarrow{H_2O_2} \mathrm{XO(2)} \xrightarrow{O_2^-} \mathrm{XO(1)} \xrightarrow{O_2^-} \mathrm{XO(0)}$$

Evidence for the involvement of XO during reperfusion comes from

studies in which a trypsin inhibitor, used to prevent the proteolytic conversion of xanthine dehydrogenase to XO [32] and allopurinol, an inhibitor of XO, afforded protection against reperfusion-induced tissue injury in heart [4,21] and kidney [27]. In addition, recent direct measurements using electron paramagnetic resonance spectroscopy, have shown that the moment of reperfusion is accompanied by a burst of oxygen free radical production in rat heart [35].

The effects of oxygen radicals on the integrity and function of various cellular components are beginning to unravel. Partially reduced oxygen species, generated by an in vitro hypoxanthine/XO system, have been shown to inhibit several important intracellular functions including Ca^{2+} uptake in the cardiac sarcoplasmic reticulum [12], the ability of liver and heart mitochondria to take up and retain Ca^{2+} [10], and respiration of isolated heart and kidney mitochondria [9,14,20].

The rate of xanthine dehydrogenase to XO conversion during ischemia depends on several factors including cell type. The experiments described below employ mitochondria isolated from rat kidney, a tissue known to double its XO concentration during 30 minutes of ischemia [32]. This paper (a) describes the Ca^{2+} releasing effects of the partial reduction products of oxygen, generated by hypoxanthine and XO, on renal mitochondria, (b) assesses the relative contributions of H_2O_2 and superoxide anion radical on Ca^{2+} efflux and (c) demonstrates the initiation of futile Ca^{2+} cycling at the inner mitochondrial membrane by the products of the hypoxanthine/XO reaction. Although these experiments employ renal mitochondria, the results may

apply to the mitochondria of other tissues which exhibit ample xanthine dehydrogenase to XO conversion and hypoxanthine accumulation during ischemia (e.g., rat intestine, heart, liver) as well [32].

MATERIALS AND METHODS

Chemicals. All chemicals and enzymes were obtained from the Sigma Chemical Company, St. Louis, Missouri (USA). Units (U) or milliunits (mU) of enzyme activity are those defined by Sigma. Stock solutions of ATP were prepared by neutralizing the tris salt to pH 7.4 with dilute KOH. Aliquots of this solution were then added to the incubation media to obtain the desired ATP concentration.

Mitochondrial Preparations. Rats were sacrificed by decapitation and the kidneys immediately removed and minced in ice cold MSE (150 mM mannitol, 130 mM sucrose, 1 mM ethylenebis (oxyethylenenitrilo-tetraacetic acid (EGTA)). The minced sample was rinsed several times with ice cold MSE and homogenized at 4°C with a Potter Elvehjem homogenizer. The homogenate was spun at 480xg to remove large cellular debris. Mitochondria were pelleted from the supernatant by centrifugation at 7700xg. The pellet was washed twice with ice cold MS (150 mM mannitol, 130 mM sucrose) and resuspended in 1.5 ml of cold MS and kept on ice. This suspension was analyzed for protein [19] and used to make the various determinations described below. All mitochondrial preparations exhibited respiratory control ratios greater than 10 using glutamate (6 mM) and malate (2 mM) as substrates. All solutions were made with deionized/quartz distilled water.

Microsomal contamination of the preparation was consistently less

than 5%. Glucose-6-phosphatase activity [3], a microsomal marker enzyme, was consistently low at 0.10 ± 0.06 (n=7) μmoles P_i released per 20 minutes per mg protein. ATP-stimulated, ruthenium red-insensitive Ca^{2+} uptake was less than 0.2 nmoles per minute per mg protein.

Endogenous Mitochondrial NAD(P)H Oxidation. NAD(P)H oxidation was monitored kinetically in intact mitochondria using a Hitachi 557 dual wavelength spectrophotometer as described by Lehninger, et al [17]. Isolated mitochondria were suspended in 65 mM KCl, 125 mM sucrose, 200 μM hypoxanthine, 20 mM tris-Cl, 0.2 mM tris-PO_4, 10 μM rotenone and 2 mM succinate at pH 7.4. Rotenone, a site I inhibitor, prevents the entry of electrons into the respiratory chain from NAD(P)H while allowing ATP synthesis via succinate and $FADH_2$. Rotenone also inhibits the reverse flow of electrons from $FADH_2$ to NAD(P)H. NAD(P)H oxidation was monitored kinetically using the wavelength pair 340-375nm. The change in optical density versus time was recorded onto chart paper.

Extramitochondrial Calcium. Extramitochondrial Ca^{2+} was monitored kinetically using the Ca^{2+} indicator, arsenazo III, and the wavelength pair 660-685nm [15]. Arsenazo III is the indicator of choice since it provides the best sensitivity when monitoring small changes at the relatively low Ca^{2+} concentrations used for these experiments [15,34]. Isolated mitochondria were suspended in 65 mM KCl, 125 mM sucrose, 200 μM hypoxanthine, 20 mM tris-Cl, 0.2 mM tris-PO_4, 50 μM arsenazo III, 10 μM rotenone and 2 mM succinate at pH 7.4. Change in optical density versus time was recorded onto chart paper.

Mitochondrial Respiration. Oxygen utilization was monitored by

conventional methods using a Clark O_2 electrode. Mitochondria (0.4-0.5 mg protein/ml) were suspended in a closed, water jacketed, glass O_2 chamber with 65 mM KCl, 125 mM sucrose, 200 μM hypoxanthine, 20 mM tris-Cl, 0.2 mM tris-PO_4, 10 μM rotenone and 2 mM succinate at pH 7.4. Temperature was held at 25°C by circulating water from a bath through the water jacketed cell. O_2 consumption was monitored as a function of time and recorded onto chart paper. In experiments in which XO was added to mitochondrial suspensions, the contribution of XO to the total O_2 consumption rate was estimated by monitoring O_2 consumption separately in incubation medium without mitochondria. XO (60 mU) alone, was found to consume 9.0 ± 0.1 nmoles O_2 per minute (n = 3).

Hypoxanthine/Xanthine Assay. The rate of conversion of hypoxanthine to xanthine by XO was determined by measuring hypoxanthine consumption and xanthine formation as a function of time. The reaction was started by adding XO (73 mU/ml) to a medium containing 65 mM KCl, 125 mM sucrose, 200 μM hypoxanthine, 20 mM tris-Cl, 0.2 mM tris-PO_4 (pH 7.4). Aliquots of 400 μl were drawn at 20 second intervals and alkalinized by adding 400 μl of 0.5 M KOH. The pH was adjusted to 6.5-7.0 with 180 μl of 1 M KH_2PO_4 and the resulting solution was filtered using an Amicon CF50A filter. The filtrate (20 μl) was assayed by HPLC for hypoxanthine and xanthine.

The HPLC system consisted of a Waters 600 Multisolvent Delivery System and Waters 490 Programmable Multi-wavelength detector. All injections were made by a Waters 712 WISP. Data acquisition and analysis was performed using a Waters System Interface Module and an IBM-AT computer equipped with Waters 820 chromatography software.

Hypoxanthine and xanthine were separated using a RESOLVE C_{18-5} (3.9mm X 15cm) column. Samples and standards were analyzed isocratically using 0.1 M KH_2PO_4 (pH 6.0) and a flow rate of 0.8 ml/min. Hypoxanthine and xanthine were detected at 254 nm. Standard curves were constructed using external standards containing known quantities of hypoxanthine and xanthine. Quantitation was based on peak area.

RESULTS

To estimate the quantity of H_2O_2 and superoxide anion radical generated in our in vitro hypoxanthine/XO system, the disappearance of hypoxanthine and the formation of xanthine were followed over time. The reaction was linear ($r = 0.97$) in the presence of 73 mU/ml XO over a period of 5 minutes. The slope of the line for hypoxanthine disappearance, 21.9 nmoles hypoxanthine per minute, was used to estimate H_2O_2 and superoxide radical production by XO. Two electrons are passed from hypoxanthine to XO per molecule of xanthine formed [8]. With a low hypoxanthine concentration and a high O_2 concentration, XO cycles between the two-electron reduced and oxidized states [26]. Under these conditions, approximately 22% of the electron flux through the enzyme occurs via the univalent pathway as determined by cytochrome c^{3+} reduction [8,14]. Therefore, approximately 8.8 nmoles of superoxide radical and 17.5 nmoles of H_2O_2 per ml·min are generated in our system using 73 mU XO/ml.

Figure 1A illustrates the Ca^{2+} releasing effect of H_2O_2 and superoxide radical on isolated renal mitochondria. Mitochondria were suspended in buffered medium as described above. Catalase and

superoxide dismutase (SOD) were used to assess the relative roles of H_2O_2 and superoxide on Ca^{2+} efflux. Four tracings are shown superimposed. All tracings were acquired under identical experimental conditions, the only variable being the presence or absence of catalase and/or SOD. Addition of Ca^{2+} caused a rapid change in optical density which returned to baseline as the mitochondria accumulated the added Ca^{2+}. After Ca^{2+} uptake was complete, XO was added to initiate H_2O_2 and superoxide radical production. SOD provided no protection against Ca^{2+} efflux. In fact, the Ca^{2+} release rate with SOD exceeded that of the control experiment (no catalase, no SOD). Catalase, however, prevented Ca^{2+} efflux with or without SOD. Dose dependent relationships exist between the ability of both catalase to prevent Ca^{2+} efflux and XO to induce Ca^{2+} efflux (data not shown). In addition, heat-inactivated catalase (100^0C for 5 minutes) had no effect on Ca^{2+} efflux. Therefore, mitochondrial Ca^{2+} efflux, induced by the products of the hypoxanthine/XO reaction, is attributed to mitochondrial H_2O_2 metabolism since efflux can be prevented by removal of H_2O_2 via catalase.

Mitochondria metabolize H_2O_2 through glutathione dependent pathways leading to oxidation of endogenous NAD(P)H [31]. Mitochondrial Ca^{2+} efflux could be prevented by providing reducing equivalents for the formation of NAD(P)H. For example, adding glutamate and malate (both 2.5 mM), in addition to succinate (2 mM), to the incubation medium (no catalase or SOD) produced tracings similar to those of Figure 1A with catalase (data not shown). Figure 1B illustrates four tracings superimposed which were acquired under

experimental conditions identical to those in Figure 1A except NAD(P)H was monitored at 340-375nm in the absence of arsenazo III. Mitochondrial NAD(P)H was rapidly oxidized upon addition of XO. Exogenous SOD increased the observed NAD(P)H oxidation rate. Catalase without SOD dramatically reduced the rate of NAD(P)H oxidation while catalase plus SOD reduced NAD(P)H oxidation even further. Again, heat-inactivated catalase had no effect.

To determine whether Ca^{2+} efflux was due to generalized mitochondrial swelling, optical density was monitored in separate experiments at 560 nm or 700 nm during the efflux period. Swelling and lysis of mitochondria would be accompanied by a decrease in optical density at both of these wavelengths. No significant change in optical density was noted (data not shown). Therefore, efflux cannot be attributed to generalized mitochondrial swelling or damage. In fact, t-butylhydroperoxide induced Ca^{2+} efflux has been shown to occur without collapse of the membrane potential in isolated liver mitochondria [1].

The Ca^{2+} efflux rate as well as the lag time to Ca^{2+} efflux are dependent on the oxidation of mitochondrial NAD(P)H. Mitochondria were suspended in medium (0.57 mg protein/ml) as described above and loaded with 18 nmoles Ca^{2+}/mg protein. When Ca^{2+} uptake was complete, various quantities of XO (7.5, 12, 30 or 45 mU/ml) were added to initiate H_2O_2 and superoxide radical production. The Ca^{2+} efflux rate and the period of time from the addition of XO to Ca^{2+} efflux (lag time) were determined at each XO concentration. Under identical conditions, the rates of NAD(P)H oxidation were determined using the same quantities of

XO. As XO concentration increased, the NAD(P)H oxidation and Ca^{2+} efflux rates also increased while the lag time to Ca^{2+} efflux decreased. The NAD(P)H oxidation rate correlates well with the Ca^{2+} efflux rate (Figure 2A) and with the inverse of lag time to Ca^{2+} efflux (Figure 2B).

Although Ca^{2+} efflux seems to depend on NAD(P)H oxidation, exogenous ATP prevents efflux without affecting NAD(P)H oxidation (Figure 3). Mitochondria were suspended in buffered medium (0.46 mg protein/ml) as described above and loaded with 22 nmoles Ca^{2+}/mg protein. After Ca^{2+} uptake was complete, ATP and XO were added. Figure 3 shows two tracings superimposed. The upper and lower tracings show changes in extramitochondrial Ca^{2+} and NAD(P)H respectively. Addition of XO is followed by a rapid oxidation of NAD(P)H, although no Ca^{2+} efflux occurs. A net Ca^{2+} efflux is seen however following the addition of oligomycin, an ATPase inhibitor. Under these experimental conditions, ATP hydrolysis prevents a net Ca^{2+} efflux since inhibition of the ATPase complex by oligomycin restores efflux. In order to further clarify the mechanism of ATP's effect, extramitochondrial Ca^{2+} was monitored in the presence of ATP and ruthenium red (data not shown). Under these conditions, ruthenium red (20 μM) prevents Ca^{2+} reuptake and a rapid efflux of Ca^{2+} is seen following XO addition (data not shown). Figure 4 shows that ATP-inhibition of Ca^{2+} efflux occurs in a dose-dependent fashion. Four tracings are shown superimposed in which various quantities of ATP were added to mitochondrial suspensions just prior to XO. As ATP concentration increased, the Ca^{2+} efflux rate decreased and the lag time to Ca^{2+} efflux increased. The Ca^{2+} efflux

rate shows a linear correlation with the logarithm of ATP concentration (insert, Figure 4). The low K_m of inhibition, 35 μM ATP, suggests that extramitochondrial (cytosolic) ATP can be avidly taken up and hydrolyzed by mitochondria to support Ca^{2+} uptake if necessary.

Hydroperoxide-induced Ca^{2+} efflux from mitochondria occurs by a pathway other than the Ca^{2+}-uniport uptake system [1]. Therefore, a net Ca^{2+} efflux would not become apparent until the efflux rate surpassed that of the uptake system. Ca^{2+} uptake by mitochondria is a high capacity, energy dependent process [5]. If H_2O_2-induced Ca^{2+} release is matched by active uptake, O_2 consumption should increase to support the futile Ca^{2+} cycle. To test this hypothesis, mitochondrial O_2 consumption was monitored in Ca^{2+}-loaded mitochondria (25 nmoles Ca^{2+}/mg protein). Addition of XO increased O_2 consumption beyond the estimated increase (see Materials and Methods) due to H_2O_2 and superoxide radical production by XO alone (Figure 5A). Ruthenium red, which prevents Ca^{2+} cycling by blocking the active Ca^{2+}-uniport [23], causes an abrupt decrease in O_2 consumption. Similar results were obtained with EGTA which prevents cycling by sequestering released Ca^{2+} (data not shown). Therefore, in the absence of ATP, H_2O_2-induced Ca^{2+} efflux increases mitochondrial O_2 consumption by initiating a futile Ca^{2+} cycle.

Figure 5B illustrates that exogenous ATP can attenuate the XO-induced increase in State 4 respiration. Experimental conditions were similar to those of Figure 5A except 200 μM ATP was added instead of ruthenium red. ATP caused an abrupt decrease in O_2 consumption which could be reversed by adding oligomycin. Since ATPase inhibition

restored O_2 consumption to a rate approximating that prior to ATP addition, exogenous ATP appears to attenuate the H_2O_2-induced increase in State 4 respiration via hydrolysis of ATP.

The experiments in Figure 5 were repeated several times using mitochondrial preparations from three different animals. Respiratory rates were determined in Ca^{2+}-loaded mitochondria (state 4) before and after XO addition and following the addition of ruthenium red or ATP and ATP plus oligomycin. To calculate the percent increase in state 4 respiration, the rate of O_2 consumption by XO (60 mU/ml) alone was also determined and subtracted from the above rates. The state 4 respiratory rate before XO addition served as the control for each experiment. The results are shown in Figure 6. H_2O_2 and superoxide radical production via XO causes a significant increase in state 4 respiration. Ruthenium red and ATP prevent the XO-induced increase in O_2 consumption while ATP in the presence of oligomycin has no effect. Similar results were obtained when, instead of XO, t-butylhydroperoxide was used to induce Ca^{2+} cycling (data not shown).

DISCUSSION

Partially reduced oxygen species appear to be involved in the cellular injury sustained during reperfusion of ischemic tissues [28,32]. During ischemia, tissue hypoxanthine concentration and XO activity rise [16,32]. Upon reperfusion, the metabolism of hypoxanthine by XO produces H_2O_2 and superoxide radical. These oxygen species can have profound effects on the metabolic function of various organelles [9-12,14,20]. Mitochondria, for example, play a key role in

intracellular Ca^{2+} homeostasis by actively sequestering and retaining Ca^{2+} when cytosolic levels are pathologically high [7,33]. Perturbation of the mitochondrial Ca^{2+} uptake/efflux systems by H_2O_2 during reperfusion may contribute to cell demise by increasing the energy requirements of the cell through a futile Ca^{2+} cycle. In a similar study, Malis and Bonventre demonstrate the potentiating effect of Ca^{2+} on respiratory function following hypoxanthine/XO treatment thereby strengthening the role of Ca^{2+} dysmetabolism in oxidant injuries [20]. The experiments described above employed levels of hypoxanthine and XO reported in ischemic tissues in an attempt to approximate, as closely as possible, the cytosolic environment during reperfusion.

The mitochondrial Ca^{2+} release shown in Figure 1A can be attributed to H_2O_2 metabolism by endogenous enzyme systems. H_2O_2, formed in vitro during the reaction of hypoxanthine with XO, is reduced to water by mitochondrial glutathione peroxidase yielding oxidized glutathione. Glutathione is re-reduced by glutathione reductase consuming NADPH. NADH is also oxidized via the transhydrogenase reaction [31]. It is well known that a decrease in the matrix $NAD(P)H/NAD(P)^+$ ratio can elicit Ca^{2+} efflux from isolated mitochondria [5,17,25]. Other oxidants have been shown to cause mitochondrial calcium release via oxidation of NAD(P)H [18,34]. Catalase, which removes H_2O_2 produced by XO, inhibited Ca^{2+} efflux (Figure 1A) and also markedly reduced the rate of intramitochondrial NAD(P)H oxidation (Figure 1B). Supplying the NADH-linked substrates, glutamate and malate, prevented Ca^{2+} efflux. Additionally, the NAD(P)H oxidation

rate correlates well with the Ca^{2+} efflux rate and the lag time to Ca^{2+} efflux. For these reasons, we conclude that mitochondrial Ca^{2+} efflux in the presence of H_2O_2 and superoxide radical generated by XO, is the result of NAD(P)H oxidation during H_2O_2 metabolism.

It is interesting to note the difference in NAD(P)H oxidation rates with catalase in the presence and absence of SOD (Figure 1B). NAD(P)H oxidation is clearly faster without SOD. This suggests intramitochondrial H_2O_2 formation from superoxide radical by endogenous mitochondrial SOD. Also, the rate constants of the three spontaneous dismutation reactions shown below need to be considered:

$$HO_2\cdot + HO_2\cdot \dashrightarrow H_2O_2 + O_2 \qquad k = 8 \times 10^5\ M^{-1}s^{-1}$$

$$HO_2\cdot + O_2\cdot^- + H^+ \dashrightarrow H_2O_2 + O_2 \qquad k = 8 \times 10^7\ M^{-1}s^{-1}$$

$$O_2\cdot^- + O_2\cdot^- + 2H^+ \dashrightarrow H_2O_2 + O_2 \qquad k = 0.2\ M^{-1}s^{-1}$$

The rate of spontaneous dismutation is extremely rapid for the perhydroxyl ($HO_2\cdot$) form of superoxide, whose pKa is 4.8 [2,30]. The proton gradient formed across the inner mitochondrial membrane may facilitate the spontaneous dismutation rate at the membrane surface forming H_2O_2 which is subsequently metabolized consuming NAD(P)H. An addition of exogenous SOD, without catalase, potentiates Ca^{2+} efflux (Figure 1A) and accelerates NAD(P)H oxidation (Figure 1B) by catalyzing the rapid dismutation of superoxide radical to H_2O_2. The additional H_2O_2 is promptly metabolized by the mitochondria leading to faster NAD(P)H oxidation and a more pronounced Ca^{2+} release.

Since the mitochondrial Ca^{2+} efflux system is separate from the

active uptake system [1], H_2O_2-induced Ca^{2+} efflux stimulates reuptake, thereby establishing a futile Ca^{2+} cycle which significantly increases mitochondrial state 4 respiration (Figure 6). Blocking the uptake system with ruthenium red (Figure 5A) or sequestering released Ca^{2+} with EGTA, reduces the state 4 respiratory rate to normal values. Exogenous ATP can also prevent the H_2O_2-induced increase in state 4 respiration (Figure 5B) as well as the net Ca^{2+} efflux. The mechanism appears to involve Ca^{2+} reuptake via ATP hydrolysis since (a) ATP's protective effect is negated by blocking the Ca^{2+} uniport uptake system with ruthenium red and (b) preventing ATP hydrolysis with oligomycin reverses the effect on both mitochondrial Ca^{2+} efflux (Figure 3) and respiration (Figures 5B and 6).

During the reperfusion of a previously ischemic tissue, the intracellular production of small qualtities of H_2O_2 and superoxide radical by XO can have profound effects on mitochondrial function. Following ischemia, cytosolic Na^+ and Ca^{2+} are high and ATP levels are low [33]. During reperfusion, cell viability hinges on effective ATP production to maintain energy charge and reverse the ionic perturbations induced by ischemia. With reperfusion, tissue O_2 tension rises, electron transport resumes and the mitochondrial electrochemical gradient is restored. Mitochondria accumulate Ca^{2+} [24] as the high cytosolic Ca^{2+} levels stimulate the Ca^{2+}-uniport uptake system. Mitochondrial Ca^{2+} transport takes precedence over oxidative phosphorylation [5]. In fact, cytosolic ATP can become hydrolyzed to support Ca^{2+} uptake (Figure 4). Therefore, effective ATP production will not resume until normal cytosolic Ca^{2+} levels are restored.

Finally, H_2O_2 production by XO during the early phases of reperfusion may initiate mitochondrial Ca^{2+} efflux, establishing a futile Ca^{2+} cycle at the mitochondrial inner membrane which can increase O_2 consumption and interfere with oxidative phosphorylation. To support this hypothesis, an increase in tissue O_2 utilization, termed 'hypermetabolism', has been reported following reperfusion of ischemic brain [33].

Several factors inherent to ischemic tissues are known to promote hydroperoxide-induced Ca^{2+} efflux from mitochondria. Efflux is enhanced by conditions which facilitate proton flux through the inner mitochondrial membrane. For example, elevated H^+ and free fatty acid concentrations promote Ca^{2+} efflux without significant uncoupling of oxidative phosphorylation [1]. As a result, higher H^+ (i.e. lower pH) and free fatty acid concentrations following ischemia [33] render mitochondria more vulnerable to H_2O_2-induced Ca^{2+} efflux and cycling. The level of endogenous mitochondrial Ca^{2+} also affects efflux. Hydroperoxide-induced Ca^{2+} efflux becomes more pronounced as endogenous mitochondrial Ca^{2+} concentrations increase [6]. Therefore, the high mitochondrial Ca^{2+} levels associated with reperfusion [24] should also facilitate H_2O_2-induced Ca^{2+} efflux and cycling. These factors and their relationship to H_2O_2-induced mitochondrial Ca^{2+} efflux and cycling may play a crucial role in cell survival during the reperfusion of ischemic tissues.

ACKNOWLEDGEMENTS

The authors wish to thank Stephanie Thompson and Debbie Nelson for their help in the preparation of the manuscript.

These studies were supported in part by a grant from the National Institutes of Health (GM-33267). Angelo A. Vlessis is an M.D./Ph.D. scholar supported by the Medical Research Foundation of Oregon.

Figure 1. Effect of extramitochondrial catalase and SOD on mitochondrial A) Ca^{2+} efflux and B) NAD(P)H oxidation. Mitochondria were suspended in buffered medium at 0.49 mg mitochondrial protein/ml in the presence of excess catalase (500 U/ml) and/or SOD (180 U/ml). After loading mitochondria with 10.2 nmoles Ca^{2+}/ mg protein, XO was added (73 mU/ml) to initiate H_2O_2 and superoxide radical production. Tracings similar to these were obtained on 3 separate occasions using different renal mitochondria preparations.

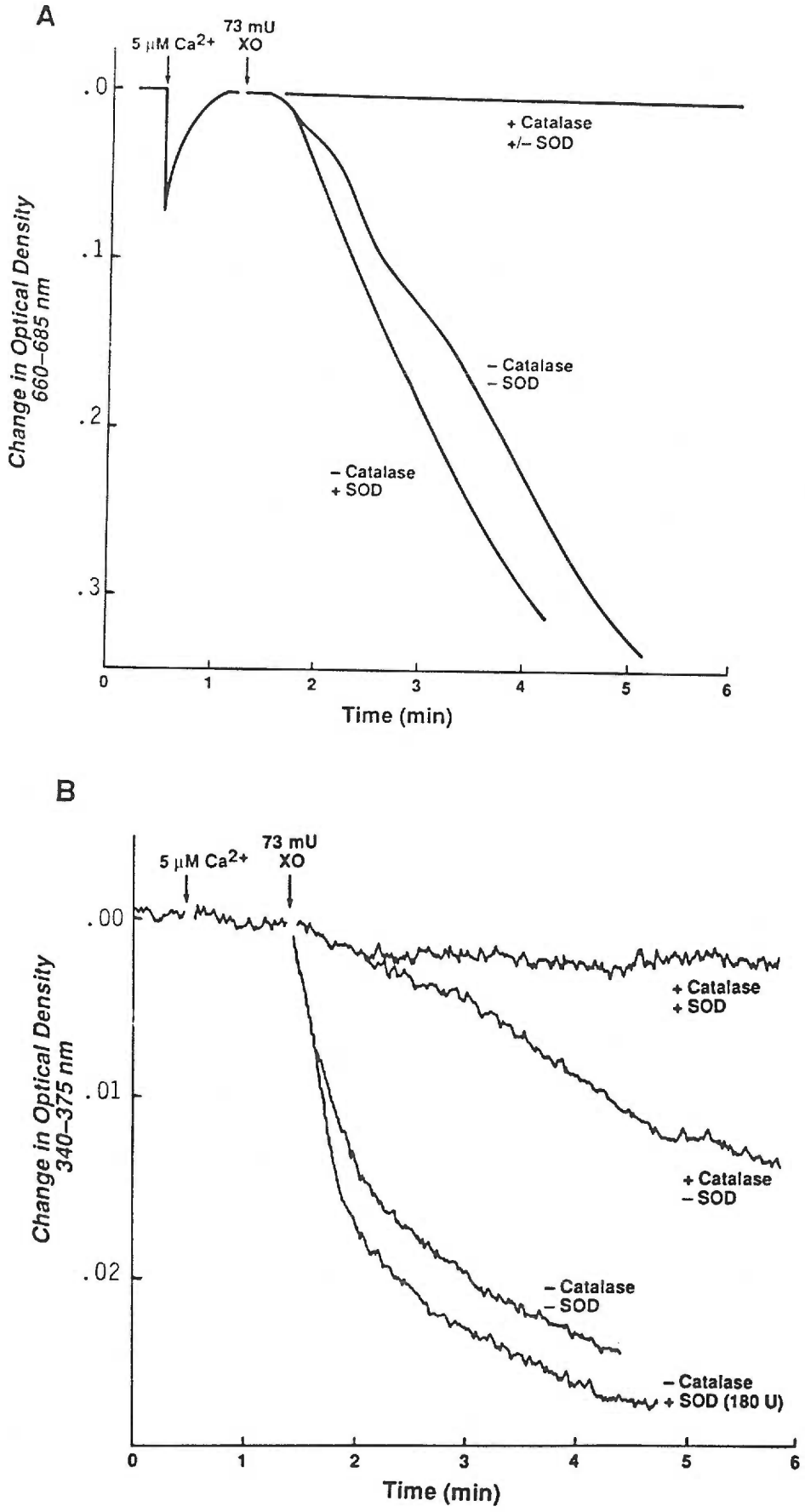
A
5 μM Ca2+
73 mU XO
.0
.1
.2
.3
+ Catalase
+/– SOD
– Catalase
– SOD
– Catalase
+ SOD
Change in Optical Density
660–685 nm
0
1
2
3
4
5
6
Time (min)
B
5 μM Ca2+
73 mU XO
.00
.01
.02
+ Catalase
+ SOD
+ Catalase
– SOD
– Catalase
– SOD
– Catalase
+ SOD (180 U)
Change in Optical Density
340–375 nm
0
1
2
3
4
5
6
Time (min)

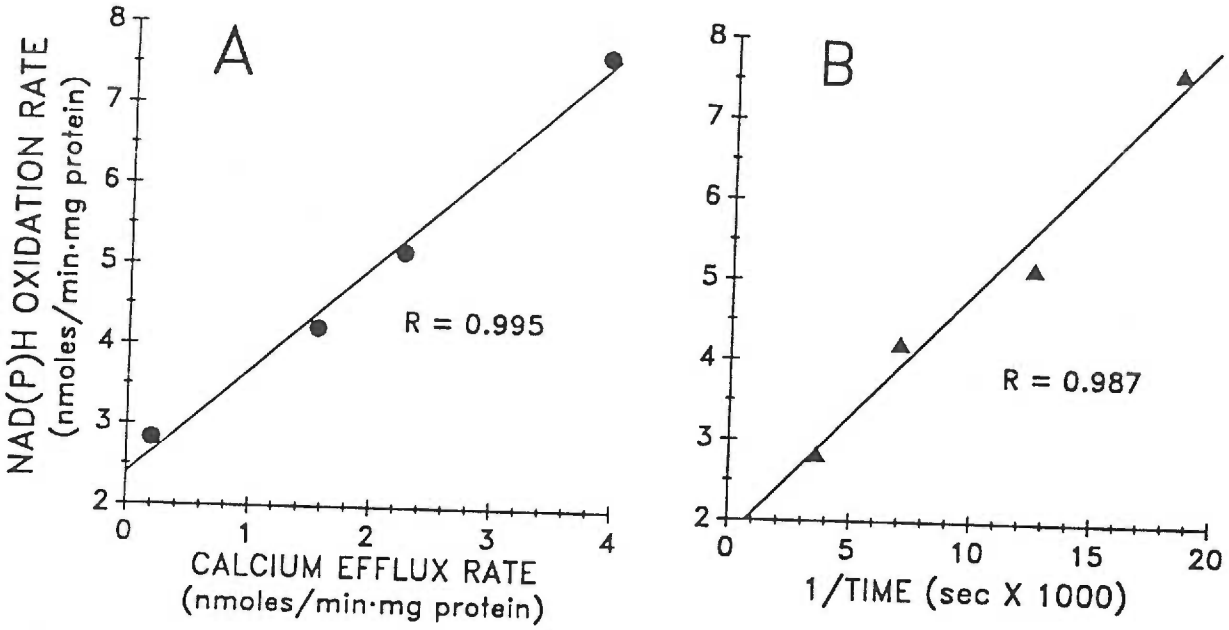

Figure 2. The rate of NAD(P)H oxidation shows a linear correlation with A) the Ca^{2+} efflux rate and B) the inverse of lag time to Ca^{2+} efflux. Mitochondria were suspended in buffered medium at 0.57 mg mitochondrial protein/ml and loaded with 18 nmoles Ca^{2+}/ mg protein. Various quantities of XO (7.5, 12, 30 or 45 mU XO/ml) were added and single determinations of lag time to Ca^{2+} efflux, Ca^{2+} efflux rate and NAD(P)H oxidation rate were made at each XO concentration. Each symbol represents the values obtained at a given XO concentration. The best fit line was calculated according to the least squares prediction equation. R is equal to the square root of the coeffecient of determination for the line.

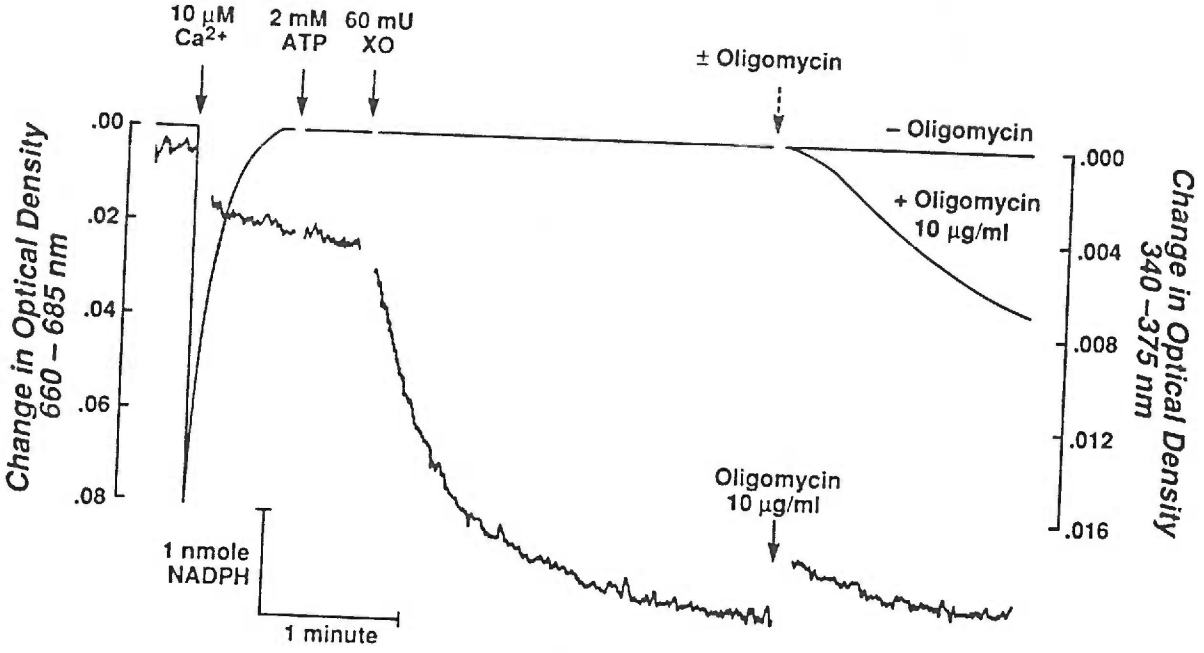

Figure 3. Effect of ATP on mitochondrial Ca^{2+} efflux and NAD(P)H oxidation. Mitochondria were suspended at 0.46 mg mitochondrial protein/ml and loaded with 22 nmoles Ca^{2+}/mg protein as described in Materials and Methods. The upper and lower tracings show changes in extramitochondrial Ca^{2+} and endogenous NAD(P)H respectively. Tracings similar to these were obtained on at least 3 separate occasions using different renal mitochondria preparations.

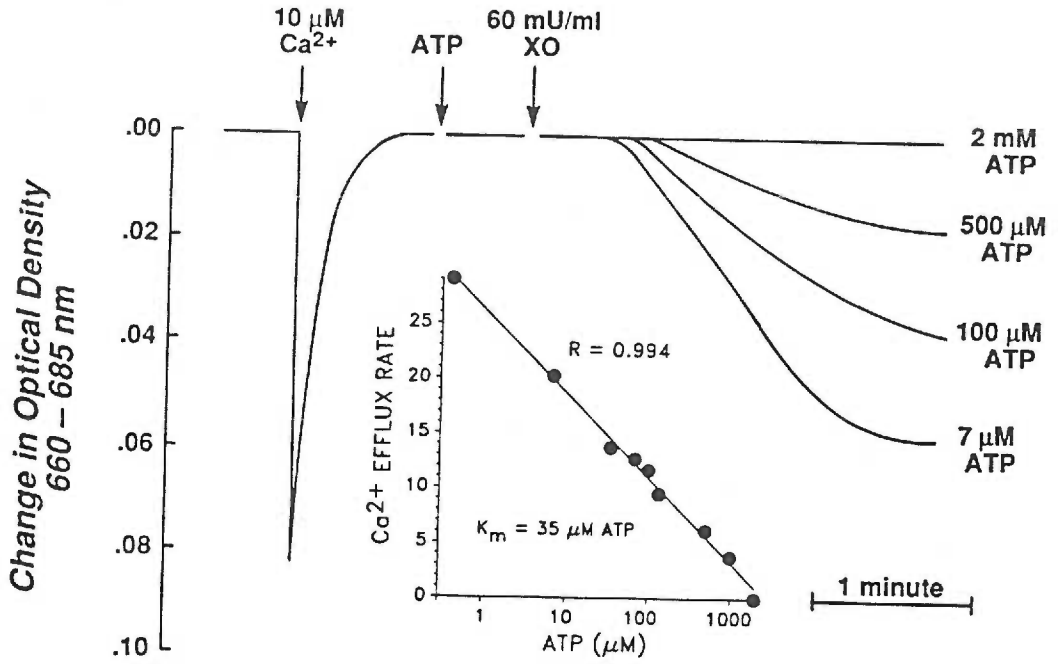

Figure 4. Exogenous ATP inhibits mitochondrial Ca^{2+} efflux in a dose-dependent manner. Mitochondria were suspended at 0.46 mg mitochondrial protein/ml and loaded with 22 nmoles Ca^{2+}/mg protein. Extramitochondrial Ca^{2+} was monitored following the addition of various quantities of ATP (0-2 mM) and XO (60 mU/ml). Four tracings are shown superimposed. The insert depicts the linear correlation between Ca^{2+} efflux rate and the logarithm of ATP concentration. The line was calculated according to the least squares prediction equation. R is the square root of the coefficient of determination for the line.

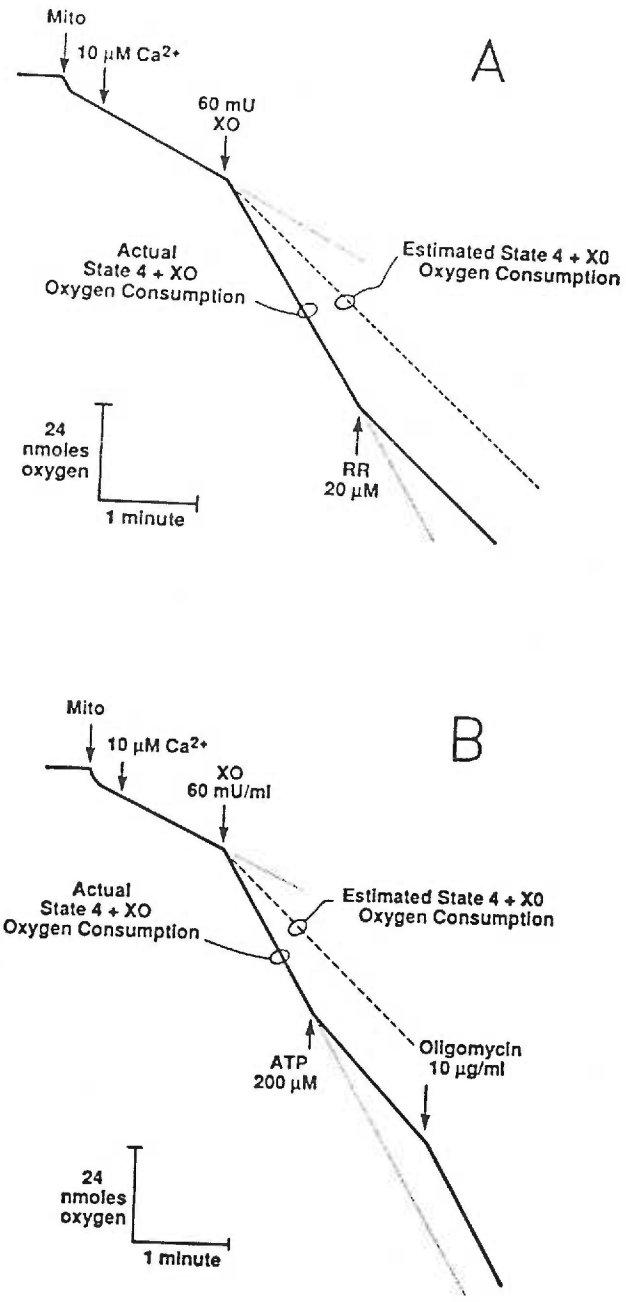

Figure 5. The effect of XO and A) ruthenium red or B) ATP and oligomycin on mitochondrial state 4 respiration. Mitochondria were suspended at 0.40 mg mitochondrial protein/ml in buffered medium and O_2 consumption was monitored as described in Materials and Methods. Tracings similar to these were obtained on at least 3 separate occasions using different renal mitochondria preparations.

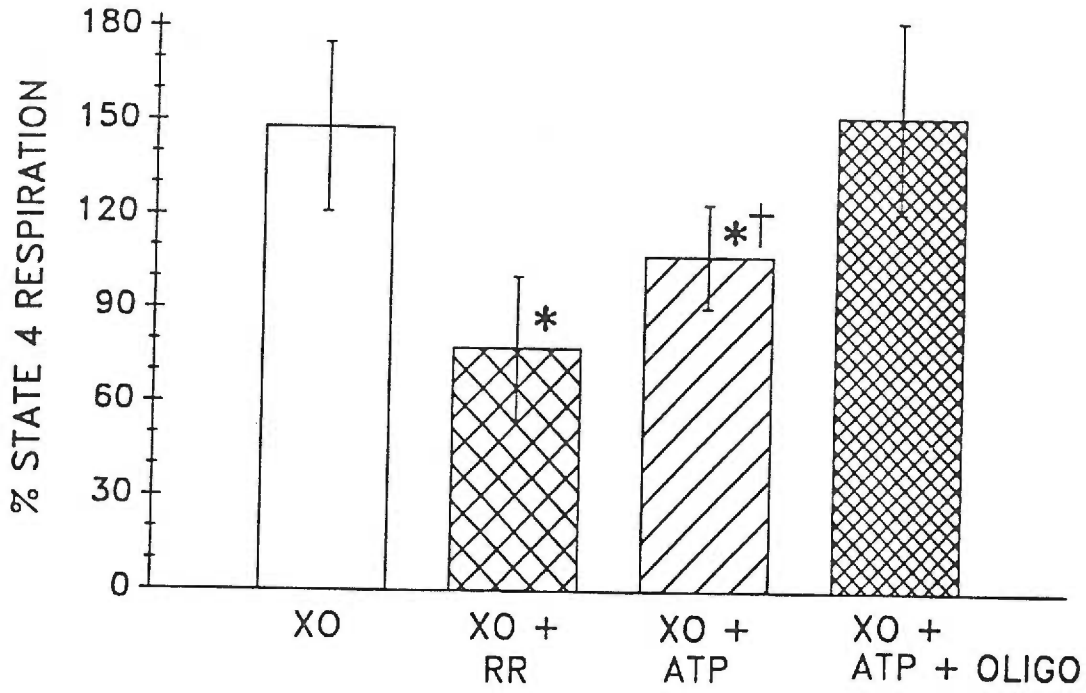

Figure 6. Effect of XO, XO and 20 μM ruthenium red (XO + RR), XO plus 200 μM ATP (XO + ATP) and XO plus 200 μM ATP and 10 μg oligomycin/ml (XO + ATP + OLIGO) on mitochondrial state 4 respiration. The number of runs in each group ranged from 5-8. The brackets include +/- one standard deviation from the mean. The results were analyzed by one-way analysis of variance (ANOVA).
* and † denote a statistical significance of $\alpha < 0.01$ from the XO and XO + ATP + OLIGO groups respectively.

REFERENCES

1. Baumhuter, S., and C. Richter. The hydroperoxide-induced release of mitochondrial calcium occurs via a distinct pathway and leaves mitochondria intact. *FEBS Letters*. 148: 271-275, 1982.

2. Behar, D., G. Czapski, J. Rabani, L.M. Dorfman and H.A. Schwartz. The acid dissociation constant and decay kinetics of perhydroxyl radical. *J Physical Chem*. 74: 3209-3213, 1970.

3. Dallner, G., P. Siekevitz and G.E. Palade. Biogenesis of endoplasmic reticulum membranes II. Synthesis of constitutive microsomal enzymes in developing rat hepatocyte. *J Cell Biol*. 30:97-105, 1966.

4. DeWall, R.A., V.A. Vasko, E.L. Stanley and P. Kezdi. Responses of the ischemic myocardium to allopurinol. *Am Heart J*. 82: 362-370, 1971.

5. Fiskum, G. and A.L. Lehninger. Mitochondrial regulation of intracellular calcium. In: *Calcium and Cell Function, Vol. II*, edited by W.Y. Cheung. New York: Academic Press, Inc., 1982, p. 39-80.

6. Frei, B., K.H. Winterhalter and C. Richter. Quantitative and mechanistic aspects of the hydroperoxide-induced release of Ca^{2+} from rat liver mitochondria. *Eur J Biochem*. 149: 633-639, 1985.

7. Freundenrich, C.C., K.W. Snowdowne and A.B. Borle. The effect of anoxia on cytosolic free calcium in kidney cells. *Fed Proc*. 43: 769, 1984.

8. Fridovich, I. Quantitative aspects of the production of superoxide anion radical by milk xanthine oxidase. *J Biol Chem*.

245: 4053-4057, 1970.

9. Guarnieri, C., C. Muscari, C. Ceconi, F. Flamigni and C.M. Caldarera. Effect of superoxide generation on rat heart mitochondrial pyruvate utilization. *J Mol Cell Cardiol.* 15: 859-862, 1983.

10. Harris, E.J., R. Booth and M.B. Cooper. The effect of superoxide generation on the ability of mitochondria to take up and retain Ca^{2+}. *FEBS Letters.* 146: 267-272, 1982.

11. Hess, M.L. and N.H. Manson. The oxygen free radical system and myocardial dysfunction. *Adv Myocardiol.* 5: 177-181, 1985.

12. Hess, M.L., E. Okabe and H.A. Kontos. Proton and free oxygen radical interaction with the calcium transport system of the cardiac endoplasmic reticulum. *J Mol Cell Cardiol.* 13: 767-772, 1981.

13. Hille, R. and V. Massey. Studies on the oxidative half-reaction of xanthine oxidase. *J Biol Chem.* 256: 9090-9095, 1981.

14. Hillered, L. and L. Ernster. Respiratory activity of isolated rat brain mitochondria following in vitro exposure to oxygen radicals. *J Cereb Blood Flow Metabol.* 3: 207-214, 1983.

15. Kendrick, N.C., R.W. Ratzlaff and M.P. Blaustein. Arsenazo III as an indicator for ionized calcium in physiological salt solutions: its use for the determination of the CaATP dissociation constant. *Anal Biochem.* 83: 433-450, 1977.

16. Kleihues, P., K. Kobayashi and K.A. Hossman. Purine metabolism in the cat brain after one hour of complete ischemia. *J Neurochem.* 23: 417-425, 1974.

17. Lehninger, A.L., A. Vercesis and E.A. Bababunmi. Regulation of calcium release from mitochondria by oxidation-reduction state of pyridine nucleotides. *Proc Natl Acad Sci USA*. 75:1690-1694, 1978.

18. Lotscher, H.R., K.H. Winterhalter, E. Carafoli and C. Richter. Hydroperoxide-induced loss of pyridine nucleotides and release of calcium from rat liver mitochondria. *J Biol Chem*. 255:9325-30, 1980.

19. Lowry, O.H., N.J. Rosebrough, A.L. Farr and R.J. Randal. Protein measurement with folin phenol reagent. *J Biol Chem*. 193: 265-275, 1951.

20. Malis, C.D., and J.V. Bonventre. Mechanism of calcium potentiation of oxygen free radical injury to renal mitochondria. *J Biol Chem*. 261: 14201-14208, 1986.

21. McCord, J.M., S.R. Ranjan and S.W. Schaffer. Free radicals and myocardial ischemia: the role of xanthine oxidase. *Adv Myocardiol*. 5: 183-189, 1985.

22. McCord, J.M. Oxygen-derived free radicals in postischemic tissue injury. *N Engl Jour Med*. 312: 159-163, 1985.

23. Moore, C.L. Specific inhibition of mitochondrial calcium transport by ruthenium red. *Biochem Biophys Res Commun*. 42:298-305, 1971.

24. Nakanishi, T., K. Nishioka and J.M. Jarmakani. Mechanism of tissue Ca^{2+} gain during reoxygenation after hypoxia in rabbit myocardium. *Am. J. Physiol*. 242: H437-H449, 1982.

25. Nicholls, N.G. and M.D. Brand. The nature of calcium ion efflux induced in rat liver mitochondria by oxidation of endogenous

nicotinamide nucleotides. *Biochem J.* 188: 133-118, 1980.

26. Olson, J.S., D.P. Ballou, G. Palmer and V. Massey. The mechanism of action of xanthine oxidase. *J Biol Chem.* 249: 4363-4382, 1974.

27. Paller, M.S., J.R. Hoidal and T.F. Ferris. Oxygen free radicals in ischemic acute renal failure in the rat. *J Clin Invest.* 74: 1156-1164, 1984.

28. Parks, D.A. and D.N. Granger. Oxygen derived radicals and ischemic-induced tissue injury. In: *Oxy Radicals and Their Scavenger Systems, Vol. 2,* edited by R.A. Greenwald and G. Cohen. New York: Elseiver Science, 1983, p. 135-144.

29. Porras, A.G., J.S. Olson and G. Palmer. The reaction of reduced xanthine oxidase with oxygen. *J Biol Chem.* 256: 9096-9103, 1981.

30. Pryor, W.A. The role of free radical reactions in biological systems. In: *Free Radicals in Biology*, edited by W.A. Pryor. New York: Academic Press, Inc., 1976, p. 1-49.

31. Reed, D.J. Regulation of reductive processes by glutathione. *Biochem Pharmacol.* 35: 7-13, 1986..

32. Roy, R.S., and J.M. McCord. Superoxide and ischemia: conversion of xanthine dehydrogenase to xanthine oxidase. In: *Oxy Radicals and Their Scavenger Systems, Vol. 2,* edited by R.A. Greenwald and G. Cohen. New York: Elsevier Science, 1983, p. 143-153.

33. Siesjo, B.K. Cell damage in the brain: a speculative synthesis. *J Cereb Blood Flow Metabol.* 1: 155-177, 1981.

34. Vlessis, A.A. and L. Mela-Riker. Selenite-induced NAD(P)H oxidation and calcium release in isolated mitochondria: rela-

tionship to in vivo toxicity. *Mol Pharmacol*. 31: 643-646, 1987.

35. Weisfeldt, M.L. Reperfusion and reperfusion injury. *Clin Res*. 35: 13-20, 1987.

SUPPLEMENTAL RESULTS

The oxidant-induced mitochondrial NAD(P)H oxidation rate shows a strong correlation with the subsequent Ca^{2+} efflux rate and the inverse of lag time to Ca^{2+} efflux (Manuscript #4). Manuscript #3 demonstrates that mitochondria from newborn animals exhibit lower NAD(P)H oxidation rates. Therefore, mitochondria from newborn animals should also exhibit a tolerance to oxidant-induced Ca^{2+} efflux. To test this hypothesis, the lag times to oxidant-induced Ca^{2+} efflux were determined in kidney and liver mitochondria from animals of various ages. The results are shown in Figure 1. Kidney and liver mitochondria isolated from newborn animals are indeed less susceptible to oxidant-induced Ca^{2+} efflux.

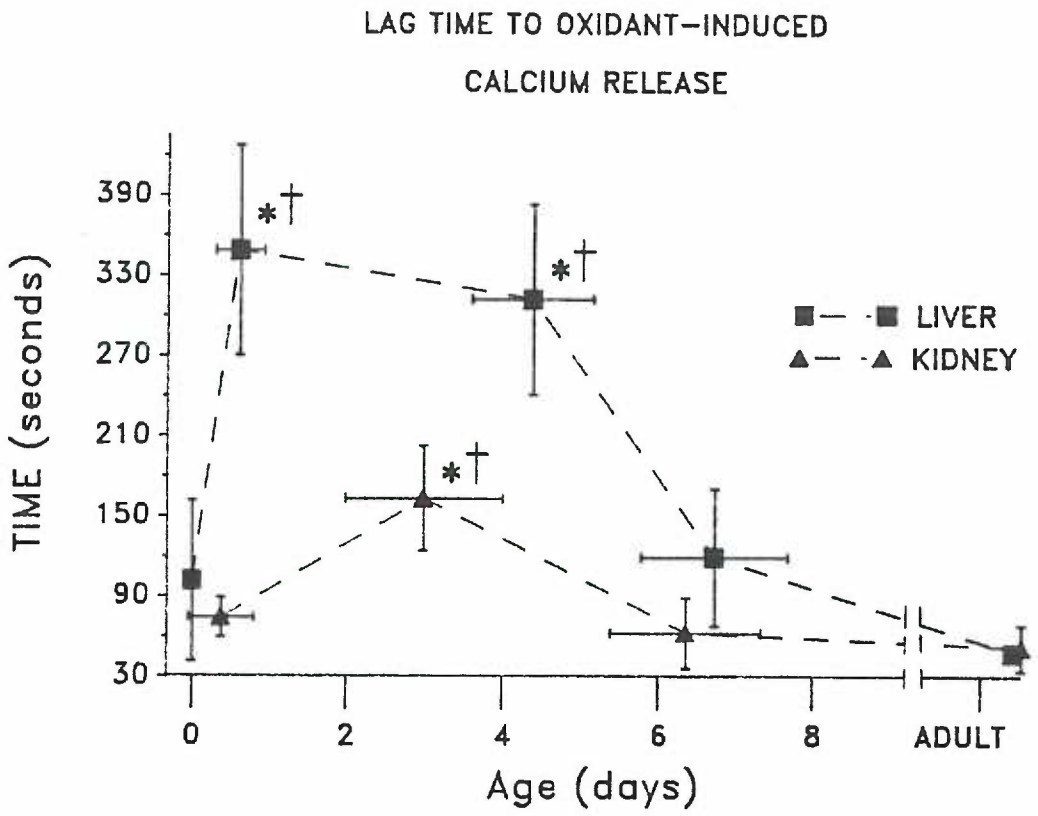

Figure 1. Age-dependent changes in lag time to oxidant-induced mitochondrial Ca^{2+} release. Extramitochondrial Ca^{2+} was monitored as described in Manuscripts #1 and #4 using fetal (Day 0), newborn and adult mitochondria. The time period between the addition of 500 μM selenite and the initiation of Ca^{2+} efflux was recorded and standardized for μmoles selenite per mg of mitochondrial protein. Each symbol depicts the mean lag time to Ca^{2+} efflux and mean age of each group. The brackets include +/- one standard deviation of the mean lag time and age. The n values averaged 4 and ranged from 3-5 animals in each group.

* and † denotes a significance of at least $\alpha < 0.02$ from the fetal and adult groups respectively.

DISCUSSION AND CONCLUSIONS

The results have already been summarized and interpreted in the Discussion sections of each manuscript. A few concluding remarks, however, will serve to solidify the material presented and emphasize its importance.

Following birth, the emerging fetus begins to exploit the benefits of aerobic metabolism by engaging the pulmonary circulation. Systemic P_aO_2 rises several-fold [1,2] and the increased availability of O_2 in various body tissues begins to influence cellular metabolism. In unicellular organisms, changes in PO_2 regulate the expression of several O_2-sensitive genes (see Introduction). A similar phenomenon may be operative in mammalian cells as the cellular PO_2 rises. Regardless of the mechanism, the rising PO_2 following birth results in elevated cytochrome oxidase and ubiquinone concentrations in heart, kidney and liver mitochondria (Manuscript #2). Oxygen seems to be the trigger since the increase in electron transport system components is not seen in animals born into a hypoxic environment [3]. A rise in mitochondrial ubiquinone concentration may increase the efficiency of electron transport through the respiratory chain since ubiquinone is believed to be the rate liming factor in electron transport [4]. Ubiquinone, however, is also the predominant site of superoxide radical formation in mitochondria [5]. The reaction of semiquinone with O_2 forms superoxide. This pathway may account for 1 - 4% of the total O_2 consumed by an animal under resting conditions [5,6]. Consequently, a rise in mitochondrial ubiquinone concentration should be accompanied by a concomitant increase in mitochondrial superoxide generation.

Interestingly, ubiquinone concentration correlates well with superoxide dismutase (MnSOD) activity during perinatal development in heart and kidney mitochondria (Figure #3-6). This suggests that an elevated MnSOD activity may be a necessary adjuvant to the rising ubiquinone levels needed for effective functioning of the high energy yielding pathways of aerobic metabolism post-birth.

Acute and chronic changes in P_aO_2 are known to alter mitochondrial respiratory activity in a predictable fashion (see Introduction). The results presented above (Figures #2-4) support the earlier work of Mela et al [1] by demonstrating a drop in pyruvate-driven respiration in heart and kidney mitochondria post-birth. Respiratory rates with other substrates, however, increase following birth. This phenomenon can be explained via the known regulatory effects of mitochondrial peroxide metabolism on substrate entry into oxidative pathways. The rising P_aO_2 post-birth is accompanied by increased generation of reactive oxygen species (e.g., H_2O_2). Evidence for this stems from elevated serum lipoperoxides and ethane/pentane expiration during the newborn period (see Introduction). Sies and Moss elegantly demonstrate that peroxide metabolism by mitochondria can severely restrict pyruvate oxidation without affecting the utilization of other substrates [7]. These changes in mitochondrial respiratory activity following birth fit a peroxide-mediated etiology. The potential influence of birth-related hormonal changes on metabolism, however, cannot be discounted [8].

In addition to modulating substrate entry into oxidative pathways, mitochondrial peroxide metabolism can also induce Ca^{2+} efflux

(Manuscript #4). Peroxide-induced mitochondrial Ca^{2+} efflux shows a strong correlation with the endogenous NAD(P)H oxidation rate (Figure #4-2). Ca^{2+} efflux stimulates reuptake thereby initiating a futile Ca^{2+} cycle across the inner mitochondrial membrane which significantly increases state 4 respiration (Figure #4-6). The mobilization of intracellular Ca^{2+} stores forms the final common pathway in various forms of oxidant-induced cell death [9].

The newborn mammal's resilience to various oxidative challenges (see Introduction) may be attributable to the developing mitochondrial antioxidant defense system which resists the oxidant-induced changes in mitochondrial Ca^{2+} homeostasis. Manuscripts #1 and #3 demonstrate that isolated liver and kidney mitochondria from newborn animals exhibit significantly lower oxidant-induced NAD(P)H oxidation rates than those of adult animals. Since mitochondrial NAD(P)H oxidation is a prerequisite for Ca^{2+} efflux (Manuscript #4), mitochondria from newborn animals should also resist oxidant-induced Ca^{2+} efflux. In fact, this is the case. Liver and kidney mitochondria from newborn animals are indeed less susceptible to oxidant-induced Ca^{2+} efflux than those of adults (Supplemental Results). Therefore, the newborn's immature mitochondrial antioxidant defense system may confer resistance to oxidative injury by resisting oxidant-induced mobilization of the mitochondrial Ca^{2+} pool which is known to increase state 4 respiration (Manuscript #4) and precede cell death [9].

Manuscript #3 reveals an interesting phenomenon which requires further emphasis. Mitochondrial glutathione reductase and peroxidase activities in sonicated mitochondria do <u>not</u> correlate consistently with

the NAD(P)H oxidation rates in intact mitochondria. For example, oxidant-induced NAD(P)H oxidation rates in adult kidney mitochondria are 3 - 4 fold higher than fetal values (Figure #3-2). Adult kidney mitochondrial glutathione reductase and peroxidase activities are, however, only 70 - 100% of fetal values (Figure #3-3). Therefore, measuring these enzyme activities in sonicated mitochondria (and possibly tissue homogenates) as an estimation of antioxidant function may be misleading since other factors appear to be regulating the activities of these antioxidant defense enzymes in situ. Monitoring the end result of oxidant metabolism, i.e., NAD(P)H oxidation, in the intact organelle (or cell) may be a more reliable index of antioxidant function. After all, the ability of these enzymes to operate within the milieu of the organelle (or cell) provides more information than individual enzyme activities under artificially optimized conditions. In fact, the conditions within the matrix (or cell) are crucial to antioxidant function since glutathione peroxidase is an allosteric enzyme subject to potent inhibition by factors normally present, e.g., coenzyme A, NADP+, NADPH and ATP [10,11]. Knowledge of the mechanisms which regulate the mitochondrial antioxidant defense system during the newborn period would be clinically valuable. As already discussed, a tolerance to oxidant-induced mitochondrial NAD(P)H oxidation and subsequent Ca^{2+} release may underlie the newborn's resistance to oxidative stress. Therapeutic approaches aimed at inhibiting mitochondrial NAD(P)H oxidation, Ca^{2+} efflux and cycling may provide a similar resilience to oxidative challenge in adult animals.

In conclusion, the most important contribution of this thesis

work is the characterization of the mitochondrial antioxidant defense system during normal perinatal development. Although many studies have focused on perinatal changes in antioxidant enzyme activities within whole tissue homogenates, the mitochondrial antioxidant enzyme system has received very little attention (see Introduction). Also, given the fact that glutathione peroxidase is an allosteric enzyme, this thesis work attempts to correlate, for the first time, the antioxidant function of intact mitochondria with the activities of the individual enzymes following sonication (Manuscript #3). In addition, normal perinatal changes in mitochondrial respiratory chain function and composition are described and correlated with the anitoxidant defense system. These combined data provide a more complete characterization of the mitochondrial O_2-dependent responses than has been previously possible. Comparison of these results with models of prematurity and other perinatal diseases may elucidate new therapeutic approaches to these clinical problems. Collectively, the research presented herein adds substantially to the current understanding of mitochondrial development during the perinatal period and establishes the importance of the mitochondrial antioxidant defense system in regulating cellular energy and Ca^{2+} metabolism.

REFERENCES

1. Mela L, Goodwin CW and Miller LD. (1976). In vivo control of mitochondrial enzyme concentrations and activity by oxygen. Am J Physiol. 231:1811-1816.

2. Harris AP, Sendak MJ and Donham RT. (1986). Changes in arterial

oxygen immediately after birth in the human neonate. J Pediatrics 109:117-119.

3. Hallman M. (1971). Changes in mitochondrial respiratory chain proteins during perinatal development. Evidence for importance of environmental oxygen tension. Biochem Biophys Acta. 253:360-372.

4. Ragan CI and Reed JS. (1986). Regulation of electron transfer by the quinone pool. J Bioenerg Biomembr. 18:403-418.

5. Boveris A. (1977). Mitochondrial production of superoxide radical and hydrogen peroxide. In: Tissue Hypoxia and Ischemia, Martin R, Coburn R, Lahiri S, Chance B (eds). Plenum Press, New York and London, pp 67-82.

6. Chance B, Sies H and Boveris A. (1979). Hydroperoxide metabolism in mammalian organs. Physiol Rev. 59:527-605.

7. Sies H and Moss KM. (1978). A role of mitochondrial glutathione peroxidase in modulating mitochondrial oxidations in liver. Eur J Biochem. 84:377-383.

8. Sutton R and Pollak JK. (1980). Hormone-initiated maturation of rat liver mitochondria after birth. Biochem J. 186:361-367.

9. Orrenius S and Nicotera P. (1986). Studies of Ca^{2+}-mediated toxicity in hepatocytes. Klin Wochenschr. 64(Suppl VII): 138-141.

10. Little C, Olinescu R, Reid KG and O'Brien PJ. (1970). Properties and regulation of glutathione peroxidase. J Biol Chem. 254:3632-3636.

11. Little C, Olinescu RM and O'Brien PJ. (1970). Inhibition of glutathione peroxidase by coenzyme A. Biochem Biophys Res Commun. 41: 287-293.

APPENDIX A

THEORY AND METHODOLOGY OF THE ARRHENIUS CALCULATION

The Arrhenius calculation is based on the *kinetic theory of matter*. In 1889, Svante Arrhenius demonstrated that reaction rate increases exponentially with temperature. If substrate concentration remains constant, the temperature dependence can be expressed entirely within the *specific rate constant*:

$$k = -Ae^{-Ea/RT} \qquad (1)$$

$$\ln k = \ln A - Ea/RT \qquad (2)$$

$$\log k = -Ea/(2.303\ RT) \qquad (3)$$

$$\frac{\log k}{1/T} = -Ea/2.303R = \text{Slope of Arrhenius Plot} \qquad (4)$$

$$Ea = (\text{Slope})(2.303\ R) \text{ in kilocalories} \qquad (5)$$

R = Universal Gas Constant
Ea = Energy of Activation
T = Temperature in degrees Kelvin
k = Specific Rate Constant
A = constant

The temperature at which the inner mitochondrial membrane changes from a gel to a liquid state is called the phase transition temperature (T_t). T_t can be determined by measuring the temperature dependent change in reaction rate of an enzyme(s) embedded within the inner mitochondrial membrane. This was done as described in Manuscript #2. Figure 1 below shows a computer generated sample Arrhenius plot of log state 3 respiratory rate versus 1/temperature in degrees Kelvin. Two lines can be drawn from this plot. The point of intersection of the two lines is T_t. Above T_t, the membrane is in the fluid state. Ea in the fluid state can be calculated from the slope of the line above T_t according to equation 5 above.

In order to accurately calculate T_t and Ea, the following program was written by myself in Apple II Pascal. With the program, the reaction rates at various temperatures can be entered into the computer. Two best fit lines are calculated according to the least squares prediction equation. The x value at the point of intersection of the two lines, T_t, is calculated as well as Ea above and below T_t, reaction rate at 37°C and the reaction rate at T_t. Screen and printer graphics routines are also provided by the program. This software was written specifically for Arrhenius type calculations since commercially available software would not adequately perform this complex series of calculations.

To my knowledge, this is the first report of computer assisted interpretation of Arrhenius data. I felt it was necessary to avoid human error in estimating best-fit lines, slope and T_t as well as removing a large portion of investigator bias.

```
(*$S+*)
PROGRAM ARRHENIUS;
USES TURTLEGRAPHICS,TRANSCEND;
LABEL 111,222,333;
TYPE  ANIMAL=RECORD
      MONTH,DAY,YEAR:0..99;
      AGE:REAL;
      ARRAY1:PACKED ARRAY[1..4,1..20] OF REAL;
      TRANSTEMP,TRANSRATE,RATE37,EA1,EA2:REAL;
      END;
      AFILE = FILE OF ANIMAL;
      VARGRAPH:PACKED ARRAY[1..80,1..80] OF 0..10;
      H,F:AFILE;
      P:INTERACTIVE;
      DATA:ANIMAL;
      ARRAY0:PACKED ARRAY[1..4,1..20] OF REAL;
      SX,SY,SXY,SX2,XMAX,XMIN,YMAX,YMIN,XINTERVAL,YINTERVAL,N:REAL;
      N1,N2,J,XM,YM,B,C,D,I,:0..100;
      NAME,CHOICE,ORGAN,PX,PY:STRING;
      XARRAY,YARRAY:ARRAY[1..80] OF REAL;
```

```
      B1,B2,T,M1,M2,SLOPE1,SLOPE2,INTER1,INTER2:REAL;

PROCEDURE MAXMIN;
 BEGIN
  YMAX:=0; YMIN:=LOG(200);
  XMAX:=(1/(273+42))*1000; XMIN:=(1/273)*1000;
  FOR B:=1 TO 20 DO
   BEGIN
      IF (ARRAY0[2,B]>XMAX) THEN XMAX:=ARRAY0[2,B];
      IF   (ARRAY0[2,B]<XMIN)   AND   (ARRAY0[2,B]<>0)   THEN
XMIN:=ARRAY0[2,B];
      IF (ARRAY0[4,B]>YMAX) THEN YMAX:=ARRAY0[4,B];
      IF (ARRAY0[4,B]<YMIN) AND (ARRAY0[4,B]<>0 THEN YMIN:=ARRAY0[4,B];
   END;
 END;

PROCEDURE WRITEGRAPH;
 BEGIN
  REWRITE(P,'PRINTER:');
  WITH DATA DO
   BEGIN
      WRITELN(P,'          ---------',AGE:2:1,' DAY',NAME,' ---------');
      PY:=CONCAT('          ',PY,'             ');
      FOR B:=1 TO 41 DO
       BEGIN
        D:=(42-B);WRITELN(P);
        WRITE(P,PY[B]);WRITE(P,YARRAY[D]:1:3:,'|');
        FOR I:=1 TO 75 DO
         CASE GRAPH[I,D] OF
      0: WRITE(P,' ');
      1: WRITE(P,'*');
      2,3,4: WRITE(P,GRAPH[I,D]);
         END;
       END;
      WRITELN(P);WRITE(P,'         ');
      FOR B:=1 TO 75 DO
        IF (B MOD 10=0) THEN WRITE(P,'|') ELSE WRITE(P,'-');
      WRITELN(P);WRITE(P,'       ',XARRAY[1]:3:1);
      FOR B:=1 TO 75 DO
      IF (B MOD 10=0) THEN WRITE(P,'      ',XARRAY[B]:1:2);
      WRITELN(P);WRITELN(P,'                          ',PX);
      CLOSE(P,LOCK);
   END;
  END;

PROCEDURE SETPOINTS;
 VAR YMN,XMN:REAL;
  BEGIN
   WRITELN('..CLEARING THE ARRAY..TURN ON PRINTER AND PLEASE WAIT..');
   FOR B:=1 TO 80 DO
        FOR C:=1 TO 45 DO GRAPH[B,C]:=0;
   WRITE('SETTING POINTS ON THE GRAPH..'); C:=0;
```

```
      REPEAT
        YMN:=0; XMN:=0; N:=0; C:=C+1;
        WRITE('.');
        IF (ARRAY0[1,C]<>0) THEN
      FOR B:=1 TO 75 DO
        IF (XARRAY[B]>=ARRAY0[2,C]) AND (YMN=0) THEN
      BEGIN
        XM:=B; XMN:=1;
      END;
        IF (YARRAY[B]>=ARRAY0[4,C]) AND (YMN=0) THEN
      BEGIN
        YM:=B; YMN:=1;
      END;
        IF (YMN=1) AND (XMN=1) THEN
      BEGIN
        GRAPH[XM,YM]:=GRAPH[XM,YM]+1; YMN:=2; XM:=2;
      END;
      END;
        UNTIL (C=20);
      WRITELN;
  END;

PROCEDURE RECALL;
 BEGIN
  REWRITE(P,'PRINTER:');
  WITH DATA DO
   BEGIN
      WRITELN(P,'      .....*****   ',NAME,'   *****.....');
      WRITE(P,'      TRANS TEMP: ',TRANSTEMP:2:1;
      WRITE(P,'      TRANS RATE: ',TRANSRATE:2:1);
      WRITELN(P,'    RATE37 -- ',RATE37:3:1);
      WRITE(P,'ENERGY OF ACTIV. ABOVE T(f) --- ',ABS(EA2):2:3);
      WRITELN(P,'                    ENERGY   OF   ACTIV.   BELOW   t(f)---
',ABS(EA1):2:3);
      WRITELN(P,'TEMP(CENT)   STATE 3 --(SUCC+ROT)');
      WRITELN(P,'----------   -------');
      FOR B:=1 TO 20 DO
        BEGIN
      IF (ARRAY0[1,B]<>0) THEN
        WRITELN(P,'   ',ARRAY1[1,B]:2:1,'      ',ARRAY1[3,B]:3:1);
      IF (ARRAY0[2,B+1]=0) THEN B:=20;
        END;
      END;
   WRITELN(P);
   CLOSE(P,LOCK);
 END;

PROCEDURE AVERINTERC;
 BEGIN
  WITH DATA DO
   BEGIN
      TRANSTEMP:=(((SLOPE1-SLOP2)/INTER2-INTER1)*1000))-273;
```

```
TRANSRATE:=EXP(2.31*((SLOPE1*((1/(TRANSTEMP+273))*1000))+INTER1));
      WRITELN('TRANSITION TEMPERATURE---> ',TRANSTEMP:2:2);
      WRITELN('TRANSITION RATE---------> ',TRANSRATE:3:1);
      RATE37:=EXP(2.303*((SLOPE2*((1/310)*1000))+INTER2));
      WRITELN('CALCULATED RATE AT 37 DEGREES-------> ',RATE37:3:1);
      EA1:=-SLOPE1; EA2:=-SLOPE2;
      WRITELN('ENERGY OF ACTIVATION ABOVE t(f) ----> ',EA2:2:3);
      WRITELN('ENERGY OF ACTIVATION BELOW t(f) ----> ',EA1:2:3);
   END;
  END;

PROCEDURE CALC;
  BEGIN
      SXY:=SXY+(ARRAY2[C,1]*ARRAY2[C,2]);
      SX2:=SX2+(ARRAY2[C,1]*ARRAY2[C,1]);
      SX:= SX+ARRAY2[C,1];
      SY:= SY+ARRAY2[C,2];
  END;

PROCEDURE EXCLUDE;
 BEGIN
  REPEAT
      WRITE('ENTER TEMP. COORDINATE OF POINT TO BE EXCLUDED-- ');
      READLN(T);
      FOR B:=1 TO 20 DO IF (ARRAY0[1,B]=T) THEN ARRAY0[1,B]:=0;
      WRITE('ANY OTHER POINTS TO BE EXCLUDED (Y/N)?');
      READLN(CHOICE);
  UNTIL (CHOICE[1]='N');
 END;

PROCEDURE TTEMP;
 BEGIN
  WRITE('FROM THE GRAPH, WHAT IS THE EXPECTED TRANSITION TEMP? ');
  READLN(T); N1:=0; N2:=0; M1:=0; M2:=0;
  FOR B:=1 TO 20 DO
   BEGIN
      IF (ARRAY0[1,B]<T) AND (ARRAY0[1,B]<>0) THEN
       BEGIN
        N1:=N1+1; ARRAY2[N1,1]:=ARRAY0[2,B]; ARRAY2[N1,2]:=ARRAY0[4,B];
       END;
      IF (ARRAY0[1,B]>T) AND (ARRAY0[1,B<>0) THEN
       BEGIN
        N2:=N2+1; ARRAY3[N2,1]:=ARRAY0[2,B]; ARRAY3[N2,2]:=ARRAY0[4,B];
       END;
     END;
  SXY:=0; SX2:=0; SX:=0; SY:=0;
  FOR C:=1 TO N1 DO CALC;
  SLOPE1:=(SXY-((SX*SY)/N1))/(SX2-((SX*SX)/N1));
  INTER1:=(SY/N1)-(SLOPE1*(SX/N1));
  SXY:=0; SX2:=0; SY:=0; SX:=0; ARRAY2:=ARRAY3;
  FOR C:=1 TO N2 DO CALC;
```

```
    SLOPE2:=(SXY-((SX*SY)/N2))/(SX2-((SX*SX)/N2));
    INTER2:=(SY/N2)-(SLOPE2*(SX/N2));
    AVERINTERC;
  END;

 PROCEDURE WORKSHOP;
  BEGIN
   WITH DATA DO
    BEGIN
       WRITE('ENTER MONTH,DAY,YEAR:  MONTH-- ');READLN(MONTH);
       WRITE('                       DAY---- ');READLN(DAY);
       WRITE('                       YEAR--- ');READLN(YEAR);
       WRITE('AGE OF ANIMAL(DAYS--ADULT=20)- ');READLN(AGE);
       WRITELN(--***----- WHEN ALL DATA ENTERED, ENTER TEMP=0---!!!');
       FOR B:=1 TO 20 DO
        FOR C:=1 TO 4 DO ARRAY1[C,B]:=0; B:=0;
       REPEAT
        B:=B+1;
        WRITE(B,'. TEMP(DEGREES CENTIGRADE)- '); READLN(ARRAY1[1,B]);
        IF (ARRAY1[1,B]<>0 THEN
         BEGIN
          ARRAY[2,B]:=(1/(ARRAY1[1,B]+273))*1000;
          WRITE('   STATE 3 RESP. RATE--------'); READLN(ARRAY[3,B]);
          ARRAY1[4,B]:=LOG(ARRAY1[3,B]);
         END;
       UNTIL ARRAY1[1,B]=0;
       ARRAY0:=ARRAY1;
    END;
   END;

 PROCEDURE WRITESCR;
  BEGIN
   INITTURTLE;
   FOR B:=1 TO 80 DO
       FOR C:=1 TO 45 DO
         IF (GRAPH[B,C]=1) THEN
          BEGIN
       PENCOLOR(NONE);
       MOVETO(B*3,C*4);
       PENCOLOR(WHITE);
       WCHAR('*');
          END;
       PENCOLOR(NONE); MOVETO(1,90);
       PENCOLOR(WHITE); MOVETO(1,1); MOVETO(279,1);
       READLN(CHOICE); TEXTMODE;
   END;

 PROCEDURE GRAPHFILE;
  BEGIN
   PX:='LOG RESP RATE'; PY:='1/TEMP(KELVIN) x 0.001';
   MAXMIN;
   XINTERVAL:=(XMAX-XMIN)/73; XARRAY[1]:=XMIN;
```

```
  YINTERVAL:=(YMAX-YMIN)/39; YARRAY[1]:=YMIN;
  FOR B:=2 TO 80 DO
      BEGIN
        J:=B-1; XARRAY[B]:=XARRAY[J]+XINTERVAL;
        IF (B<42) THEN YARRAY[B]:=YARRAY[J]+YINTERVAL;
      END;
  PY:='LOG STATE 3 RESP RATE'; PX:='1/TEMP(KELVIN) x 1000';
  SETPOINTS;
  WRITE('PRINT TO SCREEN OR TO PRINTER(TYPE "S" OR "P")?');
  READLN(CHOICE);
  IF (CHOICE[1]='P') THEN WRITEGRAPH ELSE WRITESCR;
 END;

BEGIN
      (*$G+*);
      WRITELN('---WELCOME   TO   THE   MODERN   ARRHENIUS   WORKSHOP---
');WRITELN;
333:WRITE('ENTER TISSUE TYPE (LIVER,KIDNEY,HEART)?');
      READLN(ORGAN); NAME:=ORGAN;
111:WRITELN('(A)  WORK WITH NEW ',NAME,' DATA');
      WRITELN('(B)  SWITCH TISSUE TYPE');
      WRITELN('(C)  EXIT PROGRAM');
      WRITELN('(D)  EXCLUDE POINTS FROM WORKING DATA');
      WRITELN('(E)  GRAPH THE WORKING DATA');
      WRITELN('(F)  CALCULATE TRANSTEMP, ETC. WITH WORKING DATA');
      WRITELN('(G)  RECALL WORKING DATA TO PRINTER');
      READLN(CHOICE);
      CASE CHOICE[1] OF
      'A':WORKSHOP;
      'B':GOTO 333;
      'C':GOTO 222;
      'D':EXCLUDE;
      'E':GRAPHFILE;
      'F':TTEMP;
      'G':RECALL;
      END;
      GOTO 111;
222:WRITELN('EXITING TO THE SYSTEM');
END.END.
```

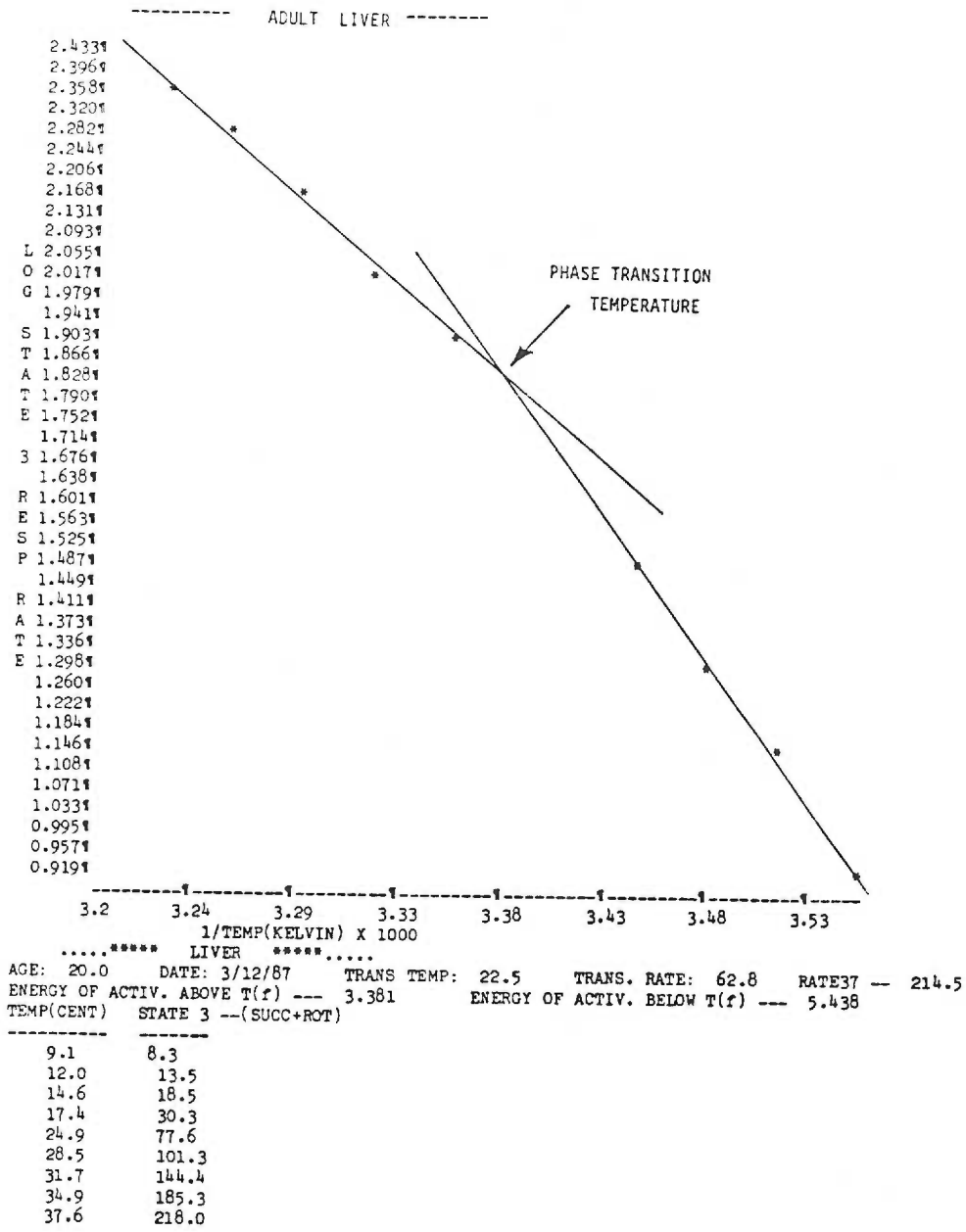

AGE: 20.0 DATE: 3/12/87 TRANS TEMP: 22.5 TRANS. RATE: 62.8 RATE37 -- 214.5

ENERGY OF ACTIV. ABOVE T(f) --- 3.381 ENERGY OF ACTIV. BELOW T(f) --- 5.438

TEMP(CENT)	STATE 3 --(SUCC+ROT)
9.1	8.3
12.0	13.5
14.6	18.5
17.4	30.3
24.9	77.6
28.5	101.3
31.7	144.4
34.9	185.3
37.6	218.0

Figure 1. Computer-generated Arrehenius plot. The data was collected as described in Manuscript #2 using liver mitochondria from an adult animal. The arrow denotes the phase transition temperature (T_t). Below the plot is a list of the calculated results and a table of the data used to make the calculations.

APPENDIX B

RESPONSES TO REVIEWER'S COMMENTS ON MANUSCRIPT #4

Comment #1-1: Following ischemia, cellular ATP would still be in excess of levels required to block the observed phenomenon.

Response: The ability of ATP to inhibit Ca^{2+} efflux is a dynamic process. Ca^{2+} efflux still occurs using 100 μM and 500 μM ATP (Figure 4), however, the effect is delayed and the rate of efflux is slower. We do not imply that a critical level of ATP is necessary to prevent efflux or inhibit cycling, only that ATP can prevent net efflux by supporting Ca^{2+} reuptake.

Comment #1-2: It is not clear from the data whether the protective effects of ATP involve inhibition of the permeability change that permits Ca^{2+} release or enhances reuptake. An experiment with ruthenium red (RR) in the absence of ATP would also test whether Ca^{2+} loss is via reversal of the uniport.

Response: In order to clarify the situation further, extramitochondrial Ca^{2+} was monitored in the presence of ATP, XO and hypoxanthine (HX) with and without RR. Without RR, ATP prevented net Ca^{2+} efflux. With RR and ATP, Ca^{2+} efflux still occurs. These data and the fact that oligomycin reverses ATP's protective effect (Figures 3, 4, 5B) support our contention that ATP prevents net Ca^{2+} efflux by supporting reuptake via ATP hydrolysis. These data have been included in the revised manuscript. The suggestion to test whether Ca^{2+} loss occurs via reversal of the uniport by incubating mitochondria with RR in the absence of ATP is inappropriate since RR blocks only the uptake of Ca^{2+} through the uniport and not the reverse flow of Ca^{2+} through the uniport.

Comment #1-3: Paragraph #1 of the results should be relocated to the discussion.

Response: The data (i.e., degradation rate of hypoxanthine) and calculations presented in this paragraph provide the reader with key information about the incubation conditions employed in the experiments subsequently described. We feel this information is essential to the reader who prefers to form his own interpretation of the results before reading the discussion.

Comment #1-4: The discussion on page 6 of the Results about the involvement of mitochondrial glutathione in the observed phenomenon is best placed in the Discussion.

Response: This change has been made in the revised manuscript.

Comment #1-5: The authors should consider measuring glutathione levels in their mitochondria.

Response: This was done. In addition, glutathione reductase and peroxidase levels were measured. The results were (mean ± S.D.).:

Gluatathione 0.23 ± 0.03, n=8 (nmoles /mg protein)
Glutathione reductase 38.3 ± 7.6, n=6 (nmoles NADPH oxidized/min/mg protein)
Glutathione peroxidase 25.6 ± 5.7, n=6 (nmoles NADPH oxidized/min/mg protein)

The results were not included in this manuscript because they are not relevant. The existance of the mitochondrial antioxidant system has been known for some time (Physiol. Reviews 59: 527-605, 1979).

Comment #1-6: The specificity of the findings for H_2O_2 could be

strengthened by showing that heat-inactivated catalase is without effect and another peroxide generating system would have similar effects.

Response: We agree. Heat-inactivated catalase was indeed without effect. Statements to that affect are included in the revised manuscript. Another form of peroxide, t-butylhydroperoxide, yields similar results causing both Ca^{2+} release (Ref. 1) and Ca^{2+} cycling (see page 11).

Comment #1-7: Information about the numbers of experiments and statistical analysis are provided only for Figure 6.

Response: Additional information about statistics and numbers are provided in the figure legends to each figure in the revised manuscript.

Comment #1-8: The conversion of xanthine dehydrogenase to XO in kidney is too slow to account for radical generation during reperfusion after commonly seen durations of ischemia (JCI 79:1564, 1987).

Response: The study cited employed non-physiological ischemia. Excised kidneys were incubated in 150 mM K_2HPO_4, 0.9% NaCl at pH 7.4, a solution similar to those used for cadaveric kidney preservation. These highly buffered, hyperosmotic and hyperkalemic conditions undoubtedly alter the mechanism under question. In vivo ischemia is associated with a cellular (1) efflux of K^+, (2) influx of Ca^{2+}, (3) lactate and H^+ accumulation and (4) swelling (JCBFM 1:155,1981). The incubation medium used in the cited study will counteract these 4

events, and create a situation much different from that seen in vivo. As a result, the normal Ca^{2+}-mediated conversion of xanthine dehydrogenase to XO is probably masked. In addition, other authors report contradictory findings arrived at under more physiological conditions, i.e., a doubling of kidney XO levels after 30 minutes of ischemia (In: Oxy Radicals and Their Scavenger Systems, Vol. 2,p. 143, 1983). Finally, dismissing the involvement of XO in renal reperfusion injury makes allopurinol preservation of renal function difficult to explain (JCI 74:1156, 1984). We do not feel that this discussion is relevant, and thus have not included it in the manuscript.

Comment #1-9: Cytosolic and mitochondrial Ca^{2+} levels may not increase in tubule cells during ischemia (Kidney Int. 33:359, 1988).

Response: The abstracts cited discuss cell Ca^{2+} during ATP-$MgCl_2$ incubation and anoxia. Our manuscript describes mitochondrial $Ca2^{+}$ cycling initiated by H_2O_2 metabolism and its importance to ischemia-reperfusion injury. The relationship between the abstracts cited and our manuscript are remote. Both abstracts, however, attempt to dissociate cellular Ca^{2+} from cell injury. The first abstract (Humes, et al) reports an increase in cellular Ca^{2+} without loss of cell viability during incubation with 2 mM ATP-$MgCl_2$ under hypoxic conditions. Is microsomal and/or mitochondrial Ca^{2+} uptake supported by ATP hydrolysis after diffusion through a damaged membrane? Does the Mg^{2+} and additional PO_4^{2-} stabilize Ca^{2+} intracellularly? The second abstract (Jacobs et al) reports modest elevations in cell Ca^{2+} despite significant cellular damage during anoxia. These findings support a

mechanism involving Ca^{2+} cycling which does occur without a significant increase in net intracellular Ca^{2+} concentration. Cell Ca^{2+} levels could conceivably be maintained by mitochondria with ATP generated from glycolysis during anoxia as demonstrated by Snowdowne et al (JBC 260: 11619, 1985) in a manuscript describing increases in Ca^{2+}_i in cultured kidney cells during anoxia. Again, we do not believe that this discussion would be helpful in the current manuscript.

Comment #1-10: Mitochondrial damage may play little role in anoxic injury(Nature 325: 78,1986).

Response: The study cited involves chemical (CN^-, iodoacetate) poisoning of cultured hepatocytes. Again, chemically induced electron transport and glycolytic inhibition in an attempt to simulate "anoxia" has little relevance to ischemia-reperfusion injury and H_2O_2-induced mitochondrial Ca^{2+} cycling. These authors, however, do describe an interesting phenomenon, i.e., net changes in cellular Ca^{2+} levels and cell viability may not be related in this type of chemical injury. No revisions were made concerning this comment.

Comment #1-11: The major parenchymal cells of heart and kidney in rabbit lack XO, yet these cells are fully susceptible to ischemic injury (Am J Physiol 252:H368, 1987).

Response: The study cited reports the apparent lack of XO and xanthine dehydrogenase in rabbit myocardium. Rat kidney and heart, however have both been shown to exhibit xanthine dehydrogenase to XO conversion by direct assay (Adv Myocardiol 5:183, 1985; Oxy Radical and Their

Scavenger Systems, Vol. 2, Greenwald RA, Cohen G, eds., p 143, 1983). Our study was conducted using rat kidney mitochondria, a tissue known to possess xanthine dehydrogenase and XO, therefore, cell damage secondary to H_2O_2 and O_2^- production by XO during reperfusion remains a valid hypothesis in this tissue. The fact that rabbit myocardium is devoid of XO suggests that XO <u>is</u> an important mediator of ischemia-reperfusion injury. Other studies on ischemic canine myocardium, which does possess XO, demonstrate a severe ischemia-reperfusion injury, i.e., one hour of ischemic followed by reperfusion induces infarction of 60% of the tissue risk (Circ Res 47:653, 1980). On the other hand, one hour of ischemia followed by reperfusion in the rabbit myocardium caused only a mild decrease (5-15% of control) in several parameters of mechanical function. Therefore, when rabbit myocardium, a tissue devoid of XO, is compared to canine myocardium, a tissue with significant xanthine dehydrogenase to XO conversion, the rabbit myocardium appears to be quite resistant to ischemia-reperfusion injury. Does the presence of XO in canine myocardium potentiate the reperfusion injury? The answer may be "yes". We do not feel this discussion is relevant and thus have not included it in the manuscript.

<u>Comment #1-12</u>: Recent direct studies of isolated rat tubules have failed to provide evidence for oxidant injury during ischemia (Kidney Int. 33:354, 1988).

<u>Response</u>: The abstract cited is interesting and supports the information presented in this manuscript in the following way. The authors show that exogenous t-butylhydroperoxide increases metabolic

rate (QO_2). Our studies show that mitochondrial peroxide metabolism induces Ca^{2+} cycling, thereby increasing O_2 consumption. This is, in fact, what the authors are observing since similar recent experiments in our laboratory show that this peroxide-induced increase in cellular O_2 consumption can be blocked with RR. The authors attempt to dissociate a decrease in mitochondrial respiratory function from oxidant injury mediated by in vitro ischemia-reoxygenation of isolated proximal tubule segments (PTS). This conclusion is premature for the following reasons. First, they assume that cellular oxidant injury is automatically accompanied by increases in lipid peroxidation products. Lipid peroxidation is initiated by hydroxyl radical which is formed from superoxide and H_2O_2. Cellular and mitochondrial antioxidant defense mechanisms function to minimize intracellular concentrations of these two oxidants via superoxide dismutase and glutathione peroxidase. In the process, glutathione and NAD(P)H become oxidized. If cellular antioxidant capacity is sufficient to overcome the oxidative stress, i.e., H_2O_2 and O_2^- are metabolized to H_2O, hydroxyl radical formation is minimized and lipid peroxidation does not occur to an appreciable extent. This manuscript demonstrates that mitochondrial H_2O_2 metabolism has deleterious effects on cell metabolism which will <u>precede</u> lipid peroxidation. Second, the abstract authors report a decrease in respiration which is probably due to sulfhydryl oxidation (Eur J Biochem 84:377, 1978) and/or loss of mitochondrial pyridine nucleotides (JBC 255:9325, 1980) in response to peroxide metabolism. These known mechanisms of oxidant induced respiratory inhibition must be ruled out before concluding that oxidants have no role in the

effect. Third, the inability of allopurinol (injected IP 18 hours prior to PTS isolation) plus exogenous catalase and SOD to protect mitochondrial respiratory function following ischemia-reoxygenation is not convincing evidence that reactive O_2 species are 'not' involved. The half-life of allopurinol and its metabolite, alloxanthine, are 2 and 18 hrs respectively. Isolation of the cells will further decrease cellular concentrations of allopurinol and alloxanthine. Does this IP injection of allopurinol effectively inhibit XO in the isolated cells? Catalase and SOD added extracellularly could not possibly sequester H_2O_2 and superoxide produced intracellularly. Based on the information provided in this abstract, the conclusion the authors make is premature and lacks sufficient experimental proof. The discussion of these differences between our manuscript and the cited abstract are superfluous.

Comment #1-13: This paper is similar to Ref. 23 except they focus on respiratory effects while this paper focuses on Ca^{2+} handling. The relationships between these observation should be more extensively discussed.

Response: Ref. 23 does indeed employ a similar experimental design, however, several key differences exist which make comparison with our work difficult. First, their HX/XO system includes 20μM $FeCl_2$ to catalyze hydroxyl radical formation from H_2O_2 and O_2^- by the Haber-Weiss reaction. This was not done in our experiments. Second, changes in respiration were studied 3 minutes post-oxygen radical treatment. Our study observes the dynamic effect of H_2O_2 metabolism during it's

generation. Finally, their animals were anesthetized with thiobarbiturate, a known respiratory chanin inhibitor, prior to mitochondrial isolation. This may contribute to the low respiratory control ratio (between 4-6) of the control groups. With these distinctions in mind, some general comments are made in the revised manuscript regarding the possible relationship between our study and Ref. 23. Any more discussion is felt to be inappropriate for this manuscript.

Comment #1-14: The statement that tissue hypoxanthine (HX) increases during ischemia is true, however the situation is more complex in that HX increases to a different extent in different cell types and the extracellular space so that the finding of increased tissue HX does not necessarily support the hypothesis advanced in this paper.

Response: We agree that the level of HX accumulation during ischemia depends on tissue/cell type, length and degree of ischemia, species, temperature, animal age, etc. Regardless of these differences, the accumulation of HX intracellularly from ATP catabolism during ischemia in mammalian cells remains a biochemical fact. If tissue HX increases in a tissue deprived of blood flow, we feel it is safe to assume that HX concentration is increased at the site of production as well as in the extracellular space. The degree of HX (and XO) accumulation will determine the extent of H_2O_2 production during reoxygenation. The small quantities of HX present intracellularly during reperfusion of ischemic rat kidney are sufficient to induce the phenomenon set forth by this manuscript, i.e., mitochondrial H_2O_2 metabolism leads to

NAD(P)H oxidation, Ca^{2+} efflux and cycling, thereby increasing the energy and oxygen demands of the cell. We feel this discussion is inappropriate for this manuscript, thus it was not included.

Comment #1-15: The general survey of the role of radicals in ischemic injury in the Introduction frequently does not indicate in which specific tissues various observation are made...generalizations are made about the roles for free radicals which we already know are very different in various tissues and cell types.

Response: The comment is very similar to Comment #1-14. The Introduction was revised to specify the exact tissue(s) in which the varuious observations were made. Radical involvement in post-ischemic injury has been studied in various tissues, species and isolated cell types. Of course, H_2O_2-induced mitochondrial Ca^{2+} release and cycling will be most likely involved in those tissues known to have ample xanthine dehydrogenase to XO conversion and HX accumulation during ischemia such as rat intestine, heart, kidney and liver. We do not state anywhere in the manuscript that this mechanism is conclusively operative in other tissues as well, only that he potential for involvement exists.

Comment #2-1: The results indicate Ca^{2+} efflux is related to NAD(P)H oxidation, however, the ATP results indicate a dissociation between Ca^{2+} efflux and NAD(P)H oxidation.

Response: NAD(P)H oxidation initiates Ca^{2+} efflux; ATP prevents a net Ca^{2+} efflux by stimulating reuptake via hydrolysis. A dissociation

exists because the phenomena are separate. This is clearly stated and proven in the Results and Discussion.

Comment #2-2: Is it possible that ATP acts by binding Ca^{2+}?

Response: No. The dissociation constant for CaATP is 1 X 10^{-4} M. The K_m for mitochondrial Ca^{2+} uptake is about 1 X 10^{-6} M. The affinity of the mitochondrial uniport for Ca^{2+} is about 100-fold higher than the affinity of ATP for Ca^{2+}. Also, a net increase in extramitochondrial Ca^{2+} in the absence of ATP following (a) oligomycin and (b) ruthenium red addition cannot be explained by Ca-ATP dissociation alone. No additonal revisions were made in the manuscript regarding this point.

Comment #2-3: ATP is likely getting hydrolyzed helping to maintain the transmitochondrial H^+ gradient.

Response: This is exactly the point being made in the manuscript - ATP hydrolysis can drive Ca^{2+} reuptake during H_2O_2-induced efflux.

Comment #2-4: If Ca^{2+} release occurs in response to NAD(P)H oxidation, then substrates reducing NAD(P) would reverse the effect of XO and HX.

Response: This was tested using glutamate and malate as NADH-linked substrates. Glutamate-malate prevents the Ca^{2+} efflux induced by XO addition. This information was added in the Results and Discussion sections.

Comment #2-5: It is unclear how the authors have taken into account the effects of solution pH with the addition of ATP in these large

quantities.

Response: A stock solution of the tris salt was prepared and neutralized to pH 7.4 with dilute KOH. Aliquots of this stock solution were then added to the incubation medium. Statements to this affect have been included in the Materials and Methods section.

Comment #2-6: It is somewhat unclear what the authors mean when they say the optical density was measured at 560nm and 700nm during the efflux period (p 7).

Response: Optical density was monitored at these wavelengths in two separate experiments during the Ca^{2+} efflux period to assess for mitochondrial swelling. These wavelengths were chosen to avoid interference induced by changes in the redox state of the cytochromes. The revised manuscript states that O.D. was measured separately at 560nm or 700nm.

Comment #3-1: Could some of the Ca^{2+} efflux that is occuring presently attributable to mitochondria really be arising from a microsomal Ca^{2+} pool?

Response: Given the large changes in Ca^{2+} seen, this is very unlikely. Although microsomal contamination in mitochondrial preparations from liver can be a problem, that of the kidney is not. The differential centrifugation method used in our laboratory as outlined in the Materials and Methods, consistently provides a preparation of mitochondria with <5% microsomal contamination. First, Ca^{2+} uptake in our preparation does not occur in the presence of RR. ATP-stimulated,

RR-insensitive, Ca^{2+} uptake was < 0.2 nmoles/min mg protein. Therefore, the contribution of contaminating microsomal Ca^{2+} transport is negligable (RR blocks the mitochondrial uniport system without affecting the microsomal Ca^{2+} uptake system. Second, the activity of glucose-6-phosphatase, a microsomal enzyme marker, in our preparation is extremely low 0.09 ± 0.06 (n = 7) μmoles of P_i generated from glucose-6-phosphate in 20 min·mg protein at 30°C. These data were added as an indication of the purity of the preparation.

Comment #3-2: The dose of catalase used in these studies is large. A dose response curve should be demonstrated. In addition, the use of an inactivated catalase as a control must be used.

Response: See Comment #1-6. The dose of catalase is not excessively large under these experimental conditions. Catalase catalyzes a first order reaction, therefore, the rate is directly proportional to enzyme and substrate concentration. One Sigma unit will decompose 1 μmole of H_2O_2/min at pH 7.0 as $[H_2O_2]$ falls from 10.3 mM to 9.2 mM. Paragraph 1 of the Results estimates that 17.5 nmoles of H_2O_2 are generated per ml·min using 73 mU XO/ml. As a result, 1 min after XO addition, assuming no H_2O_2 metabolism occurs, the $[H_2O_2]$ should be about 17.5 μM. Since the rate is proportional to [enzyme] X [substrate], a 1000-fold drop in [substrate] requires at least a 1000-fold increase in [catalase] in order to assure adequate H_2O_2 removal from the incubation medium. The dose of catalase (and XO) do show a dose response relationship with Ca^{2+} efflux rate and lag time to Ca^{2+} efflux. These data were not demonstrated in the original manuscript, however,

statements to that affect are included in the Results section of the revised manuscript.

Comment #3-3: The effect of exogenous ATP to inhibit Ca^{2+} efflux and the effect of RR to diminish futile Ca^{2+} cycling may be additive in nature. Submaximal concentrations of both should be additive...this additivity effect may provide insight into the mechanism by which the Ca^{2+} efflux may arise in the response to oxygen radical generation.

Response: This is not a feasable experiment since ATP inhibits efflux by stimulating reuptake (see Results paragr. #7 and Figure 3) through the uniport while RR blocks Ca^{2+} uptake through the same uniport. That is, RR inhibits the mechanism by which ATP has its effect, therefore, an additive effect to inhibit the increase in extramitochondrial Ca^{2+} is not possible. Substantial evidence is provided for the mechanism of Ca^{2+} efflux involving mitochondrial H_2O_2 metabolism and NAD(P)H oxidation, however, the focus of this manuscript is not on the mechanism of Ca^{2+} efflux, but that Ca^{2+} efflux occurs in response to small quantities of H_2O_2 which can induce futile Ca^{2+} cycling thereby increasing O_2 consumption.

Comment #3-4: Although the authors suggest that the Ca^{2+} efflux occurs by a route separate from the uniport system, it would be interesting to present experiments evaluating the effect of RR on Ca^{2+} efflux that develops after XO and HX treatment.

Response: This comment is very similar to Comment #1-2. Briefly, RR will not block the reverse flow of Ca^{2+} through the uniport; its only

blocks Ca^{2+} uptake. The fact that Ca^{2+} efflux occurs by another channel is supported by the findings of Baumhuter and Richter (Ref. 1), as stated in Paragraph 8, of the results, who studied t-butylhydroperoxide-induced Ca^{2+} efflux in isolated rat liver mitochondria.

Comment #3-5: "It is somewhat unclear how the estimated state 4 rate was calculated using the generated O_2 from the HX/XO reaction was calculated."

Response: The wording of the question is confusing. First, the HX/XO reaction does not generate O_2 but consumes it. The rate of O_2 consumption by XO was calculated and subtracted from the total O_2 consumption (mito + XO), i.e., mito state 4 (prior to XO addition) plus O_2 consumption by XO is equal to estimated total O_2 consumed. Clarifying statements were included in the Materials and Methods section.

APPENDIX C

ADDITIONAL DETAILS TO METHODS

This section is a collection of figures which provide additional information (spectra, chromatograms) for the interested reader concerning the methods employed in the manuscripts presented herein.

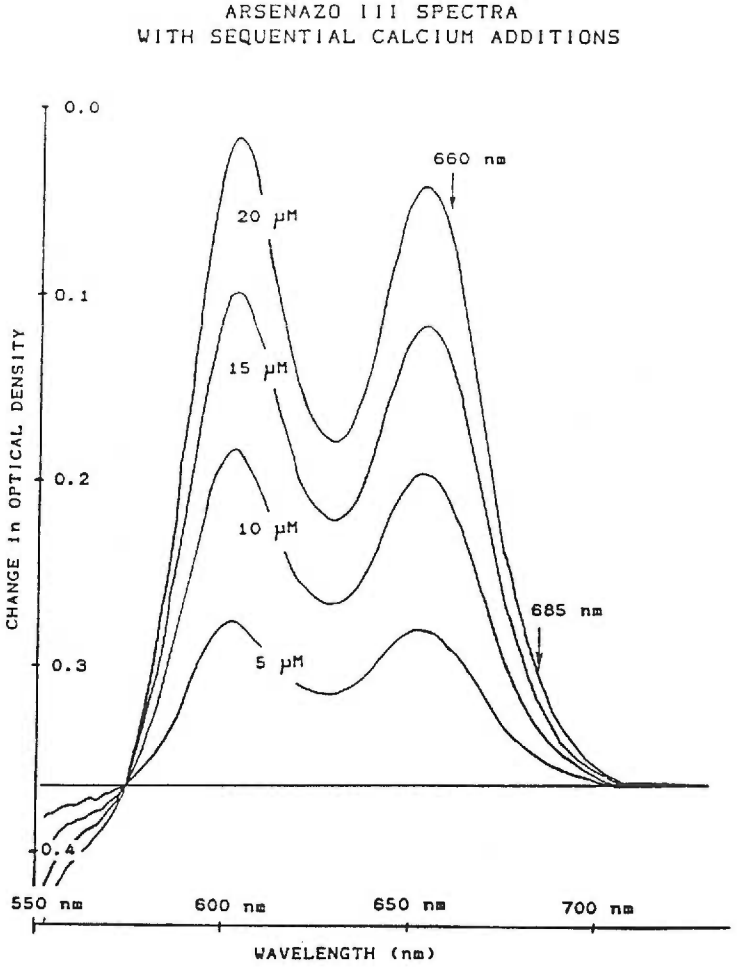

Figure 1. Changes in the arsenazo III spectrum with sequential additions of calcium. In the experiments described in Manuscripts #1 and 4, changes in extramitochondrial calcium were monitored using this calcium indicator by dual wavelength spectroscopy at 660 - 685nm. Note that micromolar changes in the cuvette calcium concentration produce large changes in the differential absorbance at these two wavelengths.

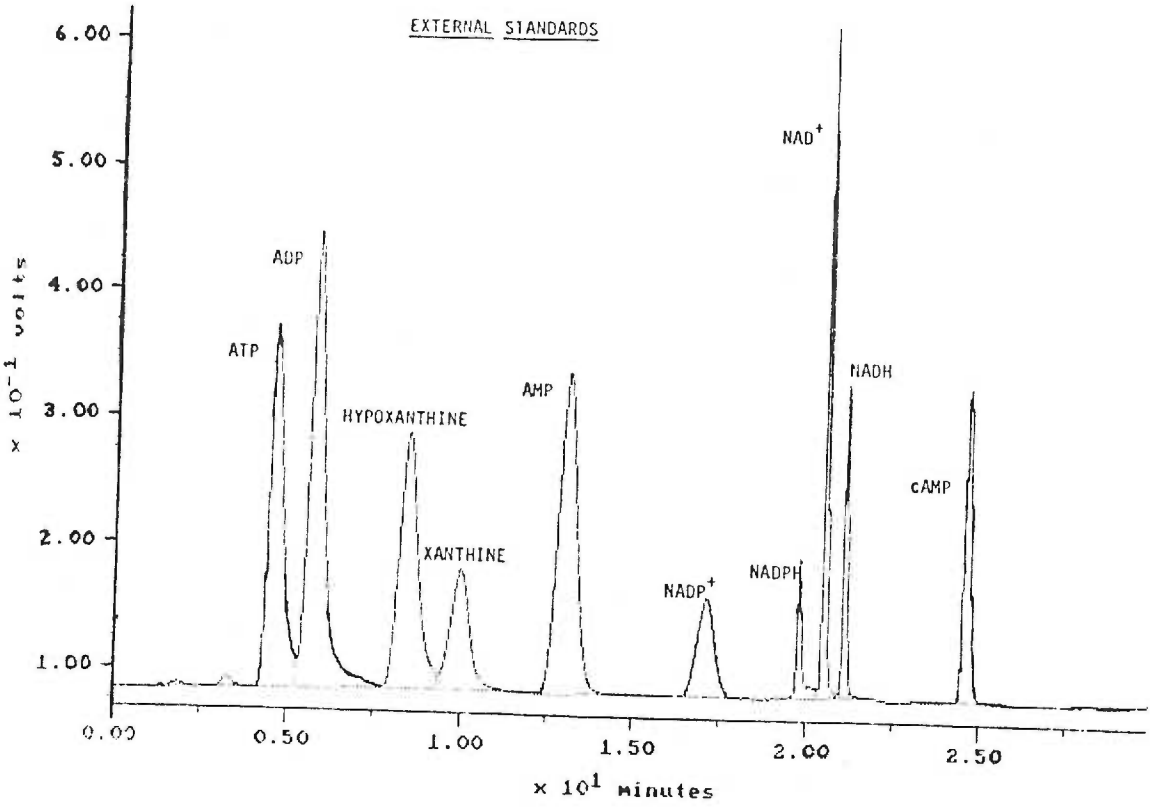

Figure 2. Sample chromatogram of external standards used for the HPLC nucleotide and hypoxanthine/xanthine assays described in Manuscripts #2, 3 and 4. Each component of the assay is labeled on the chromatogram. Details of the assay procedure are described in the manuscripts herein.

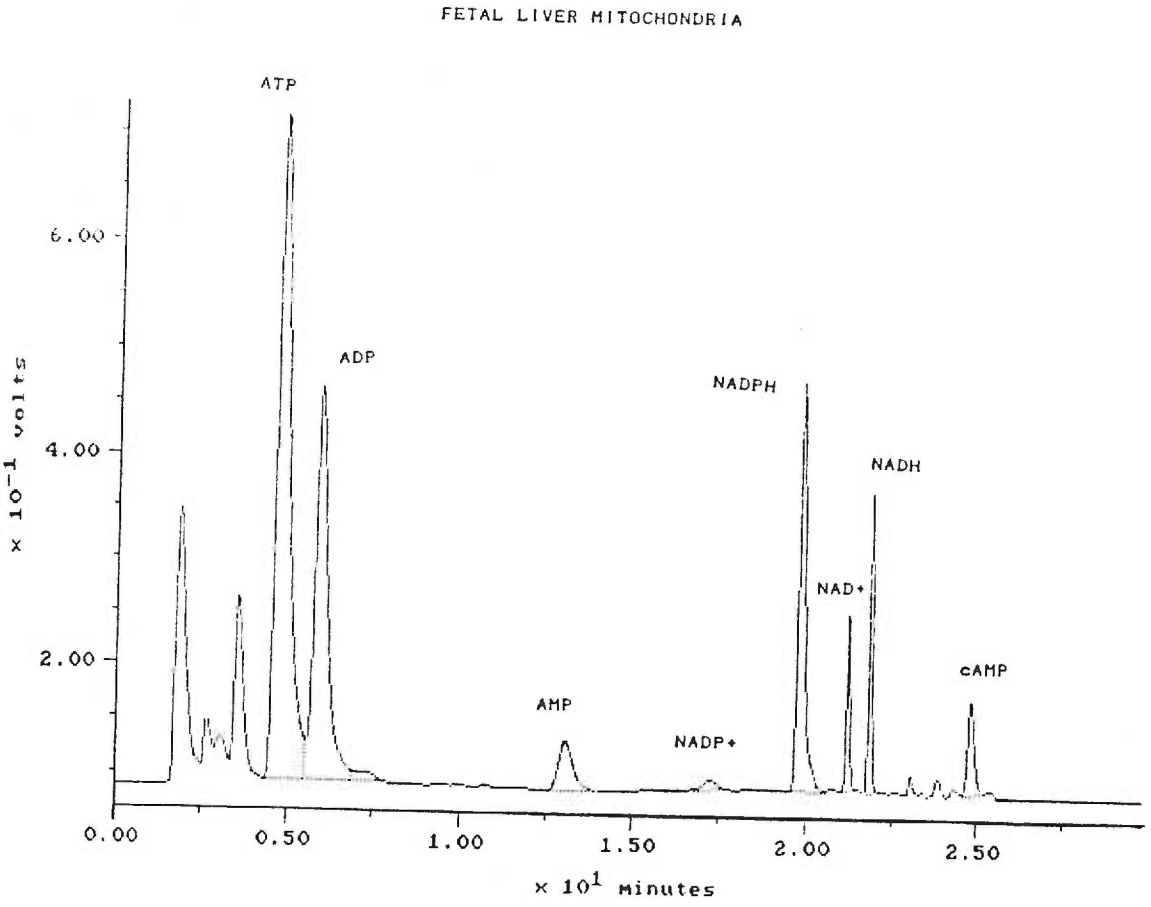

Figure 3. Sample chromatogram of the nucleotides present in liver mitochondria from a fetal animal. Details of the assay procedure are described in the manuscripts herein.

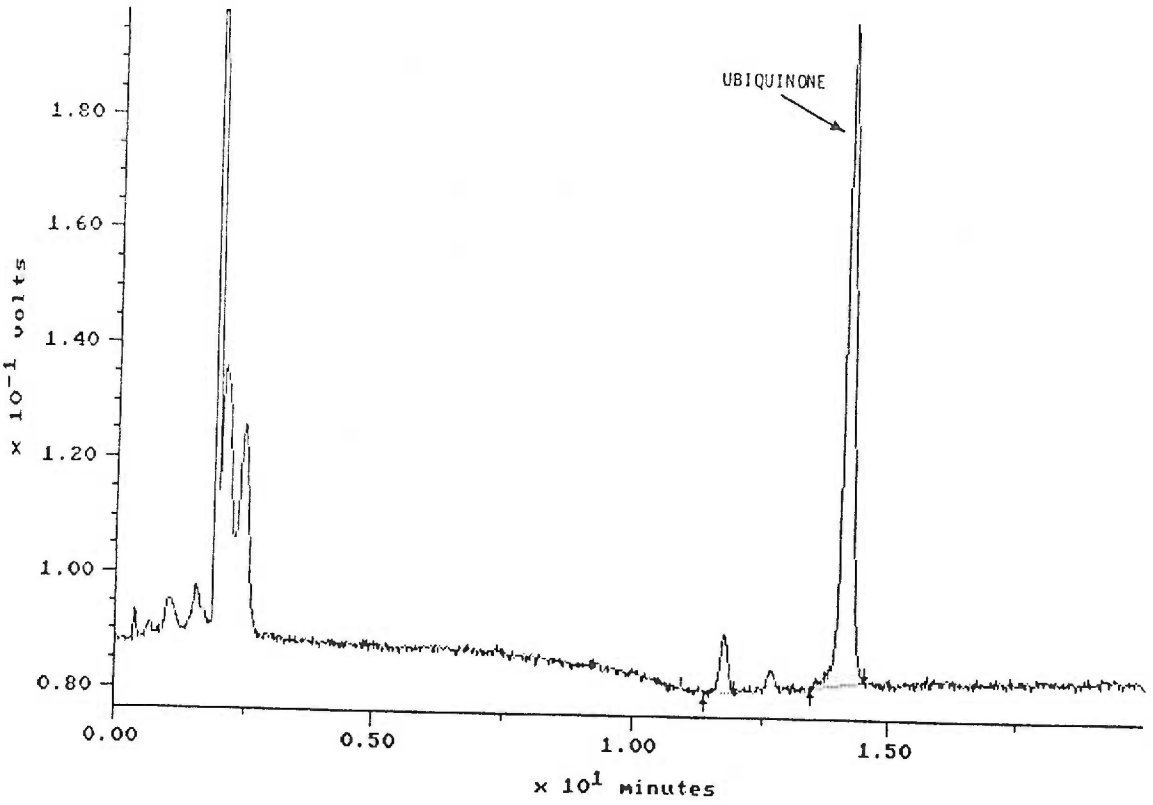

Figure 4. Sample chromatogram of ubiquinone in heart mitochondria from a 2.9 day old animal. Details of the assay procedure are described in Manuscript #2.

APPENDIX D

THE STRUCTURE AND STATES OF OXYGEN

Oxygen can exist in the following states:

$$^1O_2 \xleftrightarrow{e^-} {}^3O_2 \xleftrightarrow{e^-} \cdot O_2^- \xleftrightarrow{e^-} H_2O_2 \xleftrightarrow{e^-} HO\cdot \xleftrightarrow{e^-} H_2O$$

singlet	triplet	superoxide radical	hydrogen peroxide	hydroxyl radical	water

Triplet oxygen has 16 electrons, and therefore has electrons in the anti-bonding $2p\pi^*$-orbital. It's configuration is $...2p\pi^4\ 2p\sigma^2\ 2p\pi^{*2}$ with 2 bonds between the oxygen atoms. The double bond is a single σ-bond plus a single π-bond which is a common structure of double bonds. Energetic considerations suggest that $2px\pi^*\ 2py\pi^*$ is a better arrangement for the $2p\pi^*$ electrons than $(2px\pi^*)^2$ because the electrons are further apart and repel each other less. Since these two electrons occupy different space orbitals, they are no longer required to have opposed spins. Based on Hund's rule, electrons with parallel spins have a lower energy than a corresponding pair with opposed spins. These parallel spinning electrons give rise to a magnetic moment which makes triplet oxygen magnetic. Reactions between triplet oxygen and diamagnetic substances are slow, but reactions with paramagnetic substances are favored because changes in spin need not occur in the collision complex. Examples of favored reactions are (1) the oxygenation of paramagnetic transition metals, (2) dimerization of oxygen and (3) reversible reaction of O_2 with aromatic compounds in their triplet states.

Singlet oxygen is formed by the excitation of the electrons in the $2p\pi^*$-orbital of triplet oxygen. Two singlet states of oxygen exist: (1) The $^1\Sigma g^+$ state, where the two anti-bonding electrons occupy the same π^* -anti-bonding orbital as in the ground state, but with anti-

parallel spins. (2) The $^1\Delta g$ state, where both antibonding electrons are localized in one π^* -antibonding orbital with anti-parallel spins; the second orbital is empty. These singlet states show enhanced electron affinity and are very reactive.

The addition of an electron to triplet oxygen forms superoxide anion. It has two electrons with anti-parallel spins in the πx^* orbital with a single unpaired electron in the πy^* orbital. This oxygen species is in pH-dependent equilibrium with the perhydroxyl radical:

$$\cdot O_2^- + H^+ \underset{}{\overset{pk_a = 4.88}{<----------->} } \underset{\text{perhydroxl radical}}{\cdot HO_2}$$

Superoxide radical is a redox reactive species which is removed from biological systems via dismutation. However, spontaneous dismutation at biological pH's is unfavorable due to the charge on the superoxide molecule. Superoxide dismutases help to speed up dismutation and prevent cellular damage.

One-electron reduction of superoxide radical forms H_2O_2. This is the most stable intermediate in the reduction of triplet oxygen. Both the πx^* and πy^* orbitals are occupied by 2 electrons each, both possessing anti-parallel spins. H_2O_2 is cytotoxic but the exact mechanism of this toxicity has not been elucidated. Toxicity may be related to its intracellular metabolism or by reaction with superoxide radical (or Fe^{++}) which gives rise to the extremely reactive hydroxyl radical.

One electron reduction of H_2O_2 yields hydroxyl radical plus

hydroxyl anion. The volatile state of this highly reactive oxygen species is attributed to an unpaired electron in the σ^* orbital. Hydroxyl radical is an important component of oxygen toxicity and can be produced catalyticly from H_2O_2 in the presence of ferrous iron via the Haber-Weiss reaction.

The complete reduction of oxygen results in the formation of H_2O; all anti-bonding orbitals contain paired electrons with anti-parallel spins. This species of oxygen is very stable.

The structure of oxygen makes it fit for use in biological systems for the following reasons:

(a) O_2 has a favorable ΔG of reduction to H_2O (-52 kcal/mole).

(b) O_2 is a gas which is soluble in lipid and H_2O.

(c) H_2O exists in the liquid phase at room temperature.

(d) H_2O extraction is a main biosynthetic mechanism in DNA, RNA protein, etc., synthesis.

(e) O_2 reactions are catalyzed by transition metals and flavins.

(f) Redox potentials for the reduction of O_2 to H_2O at pH 7 are unfavorable at the first step but favorable for subsequent steps.

(g) The specific gravity of ice and water are favorable for life in aqueous media.

The diagram below depicts the redox potentials (V = volts) and the bond lengths (A = angstroms) of the various stages of oxygen reduction:

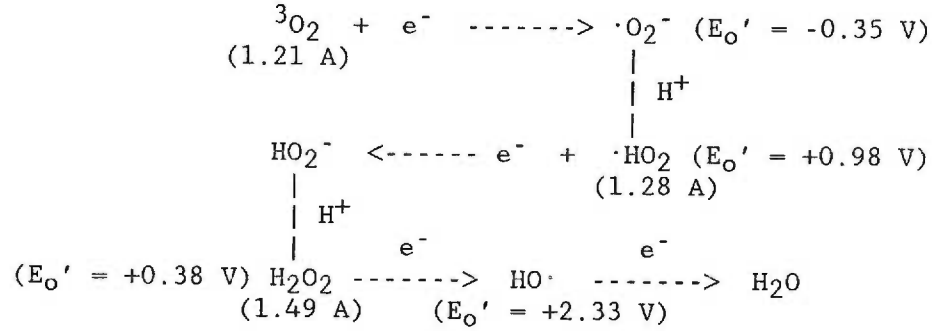

The oxidizing power of oxygen comes from the second, third and fourth additions of electrons. As the bond lengths increase, the strength of the O-O bond decreases.

Oxygen toxicity is believed to occur via singlet oxygen, hydroxyl radical and, to a lesser extent, superoxide anion. Singlet oxygen can add to double bonds forming peroxides. Peroxide formation could after the functional integrity of many cellular components (e.g., peroxides formed from polyunsaturated acyl chains in the inner mitochondrial membrane can alter membrane fluidity). Hydroxyl radical, having a redox potential of +2.33 volts, is an extremely strong oxidant and will pull electrons from almost any molecule in its immediate environment, resulting in damage to many cellular constituents including DNA. The toxicity of superoxide anion is believed to stem from its ability to form $HO\cdot$ from H_2O_2 according to the following reaction:

$$\cdot O_2^- + H_2O_2 \xrightarrow{Fe} \cdot OH + OH^- + O_2$$

Superoxide anion and H_2O_2 concentrations inside the cell are kept minimal by dismutases, peroxidases and catalases, thereby, reducing the formation of hydroxyl radical.

The thermodynamic, kinetic and chemical properties of oxygen, which are a reflection of oxygen's electronic structure, make it suitable for use in biological systems. However, these same properties also impose their limitations via the formation of toxic intermediates.

Moore, Walter J. 1983. Basic Physical Chemistry. Prentice-Hall, Inc., New Jersey, U.S.A.

APPENDIX E

MITOCHONDRIAL CALCIUM METABOLISM DURING TISSUE REPERFUSION

Perspectives in Shock Research, Vol.II, in press.

MITOCHONDRIAL CALCIUM METABOLISM DURING TISSUE REPERFUSION

Angelo A. Vlessis and Leena Mela-Riker

Departments of Surgery and Biochemistry

Oregon Health Sciences University, Portland, Oregon 97201

INTRODUCTION

The mitochondrion's role in cell metabolism under normal, and ischemic conditions and during reoxygenation is, unquestionably, of paramount importance. Under normal conditions, mitochondria oxidize various substrates to conserve energy for ATP production and ion transport. Energy from the mitochondria is delivered to the cytosol as ATP which functions to maintain plasma membrane and endoplasmic reticulum ATP-dependent ion pumps. The mitochondrial and plasma membrane electrochemical gradients are essential for normal cell function and viability. During ischemia, O_2 and substrate delivery to the cell ceases. Without O_2, the energy yielding electron transport process halts. The mitochondrial electrochemical gradient quickly dissipates resulting in release of endogenous mitochondrial Ca^{2+} into the cytosol via reversal of the Ca^{2+}-uniport (Fiskum and Lehninger,

1982). As mitochondrial ATP production stops, glycolytic activity increases, leading to tissue lactate accumulation (Siesjo, 1981). The demand for ATP soon exceeds the glycolytic capacity for its production and cytosolic ATP becomes catabolized in a stepwise fashion to hypoxanthine (DeWall et al., 1971). Elevated cytosolic Ca^{2+} is believed to activate a Ca^{2+}-dependent protease which converts xanthine dehydrogenase to xanthine oxidase (Roy and McCord, 1983).During reperfusion, tissue PO_2 rises and xanthine oxidase catalyzes the conversion of hypoxanthine to xanthine with the intracellular production of H_2O_2 and superoxide anion radical (McCord, 1985). These partially reduced O_2 species are believed to contribute to the additional cellular insult imposed by reoxygenation, termed reperfusion injury (Weisfeldt, 1987). Reoxygenation also permits mitochondrial electron transport to continue. Mitochondrial Ca^{2+} uptake and oxidative phosphorylation resume, and mitochondria begin to restore normal cytosolic free Ca^{2+} levels. The accumulation of Ca^{2+} in mitochondria during reoxygenation reflects this process. Interestingly, the quantity of accumulated Ca^{2+} correlates inversely with mechanical function and tissue ATP content post-reoxygenation (Nakanishi et al., 1982). Tissue lactate, free fatty acid accumulation (Siesjo and Wieloch, 1985) and mitochondrial Ca^{2+} uptake, as well as the intracellular production of H_2O_2 and superoxide (McCord, 1985), can have profound effects on cellular energy metabolism and viability during ischemia and reoxygenation.

H_2O_2 AND CALCIUM METABOLISM

Under normal conditions, Boveris predicts that 1-4% of all O_2 consumed by an animal is via univalent pathways in mitochondria forming superoxide anion radicals (Boveris, 1977). Superoxide dismutates, either spontaneously or enzymatically, to H_2O_2. Mitochondria then metabolize H_2O_2 via glutathione peroxidase forming glutathione disulfide (GSSG) from glutathione. GSSG is re-reduced via glutathione reductase oxidizing NADPH. NADH can also be oxidized via the transhydrogenase reaction (Chance et al., 1979). Mitochondrial NAD(P)H oxidation, via acetoacetate (Lehninger et al., 1978), various peroxides (Frei et al., 1985) or other oxidants such as selenite (Vlessis and Mela-Riker, 1987), leads to mitochondrial Ca^{2+} efflux. The Ca^{2+} efflux pathway is distinct from the Ca^{2+}-uniport uptake system and appears to involve a $Ca^{2+}/2H^{+}$ antiport mechanism (Baumhuter and Richter, 1982). Efflux can be potentiated by post-ischemic conditions which facilitate proton translocation from the extramitochondrial space to the matrix such as the elevated free fatty acid levels and decreased cellular pH (Frei et al., 1985). Ca^{2+} efflux is also potentiated by higher intramitochondrial Ca^{2+} loads (Frei et al., 1985), a condition which occurs during reoxygenation of ischemic tissues (Nakanishi, 1982). In summary, during reoxygenation, H_2O_2 formation and reduction may alter cellular Ca^{2+} balance through the oxidation of mitochondrial NAD(P)H.

MITOCHONDRIAL Ca^{2+} METABOLISM AND ENERGY PRODUCTION

The mitochondrial Ca^{2+}-uniport uptake system operates electrophoretically in response to a negative inside membrane potential developed

and maintained by electron transport or ATP hydrolysis (Mela, 1977). Mitochondrial Ca^{2+} uptake assumes a high priority and will proceed at the expense of ATP production (Fiskum and Lehninger, 1982). Since mitochondrial Ca^{2+} efflux occurs by an independent electroneutral $Ca^{2+}/2H^{+}$ antiport mechanism, efflux may stimulate reuptake, leading to futile Ca^{2+} cycling across the inner membrane which would increase O_2 and energy consumption and decrease ATP production.

O_2 CONSUMPTION AND ENERGY PRODUCTION IN ISCHEMIA-REOXYGENATION

During the reperfusion of a previously ischemic tissue, small quantities of H_2O_2 and superoxide, produced intracellularly via xanthine oxidase, can have profound effects on mitochondrial function. Figure 1, Manuscript #4, shows a typical in vitro experiment in which mitochondrial NAD(P)H oxidation and Ca^{2+} efflux are induced by small quantities of H_2O_2 and superoxide generated by xanthine oxidase in the presence of hypoxanthine. The resulting Ca^{2+} efflux requires H_2O_2 metabolism since efflux could be prevented by adding catalase, but not superoxide dismutase, to the incubation medium (data not shown). Experiments identical to those of Figure 1, Manuscript #4, were repeated using various quantities of xanthine oxidase to elicit different rates of H_2O_2 and superoxide production. NAD(P)H oxidation rates, as well as Ca^{2+} efflux rates and lag times to Ca^{2+} efflux were calculated at each xanthine oxidase concentration. The NAD(P)H oxidation rates correlated well with the Ca^{2+} efflux rate (R=0.99) and inverse of lag time to Ca^{2+} efflux (R=0.98). To determine whether

H_2O_2-induced Ca^{2+} efflux initiated reuptake, O_2 consumption was monitored versus time in the mitochondrial suspension under state 4 conditions. The addition of xanthine oxidase increased the state 4 respiratory rate to 148 +/- 27% (n=8) of control values. Additions of ruthenium red, which prevents Ca^{2+} cycling by blocking the Ca^{2+}-uniport uptake system, decreased O_2 consumption to below control values (77 +/- 23%, n=5). Similar results were obtained with EGTA which prevents Ca^{2+} cycling by sequestering released Ca^{2+}. In conclusion, small quantities of H_2O_2 and superoxide, produced by xanthine oxidase, can induce Ca^{2+} efflux and cycling across the inner mitochondrial membrane leading to a significant ($p<0.001$) increase in state 4 respiration. Therefore, during the reperfusion of an ischemic tissue, H_2O_2 and superoxide generated intracellularly from accumulated hypoxanthine and xanthine oxidase may induce Ca^{2+} efflux and cycling resulting in increased cellular O_2 consumption, ineffective ATP production and, as a consequence, decreased cell viability.

REFERENCES

1. Baumhuter S, Richter C (1982). The hydroperoxide-induced release of mitochondrial calcium occurs via a distinct pathway and leaves mitochondria intact. FEBS Lett 148:271-275.

2. Boveris A (1977). Mitochondrial production of superoxide radical and hydrogen peroxide. In Reivich M, Coburn R, Lahiri S, Chance B (eds): "Tissue Hypoxia and Ischemia," New York and London: Plenum Press, pp 67-82.

3. Chance B, Sies H, Boveris A (1979). Hydroperoxide metabolism in

mammalian organs. Physiol Rev 59:527-605.

3. DeWall RA, Vasko VA, Stanley EL, Kezdi P (1971). Responses of the ischemic myocardium to allopurinol. Am Heart J 82:362-370.

4. Fiskum G, Lehninger AL (1982). Mitochondrial regulation of intracellular calcium. In Cheung WY (ed): "Calcium and Cell Function, Vol II," New York: Academic Press, Inc., pp 39-80.

5. Frei B, Winterhalter KH, Richter C (1985). Quantitative and mechanistic aspects of the hydroperoxide-induced release of Ca^{2+} from rat liver mitochondria. Eur J Biochem 149:633-639.

6. Lehninger AL, Vercesi A, Bababunmi EA (1978). Regulation of Ca^{2+} release from mitochondria by the oxidation-reduction state of pyridine nucleotides. Proc Natl Acad Sci USA 75:1690-1694.

7. McCord JM (1985). Oxygen-derived free radicals in post-ischemic tissue injury. N Engl Jour Med 312:159-163.

8. Mela L (1977). Mechanism and physiological significance of calcium transport across mammalian mitochondrial membranes. In Bronner F, Kleinzeller A (eds): "Current Topics in Membranes and Transports, Vol 9," New York: Academic Press, Inc., pp 321-362.

9. Nakanishi T, Nishioka K, Jarmakani JM (1982). Mechanism of tissue Ca^{2+} gain during reoxygenation after hypoxia in rabbit myocardium. Am J Physiol 242:H437-H447.

10. Roy RS, McCord JM (1983). Superoxide and ischemia: conversion of xanthine dehydrogenase to xanthine oxidase. In Greenwald RA, Cohen G (eds): "Oxy Radicals and Their Scavenger Systems, Vol 2," New York: Elsevier Science, pp 143-153.

11. Siesjo BK (1981). Cell damage in the brain: a speculative

hypothesis. J Cereb Blood Flow Metabol 1:155-177.

12. Vlessis AA, Mela-Riker L (1987). Selenite-induced NAD(P)H oxidation and calcium release in isolated mitochondria: relationship to in vivo toxicity. Mol Pharmacol 31:643-646.

13. Weisfeldt ML (1987). Reperfusion and reperfusion injury. Clin Res 35:13-20.